

UNIVERSITÀ DEGLI STUDI DI PADOVA

Dipartimento di Fisica e Astronomia “Galileo Galilei”

Corso di Laurea Magistrale in Fisica

Tesi di Laurea

Electroweak Physics at Very High Energy

Relatore

Prof. Massimo Passera

Laureando

Lorenzo Ricci

Anno Accademico 2017/2018

*The completion of this thesis would not have been possible without the support,
understanding and guidance of Prof. Andrea Wulzer.*

Contents

1	Introduction	7
2	Massive gauge theories	9
2.1	Spontaneous symmetry breaking	9
2.1.1	Global symmetries	9
2.1.2	The Higgs mechanism	10
2.2	Non-Abelian gauge theories quantised	11
2.2.1	The R_ξ gauges	14
2.3	The Higgs-Kibble model	14
2.4	The Equivalent Gauge	16
3	Soft-Collinear double-logs	19
3.1	Sudakov form factor in QED	20
3.2	Virtual emissions in non-Abelian gauge theories	24
3.3	Exclusive cross-section in massive gauge theories	27
3.4	Inclusive cross-sections	29
3.4.1	A diagrammatic approach	30
3.4.2	The Coherent States Formalism	32
3.4.3	Comparison of the two formalisms	35
4	NLO heavy singlet VBF production	39
4.1	Self-energies and Slavnov-Taylor identities	40
4.1.1	Transverse W , S and h	40
4.1.2	“Unphysical fields” and Slavnov-Taylor	42
4.2	$W_0W_0 \rightarrow SS$ at one loop	44
4.3	$W_0W_0 \rightarrow SS + X$	48
4.4	$W_0W_0 \rightarrow SS$ in the Equivalent Gauge	49
5	Conclusions	55
	Appendices	56
A	Feynman rules and renormalization scheme	57
A.1	Feynman Rules	57
A.2	Renormalization scheme	60
B	One-loop integrals	61
B.1	Passarino-Veltman tensor integral decomposition	61
B.2	One-loop scalar integrals	62
C	Feynman diagrams and analytical results	67
C.1	High energy expansion	67
C.2	Feynman diagrams	69

Chapter 1

Introduction

Massive gauge theories are an essential topic in Quantum Field Theory, on which we base our theoretical comprehension of Electroweak interactions. This comprehension is concretely embodied in the Standard Model (SM) theory, which recently received a fundamental experimental confirmation with the discovery of the Higgs particle at the LHC. The SM, following the general scheme of massive gauge theories, is based on a local symmetry group $(SU(2)_L \times U(1)_Y)$, which gets spontaneously broken by the Vacuum Expectation Value (VEV) acquired by some scalar field (the Higgs doublet), which transforms in a non-trivial representation of the gauge group. The spontaneous symmetry breaking produces a mass m for some of the gauge fields, leading to a model with spin-one massive force carriers. In the SM those are the W^\pm and Z weak bosons, with $m \sim 100$ GeV.

The SM theory has been extensively probed experimentally in the $E \ll m$ and $E \simeq m$ energy range. The $E \gg m$ range is instead essentially unexplored, with the LHC having started probing TeV-scale Electroweak process only very recently and with low statistics. Progress in this direction will come from the continuation of the LHC experimental program, and from future colliders. These futures experimental prospects motivate theoretical studies on the behaviour of massive gauge theories at high energy, a topic which presents a number of delicate and interesting aspects, whose complete theoretical comprehension is still missing. This thesis deals with some of those aspects, with a twofold aim. First, we review the intricate literature on high energy massive gauge theories trying to clarify and to improve it in some aspects. Second, we concretely verify the general results for a specific process, which we study at the next to leading order in the loop expansion.

Concretely, two massive gauge theories high energy theorems have been considered: the Equivalence Theorem and the theory of Sudakov double logs of IR nature. The Equivalence Theorem is an extremely useful (and well-known) result, according to which scattering amplitudes involving 0-helicity massive vector bosons in the external legs can be equivalently computed at high energy, by replacing the gauge boson with the corresponding Goldstone boson. What is much less known is that the theorem can be generalized to an exact reformulation (at all orders in m/E) of the habitual amplitude calculation strategy. This is the so-called “Equivalent Gauge”, which we concretely apply at one loop, verifying its validity in a very non-trivial manner. The double logs of Sudakov type are another interesting aspects of massive gauge theories and there are several reasons why studying their effects on high energy processes. In the first place these corrections, of the form $\alpha \log^2(E^2/m^2)$ (where $\alpha = g^2/(4\pi)$ is the perturbative expansion parameter), are the largest corrections to Born amplitudes and are sizeable for TeV scale processes. Second, since they originate from the exchange of soft and collinear gauge bosons, these infrared corrections are somehow universal, depending only on the known “low energy” SM and not on the high energy dynamics which might contain new physics. Being able to deal with those effects within the SM will thus allow us to extract and isolate new physics effects at high energy. There are, moreover, remarkable and peculiar properties which concerns these double logs in the case of massive gauge theories, that make their treatment different from the QCD and QED ones. In particular, gauge bosons cannot become infinitely soft because of their finite mass, hence

any gauge boson emission is experimentally observable in line of principle. Correspondingly, also fully exclusive (i.e. without the emissions of additional particles) processes become observable in the case massive gauge theories. This does not bring a conceptual problem, since the infrared divergences in the loops are regulated by the finite gauge fields mass, but it poses a practical problem: at high energy terms like $\alpha \log^2(E^2/m^2)$ make perturbation theory breakdown and resummation mandatory. Suitable techniques, therefore, need to be developed. Another characteristic aspect concerns the fact that, in massive gauge theories, the gauge symmetry breakdown obliges us to consider processes that are not averaged over the “Electroweak” color of the initial states of the reaction. For instance at lepton colliders only electrons and positrons collide, while averaging over color would imply considering also neutrino-initiated process. As we will see, color averaging (guaranteed by the confinement hypothesis in QCD) is precisely what makes double logs coming from virtual emissions cancel against those coming from real emissions, in inclusive QCD observables. Therefore in the Electroweak SM it is impossible to define observables free of these large double logs so that dealing with them is of fundamental importance.

This thesis is organized as follows. In chapter 2, after a brief general review on massive gauge theories, we introduce, in section 2.3, the model we employ for the explicit calculations presented in this work. Then, in sect. 2.4, we present the Equivalence Theorem and the Equivalent Gauge. Chapter 3 deals with the resummation of double logs of Sudakov type. First, in sects. 3.1 and 3.2, we review the general method of the infrared evolution equation to take account double logs, coming from loop integration. Then, in section 3.3, we show that these approaches are also applicable in the case of massive gauge theories. In section 3.4.1 we extend our approach to include double logs coming from phase space integration of real soft gauge bosons, reproducing existing result with an original methodology. In chapter 4, we focus on a specific process and we perform the full Next to Leading Order (NLO) computation in order to compare it, at double log level, with the result predicted in the previous chapter. Finally, in sect. 4.4, we repeat the calculation within the formalism of the Equivalent Gauge and find perfect agreement. Ours is the first one-loop calculation to be performed in the Equivalent Gauge, and the first time that the validity of the approach has been verified at one loop level. Finally, in chapter 5, we report our conclusions.

Chapter 2

Massive gauge theories

2.1 Spontaneous symmetry breaking

This section provides a concise introduction to the concept of spontaneous symmetry breaking. We will first consider the case of a field theory with a global symmetry group, next we switch to the case of a local symmetry. The discussion is performed at classical level, quantization will be described in sect. 2.2.

2.1.1 Global symmetries

Let us consider, for definiteness, the specific model built of N real scalar fields $\phi^i(x)$, with Lagrangian

$$\mathcal{L} = \frac{1}{2} \partial_\mu \Phi^T \partial^\mu \Phi + \frac{1}{2} \mu^2 \Phi^T \Phi - \frac{\lambda}{4} (\Phi^T \Phi)^2, \quad (2.1)$$

where Φ^T is defined as the vector (ϕ_1, \dots, ϕ_N) and λ, μ are real and positive parameters. The Lagrangian of eq. (2.1) is manifestly invariant under the N -dimensional orthogonal group $O(N)$ as we can prove by acting on Φ as

$$\Phi \rightarrow R \Phi, \quad (2.2)$$

where R are representation of $O(N)$ group's element and obviously $R^T R = \mathbf{1}$.

The ground state corresponds to the configurations $\Phi_0^T \equiv (\phi_1^0, \dots, \phi_N^0)$ which minimize the potential energy and so it must be a solution of

$$\left. \frac{\partial V}{\partial \phi^i} \right|_{\Phi = \Phi_0} = \mu^2 \phi_0^i + \lambda \phi_0^i \Phi_0^T \Phi_0 = 0 \quad \implies \quad |\Phi_0^2| = v \equiv \sqrt{\frac{\mu^2}{\lambda}}, \quad (2.3)$$

where v is called vacuum expectation value (VEV) of ϕ . We can notice that the previous condition determines the length of the vector Φ_0 to be non vanishing. Hence the VEV points along a definite direction, breaking the continuous group of eq. (2.2). Let us choose the minimum

$$\Phi_0^T \equiv (0, \dots, v), \quad (2.4)$$

and define a new set of fields

$$\Phi^T(x) = (\pi^1(x), \dots, \pi^{N-1}(x), v + \sigma(x)) \equiv (\boldsymbol{\pi}^T, v + \sigma). \quad (2.5)$$

The Lagrangian becomes

$$\mathcal{L} = \frac{1}{2} \partial_\mu \boldsymbol{\pi}^T \partial^\mu \boldsymbol{\pi} + \frac{1}{2} (\partial_\mu \sigma)^2 - \frac{1}{2} (2\mu^2) \sigma^2 - \sqrt{\lambda} \mu \sigma^3 - \sqrt{\lambda} \mu \boldsymbol{\pi}^T \boldsymbol{\pi} \sigma - \frac{\lambda}{4} \sigma^4 - \frac{\lambda}{2} \boldsymbol{\pi}^T \boldsymbol{\pi} \sigma^2 - \frac{\lambda}{4} (\boldsymbol{\pi}^T \boldsymbol{\pi})^2. \quad (2.6)$$

As we can see, the σ field has mass, while the $N - 1$ “ π ” fields remain massless. At the same time we can note that the symmetry group, from $O(N)$ is broken to $O(N - 1)$, corresponding to rotation that leave the VEV in eq. (2.3) invariant.

This appearance of massless particles as a consequences of spontaneous symmetry breaking procedure is a general result known as the Goldstone theorem. We give a short proof of it below.

Let us consider a model with N real scalar fields Φ and a generic Lagrangian

$$\mathcal{L}(\Phi, \partial_\mu \Phi) \equiv \frac{1}{2} \partial_\mu \Phi^T \partial^\mu \Phi - V(\Phi) \quad (2.7)$$

Let Φ_0 be a constant field which minimize the potential $V(\Phi)$, so that

$$\left. \frac{\partial}{\partial \phi_i} V(\Phi) \right|_{\Phi=\Phi_0} = 0. \quad (2.8)$$

Since Φ_0 is a configuration of minimum, we can expand the potential $V(\Phi)$ around it, obtaining

$$V(\Phi) = V(\Phi_0) + \frac{1}{2} (\phi_i - \phi_{i,0}) (\phi_j - \phi_{j,0}) M_{ij}^2 + \dots, \quad (2.9)$$

where M_{ij}^2 is the symmetric matrix which give mass to particles

$$M_{ij}^2 \equiv \left. \frac{\partial^2 V(\Phi)}{\partial \phi_i \partial \phi_j} \right|_{\Phi=\Phi_0}, \quad (2.10)$$

and by definition it is not negative-defined. Now let us suppose the Lagrangian of eq. (2.7) to be invariant under a continuous transformation with the relative infinitesimal form

$$\Phi \rightarrow \Phi + \lambda \Delta(\Phi), \quad (2.11)$$

where $\Delta(\Phi)$ is some function of the field Φ and λ is an infinitesimal parameter. The invariance of the Lagrangian imply that

$$V(\Phi) = V(\Phi + \lambda \Delta(\Phi)), \quad (2.12)$$

and so

$$\Delta_i(\Phi) \frac{\partial}{\partial \phi_i} V(\Phi) = 0. \quad (2.13)$$

Differentiating the previous equation we get

$$\left(\frac{\partial \Delta_i}{\partial \phi_j} \right)_{\Phi_0} \left(\frac{\partial V}{\partial \phi_i} \right)_{\Phi_0} + \Delta_i(\Phi_0) M_{ij}^2 = 0. \quad (2.14)$$

The first term of the previous equation, vanish if Φ_0 is a minimum, therefore we have that the second term must be zero. This condition is exactly the Goldstone theorem: if the transformation leaves the vacuum unchanged, then $\Delta(\Phi_0) = 0$ and the eq. (2.14) is trivially satisfied. Otherwise, $\Delta_i(\Phi)$ is a null vector of M^2 , corresponding to a massless particle. The Goldstone theorem, therefore, can be stated: for each linear symmetry generator which is broken by the vacuum there exists a massless particle.

2.1.2 The Higgs mechanism

As a first example of a gauge theory with SSB, let us consider a complex scalar field ϕ , coupled to an electromagnetic (Abelian) field

$$\mathcal{L} = -\frac{1}{4} F^{\mu\nu} F_{\mu\nu} + |D_\mu \phi|^2 - V(\phi), \quad (2.15)$$

where $D_\mu = \partial_\mu + ieA_\mu$. This Lagrangian is invariant under a local $U(1)$ transformation

$$\phi(x) \rightarrow e^{i\lambda(x)}\phi(x), \quad A_\mu \rightarrow A_\mu - \frac{1}{e}\partial_\mu\lambda(x). \quad (2.16)$$

Let us choose, now, the potential

$$V(\phi) = -\mu^2|\phi|^2 + \frac{\lambda}{2}(|\phi|^2)^2. \quad (2.17)$$

Analogously to the case discussed before (of a global symmetry), when the field ϕ acquires a vacuum expectation value the $U(1)$ symmetry will be broken. The minimum of the potential occurs at

$$\langle\phi\rangle = v = \sqrt{\frac{\mu^2}{\lambda}}. \quad (2.18)$$

Expanding the Lagrangian around the vacuum state and decomposing ϕ as

$$\phi(x) = v + \frac{1}{\sqrt{2}}(h(x) + i\pi(x)), \quad (2.19)$$

the potential $V(\phi)$ becomes

$$V(\phi) = -\frac{1}{2\lambda}\mu^4 + \frac{1}{2}2\mu^2h^2 + \dots, \quad (2.20)$$

We can see, in light of the Goldstone theorem discussed before, that along with the broken generator of the symmetry group, a massless scalar field (a Goldstone boson) is present. If we look at the kinetic term, we find

$$|D_\mu\phi|^2 = \frac{1}{2}(\partial_\mu h)^2 + \frac{1}{2}(\partial_\mu\pi)^2 + \sqrt{2}e\phi_0 A_\mu\partial^\mu\pi + e^2\phi_0^2 A_\mu A^\mu + \dots, \quad (2.21)$$

which contains, on top of the ordinary kinematic terms, a kinetic mixing between the photon and the Goldstone and a photon mass term. We will see in the next section how to quantize this Lagrangian and to read out the physical spectrum of the theory. However we can already anticipate the result by noticing that by performing a gauge transformation, it is possible to set the Goldstone π to zero, going to the so called ‘‘Unitary gauge’’. In this gauge it is easy to read the particle content, which contain no massless Goldstone particle, a massive ‘‘Higgs’’ scalar h with mass $m_h = \sqrt{2}\mu$ and a massive ‘‘photon’’ with $m_A^2 = 2e^2v^2$ from the last term in the previous equation.

2.2 Non-Abelian gauge theories quantised

We now turn to non-Abelian gauge theories and their covariant quantization. We focus on the pure Yang-Mills theory, without additional particles, for most of the section. Extra matter (fermion, scalar) fields do not change the discussion in any way, hence they will be omitted until section 2.3, where additional scalar fields will be included.

The Yang-Mills Lagrangian reads

$$\mathcal{L}_{YM} = -\frac{1}{4}\int d^4x \sum_a F^{\mu\nu,a}F_{\mu\nu}^a, \quad (2.22)$$

where

$$F^{\mu\nu} \equiv F^{\mu\nu,a}T^a = \partial^\mu A^\nu - \partial^\nu A^\mu - i[A^\mu, A^\nu], \quad (2.23)$$

and

$$A_\mu(x) \equiv A_\mu^a T^a. \quad (2.24)$$

The T^a matrices are the Hermitian generators of the gauge group algebra and they obey to the commutation relation

$$[T^a, T^b] = i f^{abc} T^c .$$

The indexes run from 1 to the dimensionality of the group, corresponding to the existence, in eq. (2.24), of one A_μ^a gauge field for each generator. Under a gauge transformation $U(\Lambda) = \exp(i g \Lambda)$, with $\Lambda(x) = \Lambda^a(x) T^a$, the gauge field transforms as

$$A_\mu \rightarrow (A_\Lambda)_\mu = U A_\mu U^\dagger - i U (\partial_\mu U^\dagger) . \quad (2.25)$$

It is easy to check that the field strength in eq. (2.23) transforms as $F \rightarrow U F U^\dagger$, and therefore the Lagrangian in eq. (2.22) is invariant under gauge transformations.

The quantization of the theory is best illustrated in the path integral formalism. Physical quantities in gauge theories are gauge-invariant correlators of the form

$$\langle \mathcal{O}[A] \rangle = \frac{\int \mathcal{D}A \mathcal{O}[A] (i \int d^4x \mathcal{L}_{YM})}{\int \mathcal{D}A (i \int d^4x \mathcal{L}_{YM})} , \quad (2.26)$$

where $\mathcal{O}[A_\Lambda] = \mathcal{O}[A]$ However being the Lagrangian of eq. (2.22) invariant under the local transformation in eq. (2.25) there exist a direction in the field space where the integrand is constant, and the path integral in eq. (2.26) diverges. The Faddeev-Popov approach to the quantization of gauge theory allows to deal with this issue. We proceed by introducing a set of gauge fixing conditions of the form

$$f_a[A](x) = 0 . \quad (2.27)$$

This is obtained by multiplying the path integral of eq. (2.26) by the following identity,

$$1 = \int \prod_a d\Lambda^a(x) \delta(f_a[A_\Lambda](x) - \Omega^a(x)) \det \left[\frac{\delta f_a[A_\Lambda(x)]}{\delta \Lambda_b(y)} \right] , \quad (2.28)$$

where A_Λ is the gauge field A transformed by a parameters Λ , as in eq.(2.25), whose infinitesimal version is

$$(A_\Lambda)_\mu^a = A_\mu^a + \frac{1}{g} D_\mu \Lambda^a . \quad (2.29)$$

Here D_μ is the canonical covariant derivative, defined as

$$(D_\mu \Lambda)_a = \partial_\mu \Lambda_a + g f^{abc} A_\mu^b \Lambda_c . \quad (2.30)$$

We note that if the gauge fixing f_a is linear, then $\delta f_a(A_\Lambda)/\delta \Lambda$ is independent of Λ . The field $\Omega^a(x)$ in eq. (2.28) is an auxiliary field over which we will integrate over.

After some manipulation, by exploiting the gauge invariance of \mathcal{L}_{YM} and \mathcal{O} , it is possible to find that the functional integral in eq. (2.26) can be written as follows

$$\int \mathcal{D}A \mathcal{O}[A] e^{i \int d^4x \mathcal{L}_{YM}(x)} = \left(\int \mathcal{D}\Lambda \right) \int \mathcal{D}A \mathcal{O}[A] \delta(f^a[A] - \Omega^a) e^{i S[A]} \det \left[\frac{\delta f^a(A_\Lambda)}{\delta \Lambda^b} \right]_{\Lambda=0} . \quad (2.31)$$

The (infinite) volume of the local gauge group is now factorized and it drops out from eq. (2.26). The determinant on the RHS of the previous equation is the so-called Faddeev Popov determinant and it can be expressed as a functional integral over a new set of scalar anticommuting fields (the ghost and antighost fields) belonging to the adjoint representation, as

$$\det \left[\frac{\delta f_a[A_\Lambda]}{\delta \Lambda_b} \right]_{\Lambda=0} = \int \mathcal{D}\omega(x) \mathcal{D}\bar{\omega}(x) e^{i \int d^4x \mathcal{L}_{GH}} , \quad (2.32)$$

where

$$\mathcal{L}_{GH} = \int d^4x \bar{\omega}_a(x) \frac{\delta f_a(A_\Lambda(x))}{\delta \Lambda^b} \omega^b(x). \quad (2.33)$$

Finally, we notice that eq. (2.26) is by construction independent of $\Omega^a(x)$. Hence, up to an irrelevant multiplicative factor we can integrate over $\Omega^a(x)$, weighting the integrand with the Gaussian factor $\exp\left(-\frac{1}{2\xi} \sum_a (\Omega^a)^2\right)$.

In summary we conclude that the gauge invariant correlators of the original theory, such as in eq. (2.30), are equal to those computed with a new Lagrangian which can be written as

$$\mathcal{L}_F = \mathcal{L}_{YM} + \mathcal{L}_{GH} + \mathcal{L}_{GF}, \quad \mathcal{L}_{GF} = -\frac{1}{2\xi} (f^a)^2 \quad (2.34)$$

For instance the standard Lorentz gauge choice $F^a = \partial^\mu A_\mu^a$ gives

$$\mathcal{L}_{GH} = -\bar{\omega}^a \partial^\mu D_\mu \omega^a, \quad \mathcal{L}_{GF} = -\frac{1}{2\xi} (\partial_\mu A^{\mu a})^2. \quad (2.35)$$

It is convenient to further rewrite the theory by introducing the so-called Nakanishi Lautrup auxiliary field, with the Lagrangian defined as

$$\mathcal{L}_B = \frac{1}{2\xi} B^a B^a + B^a f^a(A). \quad (2.36)$$

This is trivially equivalent to eq. (2.34) because the B field, which has polynomial action, it can be easily integrate out. In summary our full Lagrangian is now

$$\mathcal{L}_{YM} = -\frac{1}{4} \int d^4x \sum_a [F^{a,\mu\nu} F_{a,\mu\nu}] + \frac{1}{2\xi} (B^a)^2 + B^a \partial^\mu A_\mu^a + \bar{\omega}^a (-\partial^\mu D_\mu) \omega^b. \quad (2.37)$$

A very important property of this Lagrangian is its invariance under a certain global symmetry, the so called BRST symmetry. Indeed, consider an infinitesimal anticommuting parameter ϵ and define the following variations.

$$\begin{aligned} \delta A_\mu^a &= \epsilon D_\mu^{ac} \omega^c & \delta \omega^c &= -\frac{1}{2} g \epsilon f^{abc} \omega^b \omega^c, \\ \delta \bar{\omega}^a &= \epsilon B^a, & \delta B^a &= 0. \end{aligned} \quad (2.38)$$

It is easy to check by direct computation that \mathcal{L} is invariant. Another important property of BRST transformation is that, they are “nilpotent”, i.e. it squares to zero. Namely, let $Q\phi$ be the BRST transformation for the field ϕ (in this case $\phi = \{A_\mu^a, \omega^a, \bar{\omega}^a, B^a\}$)

$$Q^2\phi = 0. \quad (2.39)$$

Now, consider the Hilbert space \mathcal{H} of our states. Since the operator Q is nilpotent and it commutes with the Hamiltonian of the theory (i.e. the BRST charge is conserved), then Q divides \mathcal{H} into three subspace. Let \mathcal{H}_1 be the subspace of the states with are not annihilated by Q . Let \mathcal{H}_2 be the subspace of the states of the form $|\phi_2\rangle = Q|\phi_1\rangle$ and finally \mathcal{H}_0 the space of the states $Q|\phi_0\rangle = 0$. \mathcal{H}_0 and \mathcal{H}_2 are the so-called spaces of close and exact states respectively. Without entering in details (see for instance Ref. [18]) it comes out that the physical Hilbert space is the cohomology of the operator Q , i.e. poorly speaking, the state which are close ma non exact under the BRST charge operator. So that, in particular, we have

$$Q|Phy\rangle = 0, \quad \text{but} \quad |Phy\rangle \neq Q|\phi\rangle, \quad (2.40)$$

where $|Phy\rangle$ is a generic physical state.

2.2.1 The R_ξ gauges

In order to illustrate the problem of massive gauge theories quantization in a simple context, let us discuss the Abelian gauge theory of eq. (2.15). By parametrizing the scalar field as in eq. (2.19), the Lagrangian reads

$$\mathcal{L} = -\frac{1}{4}(F_{\mu\nu})^2 + \frac{1}{2}(\partial_\mu h - eA_\mu\pi)^2 + \frac{1}{2}(\partial_\mu\pi + eA_\mu(v+h))^2 - V(\phi). \quad (2.41)$$

In spite of the spontaneous breaking the Lagrangian continues to be invariant under the local gauge group in eq. (2.16). When expressed in terms of the fields π and σ , the local symmetry, at infinitesimal level, acts as

$$h(x) \rightarrow h(x) - \lambda(x)\pi(x), \quad \pi(x) \rightarrow \pi(x) + \lambda(x) \left(\sqrt{2}v + h(x) \right). \quad (2.42)$$

In order to quantize the theory, therefore, we need to follow the method of Faddeev Popov described previously. A particularly convenient choice of the gauge fixing, in this case, is the so-called R_ξ functional

$$f[A] = \partial_\mu A^\mu - m_A \xi \pi. \quad (2.43)$$

With this choice, the ghost Lagrangian is

$$\mathcal{L}_{GH} = \partial^\mu \bar{\omega} \partial_\mu \omega - m_A^2 \xi \bar{\omega} \omega - \frac{m_A^2}{v} \xi \bar{\omega} \omega h, \quad (2.44)$$

and the gauge-fixing term is

$$\mathcal{L}_{GF} = -\frac{1}{2\xi} f[A]^2 = -\frac{1}{2\xi} (\partial_\mu A^\mu)^2 - \frac{1}{2} \xi m_A^2 \pi^2 + m_A \partial_\mu A^\mu \pi. \quad (2.45)$$

The great virtue of the R_ξ choice can be appreciated if we compute the quadratic Lagrangian for the gauge boson and the Goldstone fields. We obtain

$$\mathcal{L}_{quad} = -\frac{1}{2} \partial_\mu A_\nu \partial_\nu A_\mu + \frac{1}{2} \left(1 - \frac{1}{\xi} \right) (\partial_\mu A^\mu)^2 + \frac{1}{2} m_A^2 (A^\mu)^2 + \frac{1}{2} (\partial_\mu \pi)^2 - \frac{1}{2} \xi m_A^2 \pi^2, \quad (2.46)$$

where $m_A = ev$ and the original A - π kinetic mixing from the gauge fixing cancels the one that was present in the original Lagrangian. This makes particularly easy to read out the particles content of the theory. Therefore, the single-particle states are given by one spin one gauge bosons $|A_\lambda\rangle$ (where h is the helicity) with mass m_A , two massive scalars $|h\rangle$ and $|\pi\rangle$ with masses squared m_h^2 and ξm_A^2 , and the ghost/ antighost $|\omega\rangle/ |\bar{\omega}\rangle$. Furthermore, the spectrum contains a scalar particle with zero ghost number which correspond to the scalar polarization of the A field. It can be found that the BRST cohomology is composed of only the Higgs $|h\rangle$ and the triplet $|A_\lambda\rangle$.

2.3 The Higgs-Kibble model

The model we will employ in this thesis to illustrate and to verify the high-energy properties of massive gauge theories is the so-called $SU(2)$ Higgs-Kibble model, extended to include a massive scalar field which is a singlet of the $SU(2)$ gauge group. This scalar has no influence in the discussions of this chapter but it will be used later on in chapter 4 for an explicit calculations. The Higgs-Kibble model is essentially the Standard Model without fermions and $U(1)_Y$ hypercharge. Namely it is an $SU(2)$ gauge theory with one scalar Higgs doublet which takes a VEV, breaking completely the gauge group. Following the convention of Ref. [28], the Lagrangian is

$$\mathcal{L}_{HK} \equiv -\frac{1}{2} \text{Tr} [W_{\mu\nu} W^{\mu\nu}] + \text{Tr} \left[(D_\mu \mathcal{H})^\dagger D^\mu \mathcal{H} \right] - \frac{\lambda}{4} \left\{ \text{Tr} [\mathcal{H}^\dagger \mathcal{H}] - \frac{\tilde{v}^2}{2} \right\}^2 \quad (2.47)$$

where the fields are defined as

$$\mathcal{H} \equiv \frac{v+h}{2} \mathbb{1}_2 + \frac{i}{2} \sigma^a \pi_a \qquad W^\mu \equiv \frac{1}{2} \sigma^a W_a^\mu \quad (2.48)$$

in term of the three Pauli matrices σ^a . The ordinary Higgs doublet field has been represented, here, as a pseudo-real matrix \mathcal{H} , because this makes more evident the invariance of the theory under the custodial group described below. The canonical representation of \mathcal{H} as a doublet is

$$\mathcal{H} = \frac{1}{2} \begin{pmatrix} h + i\pi_3 + v & i\pi_1 + \pi_2 \\ i\pi_1 - \pi_2 & h - i\pi_3 + v \end{pmatrix} \equiv \frac{1}{\sqrt{2}} \begin{pmatrix} h_1 & -h_2^\dagger \\ h_2 & h_1^\dagger \end{pmatrix}. \quad (2.49)$$

The Higgs matrix decomposes in four real scalar fields, the physical Higgs h and the three Goldstone bosons π_a . For the sake of completeness, we report also the definition of the field strength $W^{\mu\nu}$ of the gauge connection W^μ and of the covariant derivative of the Higgs \mathcal{H}

$$W_{\mu\nu} \equiv \partial_\mu W_\nu - \partial_\nu W_\mu - ig[W_\mu, W_\nu], \qquad D_\mu \mathcal{H} \equiv \partial_\mu \mathcal{H} - igW_\mu \mathcal{H}. \quad (2.50)$$

In order to include the heavy scalar S in our model, we add to the Lagrangian

$$\mathcal{L}_s = \frac{1}{2} \partial_\mu S \partial^\mu S - \frac{1}{2} m_s^2 S^2 - \frac{1}{2} \lambda_s Tr[\mathcal{H}^\dagger \mathcal{H}] S^2 - \frac{\lambda}{4!} S^4.$$

The scalar S is coupled only to the Higgs doublet \mathcal{H} , its interaction vertexes are displayed in fig. (2.2).

On top of the $SU(2)$ gauge symmetry, the Lagrangian $\mathcal{L}_0 \equiv \mathcal{L}_{HK} + \mathcal{L}_S$ is also invariant under the custodial group $SO(3)_c$ and this is manifest by the matrix representation of the fields. In particular, the gauge group and the custodial group transformations are, respectively

$$\begin{aligned} \mathcal{H}(x) &\longrightarrow \Omega(x) \mathcal{H}(x), & \mathcal{H} &\longrightarrow \gamma \mathcal{H} \gamma^\dagger, \\ W_\mu &\longrightarrow \gamma W_\mu \gamma^\dagger, \end{aligned}$$

Unlike the gauge group, the custodial one is not broken by the Higgs VEV and we will be careful to preserve this symmetry when fixing the gauge, since we are going to make use of this symmetry later on. Following the Fadeev-Popov method, described in the previous section, we introduce the ghost and anti-ghost custodial triplets (ω_a and $\bar{\omega}_a$) and the canonical t'Hooft Feynman R_ξ gauge-fixing functional

$$f_a \equiv \partial_\mu W_a^\mu + \tilde{m} \xi \pi_a$$

For the moment we do not specify the gauge fixing parameters, otherwise, later on we will work in the specific gauge $\xi = 1$ and $\tilde{m} = m_W$. In order to obtain the ghost Lagrangian \mathcal{L}_{gh} , we take the gauge variation of f_a as in eq. (2.33), with respect to gauge parameter ω_a , obtaining

$$\mathcal{L}_{GH} \equiv -\bar{\omega}_a \delta_{\omega_a} f_a = -\bar{\omega}_a \partial_\mu (\partial^\mu \omega^a + g \epsilon^{abc} W_b^\mu \omega_c) - \frac{1}{2} g \tilde{m} \xi \bar{\omega}_a [(v+h)\omega^a + \epsilon^{abc} \pi_b \omega_c]. \quad (2.51)$$

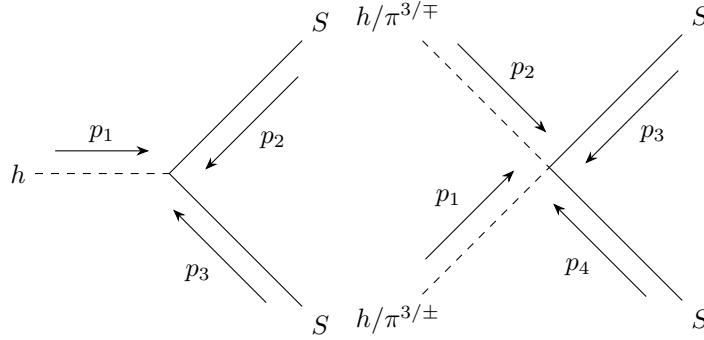
In order to make the BRST symmetry manifest, we also introduce the so-called Nakanishi-Lautrup auxiliar fields B^a and so our full Lagrangian becomes

$$\mathcal{L} = \mathcal{L}_0 + \frac{\xi}{2} B^a B_a + B^a f_a + \mathcal{L}_{gh} \quad (2.52)$$

The Lagrangian (2.52) is invariant by the BRST variation $s(\Phi)$ of Table 2.1.

Figure 2.1: BRST transformation for the Higgs-Kibble model

$$\begin{aligned}
s(W_\mu^a) &= [iQ, W_\mu^a] = \partial_\mu \omega^a + g\epsilon^{abc}W_{\mu,b}\omega_c \\
s(\pi^a) &= [iQ, \pi^a] = \frac{g}{2}(v+h)\omega^a + \frac{g}{2}\epsilon^{abc}\pi_b\omega_c \\
s(h) &= [iQ, h] = -\frac{g}{2}\omega_a\pi^a \\
s(B^a) &= [iQ, B^a] = 0 \\
s(\bar{\omega}_a) &= \{\bar{\omega}_a\} = B_a \\
s(\omega_a) &= \{iQ, \omega_a\} = -\frac{1}{2}g\epsilon_{abc}\omega^b\omega^c
\end{aligned}$$

Figure 2.2: Feynman rules for the heavy scalar S 

2.4 The Equivalent Gauge

The Equivalent Gauge is a generalization of the Equivalence Theorem, which we present following Ref [29]. First of all, let us start by defining the propagators among bare field, as

$$iG_{\bar{I}J}(p) = \int d^4x e^{ipx} \langle \Phi_{\bar{I}}(x) \Phi_J^\dagger(0) \rangle,$$

where $\Phi = \{W, \pi, h, \omega, \bar{\omega}, S\}$ denotes the whole set of bare fields of the theory. The inverse of G can be expressed as the sum of bare Feynman propagator Δ and of 1PI vacuum polarization amplitude Π

$$G^{-1} = \Delta^{-1} + \Pi.$$

Thanks to the symmetries of the Lagrangian it is possible to parametrize G^{-1} in terms of few scalar form factors (as done in [28]). The result is trivial for the propagators of the Higgs $h(G_h^{-1})$, of the scalar $S(G_S^{-1})$ and for the one of the ghost fermions G_F^{-1}

$$\begin{aligned}
G_{h/S}^{-1}(p^2) &= p^2 - M_{h/S}^2 + \Pi_{h/S}(p^2), \\
(G_F^{-1}(p^2))_b^a &= \delta_b^a \begin{pmatrix} \omega & \bar{\omega} \\ \tilde{m}^2 \xi - p^2 + \Pi_{\omega\bar{\omega}}(p^2) & 0 \end{pmatrix} \begin{pmatrix} \omega \\ \bar{\omega} \end{pmatrix}.
\end{aligned}$$

Notice that the ghost propagator is proportional to δ^{ab} because of custodial symmetry.

The result is less straightforward for the propagators of the remaining bosonic particles (π, W) (we will call it G_B). Omitting the custodial group indexes, since the propagators are diagonal in them, we have

$$G_B^{-1} = \mathcal{P}_\perp A(p^2) + \mathcal{P}^i V_i^j \mathcal{P}_j^\dagger, \quad (2.53)$$

where

$$\mathcal{P}_\perp = \begin{pmatrix} \eta_{\mu\nu} - \frac{p_\mu p_\nu}{p^2} & 0 \\ 0 & 0 \end{pmatrix}, \quad \mathcal{P}_1 = \begin{pmatrix} -i\frac{p_\mu}{p} \\ 0 \end{pmatrix}, \quad \mathcal{P}_2 = \begin{pmatrix} 0 \\ 1 \end{pmatrix}, \quad (2.54)$$

and

$$A(p^2) = \begin{pmatrix} W & \pi \\ m^2 - p^2 + \Pi_{WW}^T & 0 \\ 0 & 0 \end{pmatrix} \begin{matrix} W \\ \pi \end{matrix}, \quad (2.55)$$

$$V(p^2) = \begin{pmatrix} W & \pi \\ B(p^2) - \frac{p^2}{\xi} & p(C(p^2) - \tilde{m}) \\ p(C(p^2) - \tilde{m}) & p^2 F(p^2) - \xi \tilde{m}^2 \end{pmatrix} \begin{matrix} W \\ \pi \end{matrix}, \quad (2.56)$$

with

$$B(p^2) = m^2 + \Pi_{WW}^L(p^2), \quad C(p^2) = m + \Pi_{W\pi}(p^2), \quad p^2 F(p^2) = p^2 + \Pi_{\pi\pi}(p^2). \quad (2.57)$$

The three form factors F , B and C are not independent as it is simple to prove thanks to one the Slavnov-Taylor's identity derived in Ref. [28]. Namely

$$\langle f_a(x) f_b(y) \rangle = -i\xi \delta_{ab} \delta^4(x-y) \Rightarrow B(p^2)F(p^2) = C^2(p^2).$$

We can thus express the propagators G_B as

$$\begin{aligned} G_{\mu\nu}^{WW}(p) &= \frac{-i \left(\eta_{\mu\nu} - \frac{p_\mu p_\nu}{p^2} \right)}{A(p^2)} + i \frac{p_\mu p_\nu \xi F (\tilde{m}^2 \xi - F p^2)}{p^2 (F p^2 - C \tilde{m} \xi)^2}, \\ G_\mu^{W\pi}(p) &= -p_\mu \frac{\xi F (C - \tilde{m})}{(F p^2 - C \tilde{m} \xi)^2}, \\ G_\mu^{\pi W}(p) &= p_\mu \frac{\xi F (C - \tilde{m})}{(F p^2 - C \tilde{m} \xi)^2}, \\ G^{\pi\pi}(p) &= i \frac{F p^2 - \xi C^2}{(F p^2 - C \tilde{m} \xi)^2}. \end{aligned} \quad (2.58)$$

In order to introduce the Equivalent Gauge slightly more general identities are needed, proven in full generality in refs. [15, 16, 29]. We present here a partial derivation, by noticing that, since the physical states of the theory are in the cohomology of the BRS operator, we have

$$\langle Phy | \left\{ iQ, \omega_a(\bar{x}) \right\} | Phy' \rangle = \langle Phy | f_a(x) | Phy' \rangle = 0, \quad (2.59)$$

where we made use of the BRS transformation in table 2.1. Going to momentum space, we find

$$-i p_\mu \langle Phy | W^\mu(p) | Phy' \rangle + \tilde{m} \xi \langle Phy | \pi(p) | Phy' \rangle = 0. \quad (2.60)$$

If we express the matrix element in terms of amputated amplitude

$$\begin{aligned} \langle Phy | W^\mu(p) | Phy' \rangle &= G_{\mu\nu}^{WW}(p) \mathcal{A}[W^\nu(p)] + G_\mu^{W\pi}(p) \mathcal{A}[\pi(p)], \\ \langle Phy | \pi(p) | Phy' \rangle &= G^{\pi\pi}(p) \mathcal{A}[\pi(p)] + G_\mu^{\pi W}(p) \mathcal{A}[W^\mu(p)], \end{aligned}$$

and we use eq. (2.58), we obtain

$$-F \xi p_\nu \mathcal{A}[W^\nu(p)] + i C \xi \mathcal{A}[\pi(p)] = 0,$$

which finally gives us

$$p_\nu \mathcal{A}[W^\nu(p)] = i \frac{C(p^2)}{F(p^2)} \mathcal{A}[\pi(p)] = i \frac{B(p^2)}{C(p^2)} \mathcal{A}[\pi(p)] = i \frac{m^2 + \Pi_{WW}^L(p^2)}{m + \Pi_{W\pi}(p^2)} \mathcal{A}[\pi(p)]. \quad (2.61)$$

Let us consider a generic process with longitudinally-polarized (zero helicity) external bosons. The amplitudes reads

$$\mathcal{M} = \sqrt{Z_W} \epsilon_0^\mu(\mathbf{p}) \mathcal{A}[W_\mu(p)], \quad (2.62)$$

where Z_W is the residue at pole of the transverse W propagator, and

$$\epsilon_0^\mu(\mathbf{p}) = \frac{1}{m_W} \left\{ |\mathbf{p}|, \frac{E_{\mathbf{p}}}{|\mathbf{p}|} \mathbf{p} \right\}. \quad (2.63)$$

By noticing that $\epsilon_0 \sim p/m_W$ for $E_{\mathbf{p}} \gg m_W$, we immediately realize that it is convenient to use eq. (2.58) in order to rewrite the amplitude as

$$\sqrt{Z_W} \left(\epsilon_0^\mu(\mathbf{p}) - \frac{p^\mu}{m_W} + \frac{p^\mu}{m_W} \right) \mathcal{A}[W_\mu(p)] = \sqrt{Z_W} (\epsilon_L^\mu \mathcal{A}[W_\mu(p)] + \epsilon_\pi \mathcal{A}[\pi(p)]) \quad (2.64)$$

where

$$\epsilon_\pi = -i \frac{B(m_W^2)}{m_W C(m_W^2)} \quad \text{and} \quad \epsilon_L^\mu \equiv \epsilon_0^\mu - \frac{p^\mu}{m_W} = \frac{-m_W}{E_{\mathbf{p}} + |\mathbf{p}|} \left\{ 1, -\frac{\mathbf{p}}{|\mathbf{p}|} \right\}. \quad (2.65)$$

The result is that we can change the Feynman rule for an external longitudinal gauge bosons as follows

$$\epsilon_0^\mu \rightsquigarrow \bullet \longrightarrow \epsilon_L^\mu \rightsquigarrow \bullet + \epsilon_\pi \text{---} \bullet, \quad (2.66)$$

obtaining an exactly identical amplitude. This reformulation of the theory, dubbed ‘‘Equivalent Gauge’’ in Ref. [28], has an obvious advantage in the high energy regime. Namely, it makes use of polarization vector ϵ_L which does not grow with the energy. Therefore naive power-counting [28] straightforwardly holds at the level of individual Feynman diagrams. Indeed ϵ_L^μ not only doesn’t grow with the energy, but it decreases as $\epsilon_L^\mu \sim m_W/E$. At the leading order to the $\frac{m_W}{E}$ expansion, we can thus neglect the gauge diagrams and substitute the external longitudinal vectors with the Goldstones, as dictated by the ordinary Equivalence Theorem. Higher orders in m_W/E can be systematically included. It should be noted that the one above is only a partial derivation of the result of refs. [15, 16, 29]. We, indeed, established it only for a single longitudinal boson, while it hold for an arbitrary number of external longitudinal particles. We will not give the complete proof here, but we will verify the result explicitly, at one-loop order, for a process where two longitudinal bosons are involved.

Chapter 3

Soft-Collinear double-logs

The largest corrections to Born amplitudes at high energy are double logarithmic contributions of the form $\left(\alpha \log^2\left(\frac{E^2}{m^2}\right)\right)^n$, with m being some characteristic mass scale of the theory and $E \gg m$ the typical energy of the reaction [23]. Such corrections originate from soft and collinear gauge bosons coupled to external particle. They are also called mass singularities¹, since in massless gauge theories such as QED and QCD soft and collinear emissions formally produce infinities. Clearly, those infinities are unphysical and they cancel in physically observable cross-sections. The point is that infinitely soft photons or gluons unavoidably escape detection, hence the only final states which is worth considering are the “inclusive” ones, that allow for extra soft particles emissions. These extra “real” emissions are also singular, when integrated over the soft-collinear region of the emission phase-space, and their divergence cancels exactly the virtual singularities that are present in the loop corrections to the scattering amplitudes [3, 17, 20].

The situation is slightly different for massive gauge theories such as the SM. First of all, fully exclusive final states, with no extra soft emissions, become observables. This does not bring a conceptual problem because the divergences are regulated by the finite mass of the gauge fields such that all cross-section, including the fully exclusive ones, are now calculable in line of principle. In practice it does pose a problem, in that those calculations cannot be carried on at fixed order in perturbation theory for large E , where $\alpha \log^2 \frac{E^2}{m^2} > 1$. Resummation techniques have to be developed, as discussed below in this chapter. The second important aspect is that in massive gauge theories, we cannot, unlike in QED and QCD, define “sufficiently inclusive” cross-sections such as to cancel the double log enhancement of the radiative corrections. Therefore, we cannot define observables that can be reliably computed at a fixed order in perturbation theory. Double logs resummation is thus important at order one in any massive theory reaction, including fully inclusive processes [7]. This surprising result, namely the fact that double logs do not cancel not even in inclusive cross-sections, is due to the fact (see [6]) that the initial states of the scattering are not averaged under the massive gauge theory (EW) color. This is possible only because the gauge symmetry, unlike in QED and QCD, is spontaneously broken.

The previous discussion shows that IR effects, and double logs in particular, are extremely important in massive gauge theories. In the rest of this chapter we will review the treatment of those effects. In section 3.1 we present the original Sudakov form factor calculation for QED [24] in a form which is suited to be generalized to non-Abelian gauge theories. Then we turn to the non-Abelian case showing how to compute exclusive and inclusive cross-section, respectively in sect. 3.2 and sect. 3.4. Finally, in section 3.3, we show how to generalize this results to the case of massive gauge theories.

¹To be more precise this definition refers also to single log, we are not going to investigate.

3.1 Sudakov form factor in QED

Let us consider the high energy behaviour for an electron elastic scattering from an external field, at a fixed angle i.e. $t \equiv -2p_1 \cdot p_2 \equiv -E^2$, for $E \gg m_e, m_e$ being the electron mass. It is possible to identify the diagrams giving rise to leading virtual double logs as the ones in which a soft and almost collinear photon is exchanged between the two on-shell fermions. In particular, let us consider the first-order correction (in $\alpha = e^2/(4\pi)$) to the tree-level amplitude $\mathcal{M}_B = i\bar{u}(p_2)\gamma^\mu u(p_1)A_\mu^{ext}$, described by the following diagram

$$\mathcal{M}_{1L} = \text{diagram} = i\bar{u}(p_2)\Gamma_{1L}^\mu u(p_1)A_\mu^{ext},$$

where A^{ext} is the external field and

$$\Gamma_{1L}^\mu = -\frac{ie^2}{(2\pi)^4} \int d^4k \frac{\gamma^\nu (\not{p}_2 + \not{k} + m_e) \gamma^\mu (\not{p}_1 - \not{k} + m_e) \gamma_\nu}{((p_2 + k)^2 - m_e^2 + i\epsilon)((p_1 - k)^2 - m_e^2 + i\epsilon)(k^2 + i\epsilon)}. \quad (3.1)$$

The important region of the integration is the one in which k is soft and almost collinear to p_1 and p_2 , therefore in eq. (3.1) we can neglect factors \not{k} in the numerator and k^2 in the denominator. Using the Dirac equation $(\not{p} - m_e)u(p) = 0$, we get

$$\Gamma_{1L}^\mu \simeq -2i \frac{e^2}{(2\pi)^4} E^2 \gamma^\mu I \quad (3.2)$$

where we have defined

$$I \equiv \int \frac{d^4k}{(2k \cdot p_1 + i\epsilon)(2k \cdot p_2 + i\epsilon)(k^2 + i\epsilon)}. \quad (3.3)$$

In order to deal with this integral, it is convenient to switch to the so-called Sudakov parametrization

$$k = up_1 + vp_2 + k_\perp, \quad (3.4)$$

where k_\perp is a four-vector orthogonal to p_1 and p_2 . Without loosing of generality, we can turn into a coordinate system in which p_1, p_2 plane correspond to t, z and k_\perp to y, z coordinates. Therefore, k_\perp is purely space-like and we get $\mathbf{k}_\perp^2 \equiv -k_\perp^2$. In these coordinates the soft and collinear region is

$$\mathbf{k}_\perp^2 \ll \min\{|Eu|, |Ev|\}, \quad |u|, |v| \ll 1. \quad (3.5)$$

In this region we have

$$2k \cdot p_1 = 2um_e^2 + E^2v, \quad 2k \cdot p_2 = 2vm_e^2 + E^2u, \quad (3.6)$$

$$k^2 = um_e^2 + vm_e^2 + E^2uv + k_\perp^2 \sim E^2uv - \mathbf{k}_\perp^2. \quad (3.7)$$

Furthermore, switching to polar coordinates in the k_\perp plane, we have

$$d^4k = \frac{E^2}{4} d\theta d\mathbf{k}_\perp^2 dudv = \frac{E^2\pi}{2} d\mathbf{k}_\perp^2 dudv. \quad (3.8)$$

Notice that the integral I is manifestly IR divergent. We thus introduce an infrared cut-off² μ on the modulo of the transverse momentum, i.e. we perform the integration only in the region $\mathbf{k}_\perp^2 \geq \mu^2$. With this cut-off the integral reads

$$\begin{aligned} I(\mu^2) &= \int \frac{d^4 k}{(2k \cdot p_1 + i\epsilon)(2k \cdot p_2 + i\epsilon)(k^2 + i\epsilon)} \theta(\mathbf{k}_\perp^2 - \mu^2) \\ &= \pi \frac{E^2}{2} \int \frac{d\mathbf{k}_\perp^2 dudv}{(2um_e^2 + vE^2 + i\epsilon)(2vm_e^2 + uE^2 + i\epsilon)(+E^2uv - \mathbf{k}_\perp^2 + i\epsilon)} \theta(\mathbf{k}_\perp^2 - \mu^2). \end{aligned} \quad (3.9)$$

We can use the relation

$$\frac{i}{E^2uv - \mathbf{k}_\perp^2 + i\epsilon} = \mathcal{P} \frac{i}{E^2uv - \mathbf{k}_\perp^2} + \pi \delta(E^2uv - \mathbf{k}_\perp^2), \quad (3.10)$$

and retain only the δ -function, which restrict the integral near the mass-shell of the photon selecting, in such a way, the region of integration giving the biggest contribution. We obtain

$$I(\mu^2) \simeq -i\pi^2 E^2 \int_0^1 du \int_0^1 \frac{dv}{(2um_e^2 + vE^2)(2vm_e^2 + uE^2)} \theta\left(uv - \frac{\mu^2}{E^2}\right), \quad (3.11)$$

where we used the constraint $uv > 0$ implied by the δ -function, together with the fact that the integral is even under $(u, v) \rightarrow -(u, v)$, to write I as twice the integral for $u, v \geq 0$. It should be noticed that the upper bound on the u, v variables is arbitrary at this point, since we already made approximations in the integral which rely on $|u|, |v| \ll 1$ as in eq. (3.5). The choice of the upper bound is irrelevant since the region $u, v \sim 0$ gives the dominant (double log-enhanced) contribution to the integral.

In order to perform the integration, we switch to a new coordinate system $\{u, v\} \rightarrow \{\tau, \lambda\}$ such that

$$u = e^\lambda \sqrt{\tau}, \quad 0 \leq \tau \leq 1, \quad (3.12)$$

$$v = e^{-\lambda} \sqrt{\tau}, \quad \frac{1}{2} \log \tau \leq \lambda \leq -\frac{1}{2} \log \tau. \quad (3.13)$$

Therefore I becomes

$$\begin{aligned} I &\simeq -iE^2 \pi^2 \int_0^1 d\tau \int_{+\frac{1}{2} \log \tau}^{-\frac{1}{2} \log \tau} dy \frac{1}{4m_e^4 + E^4 + 4m_e^2 E^2 \cosh(2y)} \theta\left(\tau - \frac{\mu^2}{E^2}\right) \\ &= -\frac{i\pi^2}{E^2} \int_{\frac{\mu^2}{E^2}}^1 d\tau \operatorname{arctanh} \left(\frac{2m_e^2 - E^2}{E^2 + 2m_e^2} \tanh(y) \right) \Bigg|_{y=+\frac{1}{2} \log \tau}^{y=-\frac{1}{2} \log \tau}. \end{aligned} \quad (3.14)$$

After some algebra

$$I \simeq -\frac{i\pi^2}{E^2} \int_{\frac{\mu^2}{E^2}}^1 \frac{d\tau}{\tau} \log \left(\frac{2m_e^2 + E^2 \tau}{E^2 + 2m_e^2 \tau} \right). \quad (3.15)$$

The integral above can be performed in terms of dilog functions. Simple approximations, depending on the relative magnitude of μ^2 and m_e^2 , are

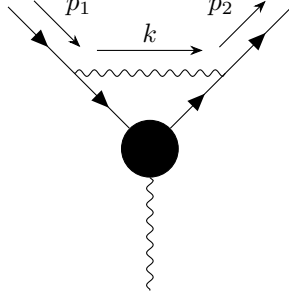
$$I \simeq \frac{i\pi^2}{E^2} R \left[\frac{E^2}{m_e^2}, \frac{m_e^2}{\mu^2} \right], \quad (3.16)$$

where we have defined

$$R \left[\frac{E^2}{m_e^2}, \frac{m_e^2}{\mu^2} \right] \equiv \begin{cases} \frac{1}{2} \log^2 \frac{E^2}{m_e^2} + \log \frac{E^2}{m_e^2} \log \frac{m_e^2}{\mu^2} & \text{for } \mu^2 \ll m_e^2 \ll E^2 \\ \frac{1}{2} \log^2 \frac{E^2}{\mu^2} & \text{for } m_e^2 \ll \mu^2 \ll E^2 \end{cases} \quad (3.17)$$

²An alternative approach would be to introduce a fictitious photon mass.

Figure 3.1: Diagram giving rise to double-logs loop correction to the electron elastic scattering process



Coming back to eq. (3.1), we have obtained that the first double log correction to the Born amplitude \mathcal{M}_B factorizes as

$$\mathcal{M}_{1L}|_{DL} = \mathcal{M}_B \times \left(-\frac{\alpha}{2\pi} R \left[\frac{E^2}{m_e^2}, \frac{m_e^2}{\mu^2} \right] \right), \quad (3.18)$$

where R was computed (see eq. (3.18)) in both regimes $\mu^2 \ll m_e^2$ and $\mu^2 \gg m_e^2$. For the generalization to non Abelian gauge theories and to the SM, $\mu^2 \gg m_e^2$ is the regime of interest. We will thus focus on the latter in what follows.

The one loop correction in eq. (3.18) diverges when the unphysical regularization parameter μ is taken to vanish. This signals the breakdown of perturbation theory and the need of all order resummation. With this purpose, we follow the scheme of the infrared evolution equation described in Ref. [12]. Let $\mathcal{M}(\mu^2)$ be the amplitude for our process at all orders in perturbation theory and with a cut-off μ on the transverse momentum of all the virtual photons running in the loops. Now, let us imagine starting from an amplitude with a cut off μ^2 and to try to compute the one with a slightly larger cut-off squared $\mu^2 + \delta\mu^2$, where $\delta\mu^2 > 0$ is an infinitesimal variation. We have,

$$\mathcal{M}(\mu^2) - \mathcal{M}(\mu^2 + \delta\mu^2) = -\delta\mu^2 \frac{\partial \mathcal{M}(\mu^2)}{\partial \mu^2}. \quad (3.19)$$

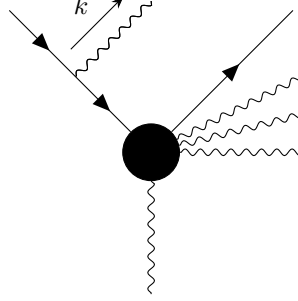
The differences between $\mathcal{M}(\mu^2)$ and $\mathcal{M}(\mu^2 + \delta\mu^2)$ is given by the loop integrals performed in the narrow region $\mathbf{k}_\perp^2 \in [\mu^2, \mu^2 + \delta\mu^2]$, where \mathbf{k}_\perp is the modulo of the virtual photons transverse momenta. At the linear order in $\delta\mu^2$, this integral is the sum of the integrals over the strips for each loop momentum. Among those, it is not hard to see that the dominant contribution comes from virtual photons exchanged from two external lines, as in fig. 3.1 The intuitive reason why this happens is that three propagators go on shell (the two fermionic plus the photon one) when the virtual photon momentum goes to zero. Hence the IR enhancement is expected to be more significant than for the other diagrams where a smaller number of propagators go on-shell. The dominance of this kind of diagrams was rigorously established in Ref. [17].

Therefore, we have

$$\begin{aligned} -\delta\mu^2 \frac{\delta \mathcal{M}(\mu^2)}{\delta \mu^2} &\simeq -i \frac{e^2}{(2\pi)^4} \int_{\mathbf{k}_\perp \in [\mu^2, \mu^2 + \delta\mu^2]} \frac{d^4 k}{(2k \cdot p_1 + i\epsilon)(2k \cdot p_2 + i\epsilon)(k^2 + i\epsilon)} \mathcal{M}(\mu^2) \\ &\simeq \delta\mu^2 \frac{\alpha}{2\pi} \frac{\partial R \left[\frac{s}{m^2}, \frac{m^2}{\mu^2} \right]}{\partial \mu^2} \mathcal{M}(\mu^2), \end{aligned} \quad (3.20)$$

where we exploited the previous calculation of $I(\mu^2)$ in eq. (3.16). From eq. (3.20) it follows

Figure 3.2: Real emissions giving rise to double log correction to the e^- elastic scattering cross section



the infrared evolution equation

$$\frac{\partial \mathcal{M}(\mu^2)}{\partial \log(\mu^2)} = K(\mu^2) \mathcal{M}(\mu^2) \quad \text{where} \quad K(\mu^2) = -\frac{\alpha}{2\pi} \frac{\partial R \left[\frac{s}{m^2}, \frac{m^2}{\mu^2} \right]}{\partial \log(\mu^2)}. \quad (3.21)$$

We can solve the evolution equation above, provided a suitable boundary condition is given. This is identified by noticing that if μ^2 was of order E^2 , no log enhancement would be encountered and the process would be calculable in perturbation theory. In particular the Born amplitude would be a valid approximation, so that we could employ the boundary condition $\mathcal{M}(\mu^2 = E^2) = \mathcal{M}_B$. Solving eq. (3.21) we obtain the resummed expression

$$\mathcal{M} = \mathcal{M}_B \exp \left(-\frac{\alpha}{2\pi} R \left[\frac{s}{m^2}, \frac{m^2}{\mu^2} \right] \right). \quad (3.22)$$

To conclude our discussion on the QED Sudakov form factor we need to include the emission of an arbitrary number of soft-photons, below a given threshold. This is essential in order to obtain a physically observable process, because soft photons cannot be detected, as previously argued. In particular we allow the radiation of an arbitrary number of real photons with transverse momentum³ $\mathbf{k}_\perp^2 < E'^2$. The real emission cross-section diverges in the region $\mathbf{k}_\perp \rightarrow 0$ of the phase space integral and so we regularize this divergence with the lower cutoff $\mathbf{k}_\perp^2 > \mu^2$. The same cutoff is also employed to regularize the loop integrals as in the previous calculation.

We are, thus, looking for inclusive cross-section $\sigma(E'^2; \mu^2)$ and in order to find it we need an infrared evolution equation for real emissions (similar to eq. (3.21) for virtual emissions). We suppose, therefore, to increase the threshold E' by an infinitesimal quantities $E'^2 \rightarrow E'^2 + \delta E'^2$, consequently we have that

$$\sigma(E'^2 + \delta E'^2, \mu^2) - \sigma(E'^2, \mu^2) = \delta E'^2 \frac{\partial \sigma(E'^2, \mu^2)}{\partial E'^2}. \quad (3.23)$$

The differences between $\sigma(E'^2 + \delta E'^2, \mu^2)$ and $\sigma(E'^2, \mu^2)$ is now given by the phase space integration $\mathbf{k}_\perp^2 \in [E'^2, E'^2 + \delta E'^2]$, where \mathbf{k}_\perp^2 is the modulo squared of the transverse four momenta of the real photons emitted. The leading contribution, in this case, comes from the emission of a soft particle from an external line (see fig. 3.2). The intuitive reason is analogue to the previous one: when the photon momentum goes to zero the fermion propagators together with the phase space factor go to infinity in this kind of diagrams. Therefore, it is straightforward to find

$$\delta E'^2 \frac{\partial \sigma(E'^2, \mu^2)}{\partial E'^2} \simeq d\sigma(E'^2, \mu^2) \times \int_{\mathbf{k}_\perp^2 \in [E'^2, E'^2 + \delta E'^2]} dw_k. \quad (3.24)$$

³In the first derivation of Abrikosov in [1], the author used as a threshold a maximum energy of non detection instead of a cut-off on the transverse momentum.

where the integral over phase space is

$$\begin{aligned} \int_{\mathbf{k}_\perp^2 \in [E'^2, E'^2 + \delta E'^2]} dw_k &= \frac{e^2}{2} \int_{\mathbf{k}_\perp^2 \in [E'^2, E'^2 + \delta E'^2]} \frac{d^3 \mathbf{k}}{(2\omega_{\mathbf{k}})(2\pi)^3} \frac{2p_1 \cdot p_2}{(p_1 \cdot k)(p_2 \cdot k)} \\ &= \frac{e^2}{2(2\pi)^3} \int_{\mathbf{k}_\perp^2 \in [E'^2, E'^2 + \delta E'^2]} \frac{d^4 k}{(p_1 \cdot k)(p_2 \cdot k)} \delta(k^2). \end{aligned} \quad (3.25)$$

Noticing that this last integral is proportional to $dI/d\mu^2$

$$\frac{\partial \sigma(E'^2, \mu^2)}{\partial \log(E'^2)} = K'(E'^2) \sigma(E'^2, \mu^2), \quad (3.26)$$

where, now, the kernel is

$$K'(E'^2) = -2K(E'^2). \quad (3.27)$$

Eq. (3.26) has to be solved with the appropriate choice of the boundary condition. In particular we use that when $E'^2 = \mu^2$ the phase space for the extra particles emission closes and no extra particles can be produced. Therefore $\sigma(E'^2, \mu^2)$ has to match with the exclusive cross-section, with not extra emissions

$$\sigma(E'^2 = \mu^2, \mu^2) = \sigma^{exc}(\mu^2) = \sigma_B \times \exp\left(-\frac{\alpha}{\pi} R \left[\frac{E^2}{m^2}, \frac{m^2}{\mu^2}\right]\right), \quad (3.28)$$

where $\sigma^{exc}(\mu^2)$ is obtained squaring eq. (3.39). Finally, we find

$$\sigma(E'^2, \mu^2) = \sigma_B \exp\left(-\frac{\alpha}{\pi} R \left[\frac{E^2}{m_e^2}, \frac{m_e^2}{\mu^2}\right]\right) = \sigma_B \exp\left(-\frac{\alpha}{2\pi} \log^2\left(\frac{E^2}{E'^2}\right)\right). \quad (3.29)$$

In this last formula, we can see that the dependence on the unphysical IR cut-off μ cancels. This is a consequences of the Bloch-Nordsieck theorem [3]: QED observables are safe from IR divergences. Furthermore, we see that for $E' \sim E$, i.e. for a “fully inclusive” cross-section, the Sudakov log cancels and σ is well approximated by the perturbative (Born) result.

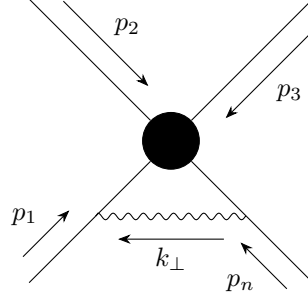
3.2 Virtual emissions in non-Abelian gauge theories

In this section we present the approach of Ref. [12] on how to compute Sudakov effects for massless simple gauge theories. The extension to non-simple groups is straightforward and needs not to be discussed here. It is non trivial, instead to generalize the derivation to massive gauge theories. We will analyze this case later on in the specific example of the Higgs-Kibble model.

Let us consider the scattering amplitude for a process with n -external legs and let us suppose to be in the simple kinematical configuration, where all the invariants $s_{i,j} \equiv 2p_i \cdot p_j \sim E^2$ are large (i.e., E is big in comparison to the masses m_i of the external particles) and of the same order. Since our aim is to compute the leading double log correction, which comes out from the radiative corrections to the process, we first have to identify the class of diagrams causing this kind of contributions. If we work in the Lorentz gauge, where all the propagators have the same pole structure of the scalar ones, part of the solution has been provided by the analysis of scalar integrals made by Kinoshita in Ref. [17]: large double-logs come only from the exchange of a soft and almost collinear virtual particle between two hard external legs⁴. An intuitive justification of this result was given in the previous section. Among these diagrams it turns out that only those where the soft-collinear virtual particle is a gauge boson actually produce double log. We momentarily accept this statement without proof until the next section where we will verify it in the more general setup of spontaneously broken theories.

⁴We remind the reader that with soft we mean that the four-momentum k of the virtual particle is such that $E_{\mathbf{k}} \ll E$, and with almost collinear we mean that if $k = up_1 + vp_2 + k_\perp$ then $k_\perp^2 \ll E^2$.

Figure 3.3: Example of diagram giving rise to virtual double logs correction



Let us consider the amplitude of the process, $\mathcal{M}^\alpha(\mathbf{P}, \mu^2)$, where \mathbf{P} indicates the set of the momenta $\mathbf{P} \equiv \{p_i\}, i = 1, \dots, n$, and $\alpha \equiv \{\alpha_i\}$ is the color index of each particle. The color index α_i runs from 1 to d_i , where d_i is the dimensionality of the representation of the particle “i”. As in the case of QED previously discussed, a cutoff $k_\perp^2 > \mu^2$ is understood in the loop integrals. In order to write down the IR evolution equation in this case, we start by considering one extra vector bosons insertion on one of the external legs. If the extra boson is soft, this gives

$$g \frac{\epsilon^*(k) \cdot p_i}{k \cdot p_i} (T^a(i))_{\alpha'}^\alpha \mathcal{M}^{\alpha'}(\mathbf{P}, \mu^2), \quad (3.30)$$

where the sum over α' (i.e., on each of the α_i index), is understood. In the previous expression, $\epsilon(k)$ is the polarization vector of the emitted boson and “a” its gauge index (in the adjoint representation). The gauge coupling of the theory is denoted as “g”. The generator $T^a(i)$ acts on the α tensorial indexes and it is given by $(T^a(i))_{\alpha'}^\alpha \equiv \delta_{\alpha'}^{\alpha_1} \dots (T^a)_{\alpha'_i}^{\alpha_i} \dots \delta_{\alpha'_n}^{\alpha_n}$. Notice that the form of eq. (3.30) is independent of the nature (fermions, gauge bosons or scalar) of the external particle “i” to which the soft bosons are attached. This result is dubbed as non-Abelian generalization of the “Gribov Theorem” in Ref. [12], and it can be readily established by direct calculation.

Let us now consider an infinitesimal variation of the cut-off μ , it correspond obviously to

$$\mathcal{M}^\alpha(\mathbf{P}, \mu^2) - \mathcal{M}^\alpha(\mathbf{P}, \mu^2 + \delta\mu^2) = -\delta\mu^2 \frac{\partial \mathcal{M}_B^\alpha(\mathbf{P}, \mu^2)}{\partial \mu^2}. \quad (3.31)$$

This variation is given, as we argued before, to the exchange of soft and collinear gauge bosons between external legs (as in fig. 3.3), with the loop integral performed in the region $k_\perp^2 \in [\mu^2, \mu^2 + \delta\mu^2]$. Using eq. (3.30) for two external legs and summing over the polarization of the intermediate virtual boson we have

$$\begin{aligned} -\delta\mu^2 \frac{\partial \mathcal{M}^\alpha(\mathbf{P}, \mu^2)}{\partial \mu^2} = \\ -\frac{i}{2} \frac{g^2}{(2\pi)^4} \sum_{j,l=1, j \neq l}^n \int_{k_\perp^2 \in [\mu^2, \mu^2 + \delta\mu^2]} \frac{d^4 k}{k^2 + i\epsilon} \frac{p_j \cdot p_l}{(k \cdot p_j)(k \cdot p_l)} (T^a(j)T^a(l))_{\alpha'}^\alpha \mathcal{M}^{\alpha'}(\mathbf{P}, \mu^2). \end{aligned} \quad (3.32)$$

We now have to make use of the invariance of the amplitude $\mathcal{M}^\alpha(\mathbf{P}, \mu^2)$ under a global gauge group transformation i.e.

$$\delta \mathcal{M}^\alpha(\mathbf{P}, \mu^2) = 0 \implies \sum_{i=1, \dots, n} (T^a(i))_{\alpha'}^\alpha \mathcal{M}^{\alpha'} = 0, \quad (3.33)$$

and that $\sum_a T^a(i)T^a(i) = -C_i$, with C_i the Casimir of the particle “ i ”. Using the result of the previous section in eq. (3.32), we get

$$\frac{\partial \mathcal{M}^\alpha(\mathbf{P}; \mu)}{\partial \log(\mu^2)} = K(\mu^2) \mathcal{M}^\alpha(\mathbf{P}; \mu^2), \quad (3.34)$$

where

$$K(\mu^2) \equiv -\frac{1}{2} \sum_{i=1}^n \frac{\partial W_i(E^2, \mu^2)}{\partial \log(\mu^2)}, \quad \text{and} \quad W_i(E^2, \mu^2) \equiv \frac{g^2}{8\pi^2} C_i R \left[\frac{E^2}{m_i^2}, \frac{m_i^2}{\mu^2} \right]. \quad (3.35)$$

Now, integrating eq. (3.34) with the boundary condition

$$\mathcal{M}^\alpha(\mathbf{P}; \mu^2 = E^2) = \mathcal{M}^\alpha(\mathbf{P}), \quad (3.36)$$

where \mathcal{M}_B is the Born amplitude, we conclude that

$$\mathcal{M}^\alpha(\mathbf{P}; \mu) = \mathcal{M}^\alpha(\mathbf{P}) \exp \left(-\frac{1}{2} \sum_{i=1}^n W_i(E^2, \mu^2) \right). \quad (3.37)$$

Since it will be useful later on, we introduce a matrix

$$\mathcal{B}_\alpha^\alpha(E^2, \mu^2) \equiv -\sum_{i=1}^n W_i(E^2, \mu^2) \left(\delta_{\alpha_1}^{\alpha_1} \cdots \delta_{\alpha_N}^{\alpha_N} \right) \quad (3.38)$$

and we rewrite equation above as

$$\mathcal{M}^\alpha(\mathbf{P}; \mu) = \exp \left(\mathcal{B}(E^2, \mu^2) \right)_\alpha^\alpha \mathcal{M}^{\alpha'}(\mathbf{P}). \quad (3.39)$$

We will now briefly show how to extend this formalism of the IR evolution equation to resum virtual double logs for an hard process with an additional real soft emission, as derived in Ref. [12]. In particular, we consider the amplitude $\mathcal{M}_l^{\alpha,a}(\mathbf{P}, p_\perp)$ of the hard process $\mathcal{M}^\alpha(\mathbf{P})$ together with the radiation of a soft gauge boson from the hard external leg “ l ”. Let \mathbf{p}_\perp the modulo of the transverse momentum of the soft boson relative to the external leg and be a its the color index. According to eq. (3.30), we have that

$$\mathcal{M}^{\alpha,a}(\mathbf{P}, p; \mu^2) = g \frac{\epsilon^*(p) \cdot p_l}{p \cdot p_l} (T^a(l))_{\alpha'}^\alpha \mathcal{M}^{\alpha'}(\mathbf{P}; \mu^2). \quad (3.40)$$

Depending the value of the cut off μ^2 , with respect two E^2 and \mathbf{p}_\perp^2 , we can identify to cases to discuss:

- A) $E^2 > \mu^2 > \mathbf{p}_\perp^2$,
- B) $E^2 > \mathbf{p}_\perp^2 > \mu^2$.

Let us start from the simpler case (A). In computing the infinitesimal variation as in eq. (3.32) we can note that the loop integration of a soft virtual particles starting from the soft real external leg (with momentum p) will give subleading contribution. Therefore the result is the same of eq. (3.37)

$$\mathcal{M}^{\alpha,a}(\mathbf{P}, p; \mu^2)_A = \mathcal{M}^{\alpha,a}(\mathbf{P}, p; \mu^2) \times \exp \left(-\frac{1}{2} \sum_{i=1}^n W_i(E^2, \mu^2) \right). \quad (3.41)$$

The case (B) is more involved. The idea is to find two evolution equations, for generic cutoff μ'^2 , depending on whether $\mu'^2 > \mathbf{p}_\perp^2$ (A) or $\mu'^2 < \mathbf{p}_\perp^2$ (B) and to evolve separately in the two region. Then, to impose the following matching conditions

$$\mathcal{M}^{\alpha,a}(\mathbf{P}, p; \mu'^2 = E^2)_A = \mathcal{M}^{\alpha,a}(\mathbf{P}, p), \quad \mathcal{M}^{\alpha,a}(\mathbf{P}, p; \mu'^2 = \mathbf{p}_\perp^2)_A = \mathcal{M}^{\alpha,a}(\mathbf{P}, p; \mu'^2 = \mathbf{p}_\perp^2)_B. \quad (3.42)$$

Without entering in details, the only difference in computing eq. (3.32) in the region (B) is that the kernel of the equation $K(\mu'^2)$ is now

$$K(\mu'^2)_B \equiv -\frac{1}{2} \sum_{i=1}^n \frac{\partial (W_i(\mathbf{p}_\perp^2, \mu'^2) + W_A(\mathbf{p}_\perp^2, \mu'^2))}{\partial \log(\mu'^2)}, \quad (3.43)$$

where $W_A(\mathbf{p}_\perp^2, \mu'^2)$ is the extra factor relative to the soft boson, and contains the Casimir of the adjoint representation C_A . The kernel (B) is instead the same of the case (A). The final result is

$$\mathcal{M}^{\alpha,a}(\mathbf{P}, p; \mu^2) = \mathcal{M}^{\alpha,a}(\mathbf{P}, p; \mu^2) \times \exp\left(-\frac{1}{2} \sum_{l=1}^n W_l(E^2, \mu^2) - \frac{1}{2} W_A(\mathbf{p}_\perp^2, \mu^2)\right). \quad (3.44)$$

3.3 Exclusive cross-section in massive gauge theories

The cross-section for exclusive processes, obtained by squaring the amplitude with only hard external legs, are unphysical in massless gauge theories. Indeed they depend on the unphysical IR regulator μ , as we saw in the previous section. Exclusive process becomes instead observables physical in the massive case, where the scale μ physically corresponds to the vector bosons mass m . An heuristic approach for computing them, adopted in [12], is to assume that for $E \gg m$ the massive theory amplitudes approach those of the corresponding massless theory. Hence it should be sufficient to substitute $\mu^2 = m_W^2$ in eq. (3.39). Clearly the relevant massless amplitude should be considered, which duly correspond to the massive one under consideration. The only subtlety in this identification is related with the longitudinal polarized (i.e. helicity equal to zero) external vector bosons. The latter correspond to scalar Goldstone in the massless theory theory, rather than to gauge boson. In particular this implies that the Casimir factor to be employed in eq. (3.39) is not the one in the adjoint, for longitudinal external legs, but the one of the representation where the Goldstone live. In the SM, and in the Higgs Kibble model, this is the doublet of SU(2).

The heuristic approach described above turns out to be correct. The aim of this section is to put it on firmer grounds, by studying the soft-collinear virtual emissions that occur in the massive theory, and proving that at double log level they approach the massless theory ones for $E \gg m$. The analysis will be performed for simplicity in the HK model of sect. 2.3. We work in the Feynman-'t Hooft gauge ($\xi = 1, \tilde{m} = m_W$), where all propagators have the same structure of the scalar ones and we apply once again the result of Ref. [17]. According to it the class of diagrams that produce double logs is the one in which a virtual soft and almost collinear particle is exchanged between two external on-shell particles i.e. diagrams of the type in the left panel of fig. 3.4. In order to compute them, we start from evaluating the insertion of a single soft particle “ ϕ_s ” on an external leg “ ϕ ” as in the right panel of the figure. Notice that the ϕ_s emission turns ϕ into a particle ϕ' of different type or of different color.⁵ The Feynman amplitude for the insertion is, in general,

$$\epsilon_\phi(p) i \Gamma^{\phi\phi_s\phi'}(p, -q, q-p) \epsilon_{\phi_s} G^{\phi'\phi'}(p-q) \mathcal{A}[\phi'(p-q)]. \quad (3.45)$$

Now, we have to take the limit in which $\phi_s(q)$ is soft and almost collinear to $\phi(p)$ i.e. $E_q \ll E_p$ and $\mathbf{q}_\perp \ll E_q$, and identify which are the specific diagrams that effectively give the leading contribution in this limit. In order to do this analysis we need to distinguish two cases: the first one in which the external particle is a gauge boson with longitudinal polarization $\epsilon_\phi(p) = \epsilon_0^\mu(p)$ and the other one in which it is not. By inspecting the Feynman rules of the theory, we notice that the only ones that are not proportional to m_W , and hence power-like suppressed for $E \gg m_W$, are those producing the emission of a gauge boson, either from a scalar or from a gauge line. Among all the possible splittings these vertices give rise to, direct calculation reveals that IR enhancement only emerge if the soft line is a gauge field. Let us compute the splitting of a W boson with color index a and transversal

⁵“Color” refers here to the quantum number under the broken gauge group.

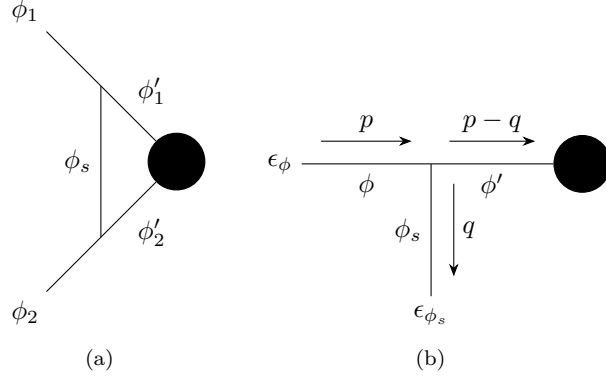


Figure 3.4

polarization ($W_\lambda^a(p)$, with $\lambda \neq 0$) into a gauge boson with color index b . Taking $q \rightarrow 0$, we find on amplitude

$$\begin{aligned}
& ig\epsilon^{abc}\epsilon_\lambda^\mu(p)\epsilon_{\lambda'}^\nu(q)\frac{\eta_{\mu\nu}p_\rho - 2\eta_{\rho\mu}p_\nu}{(p-q)^2 - m^2 + i\epsilon}\mathcal{A}[W_\rho^c(p-q)] \\
\sim_{q \rightarrow 0} & i\frac{g\epsilon^{abc}}{2p \cdot q}\left(2\epsilon_{\lambda'}(q) \cdot p\epsilon_\lambda^\mu(p)\mathcal{A}[W_\mu^c(p)] - im_W\epsilon_{\lambda'} \cdot \epsilon_\lambda(p)\mathcal{A}[\pi^c(p)]\right), \quad (3.46)
\end{aligned}$$

where we have used the Ward identity of eq. (2.61). In the previous equation we have cancelled the term proportional to the $\mathcal{A}[\pi]$ since it is mass suppressed and so, generally, subleading. Therefore eq. (3.46) can be written as

$$\frac{-gf^{abc}}{2p \cdot q}\left(2\epsilon_{\lambda'}(q) \cdot p\epsilon_\lambda^\mu(p)\mathcal{A}[W_\mu^c(p)]\right), \quad (3.47)$$

where $f^{abc} \equiv i\epsilon^{abc}$ is the hermitian generator of the group in the adjoint representation. For external scalars, i.e. for the splitting $h^i \rightarrow h^j W$, we have

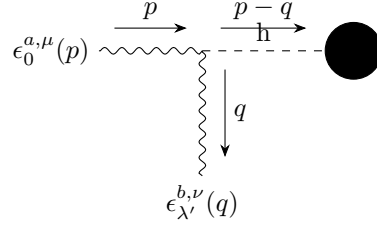
$$\begin{aligned}
& h^i \xrightarrow{p} \xrightarrow{p-q} h^j \\
& \quad \quad \quad \downarrow q \\
& \quad \quad \quad W_\mu^a
\end{aligned} = -\frac{i}{2}\sigma_j^{a,i}(2p_\mu\epsilon_\lambda^\mu(q)), \quad (3.48)$$

where we are referring to the doublet parametrization of the scalars in eq. (2.49). Therefore, we have seen that both for scalars both for transverse gauge bosons we obtained the universal coupling of eq. (3.30).

The situation is slightly more involved for longitudinal external bosons. In particular, the anomalous growth of the polarization vector with the energy does not easily allow us to conclude that m_W suppressed splitting amplitudes are irrelevant, which was the starting point of the previous discussion. Also, the non mass-suppressed splitting $W \rightarrow WW$ is more difficult to study, let us start from it. As in eq. (3.46), we have

$$\begin{aligned}
& ig\epsilon^{abc}\epsilon_0^\mu\epsilon_{\lambda'}^\nu\frac{\eta_{\mu\nu}p_\rho - 2\eta_{\rho\mu}p_\nu}{(p-q)^2 - m^2 + i\epsilon}\mathcal{A}[W_\rho^c(p-q)] \\
\sim_{q \rightarrow 0} & i\frac{g\epsilon^{abc}}{2p \cdot q}\left(2\epsilon_{\lambda'} \cdot p\epsilon_0^\mu\mathcal{A}[W_\mu^c(p)] - im_W\epsilon_0 \cdot \epsilon_{\lambda'}\mathcal{A}[\pi^c(p)]\right), \quad (3.49)
\end{aligned}$$

Figure 3.5



where we used the Slavnov Taylor identity of eq. (2.59) and the sum over c is understood. Diagrammatically, the above equation can be written as

$$\begin{aligned}
 \epsilon_0^{\mu, a}(p) \xrightarrow{p} \text{---} \bullet \xrightarrow{p-q} \text{---} \bullet \\
 \downarrow q \\
 \epsilon_{\lambda'}^{\nu, b}(q)
 \end{aligned}
 \sim_{q \rightarrow 0} i \frac{g \epsilon^{abc}}{2p \cdot q} \left(2\epsilon_{\lambda'}^b(q) \cdot p \times \epsilon_0^{c, \mu}(p) \xrightarrow{p} \bullet \right. \\
 \left. - im_W \epsilon_{\lambda'}(q) \cdot \epsilon_0(p) \times \epsilon_{\pi}^c(p) \xrightarrow{p} \bullet \right),$$

where the color index in the polarization vector in the diagrams is used to indicate the color of the respectively external particle. This result should be combined, with the mass suppressed splitting $W \rightarrow Wh$, depicted in fig. 3.5. This gives

$$ig \frac{m_W \delta^{ab} \epsilon_0(p) \cdot \epsilon_{\lambda'}}{2p \cdot q} \mathcal{A}[h(p)].$$

The expression above, despite of m_W in the numerator, is not mass suppressed since $\epsilon_0^\mu \sim p^\mu/m_W$. Therefore the full splitting to consider in the case of external longitudinal polarization vector is:

$$i \frac{g}{2p \cdot q} \left(2\epsilon^{abc} \epsilon_{\lambda'} \cdot p \epsilon_0^\mu \mathcal{A}[W_\mu^c(p)] - im_W \epsilon_0 \cdot \epsilon_{\lambda'} \left[\epsilon^{abc} \mathcal{A}[\pi^c(p)] - i\delta^{ab} \mathcal{A}[h(p)] \right] \right). \quad (3.50)$$

To conclude we have to note that, using the Equivalence Theorem in the previous equation, we immediately obtain, the same rule of eq. (3.48). In fact, using that $\epsilon_0 \cdot \mathcal{A}[W] \simeq i\mathcal{A}[\pi]$ in eq. (3.50) and using that, at high energy, $\epsilon_0^\mu \sim p^\mu/m_W$ we can rewrite eq. (3.50) as

$$- \frac{g \epsilon_{\lambda'} \cdot p}{2p \cdot q} \left(\epsilon^{abc} \mathcal{A}[\pi^c(p)] + \delta^{ab} \mathcal{A}[h(p)] \right). \quad (3.51)$$

At this point, it is straightforward to find that, using the fields representation eq. (2.49) for the Goldstone, the previous expression corresponds to eq. (3.48). And this is, exactly, eq. (3.30) for the case of a doublet of $SU(2)$.

3.4 Inclusive cross-sections

In section 3.2 we computed how to dress an hard process by virtual double log corrections to all order in perturbation theory and in sect. 3.3 we showed that those calculation applies also to massive gauge theories. The result in eq. (3.39) shows that the exclusive differential cross-section for a process (where we remember that with exclusive we mean without the emission of additional real particles) depends on the IR cut-off μ , which is a

totally unphysical parameter for massless gauge theories. In the case of SSB μ^2 is promoted to the physical parameter m_W^2 and so the gauge boson mass makes exclusive cross-section predictable quantities. However our result shows that exclusive amplitudes go to zero for $E \rightarrow \infty$, meaning that the exclusive process becomes more and more improbable with the increasing of E . Therefore exclusive quantities are not the best candidates to be compared with high energy measurements. In order to attack this problem and to end up with an useful quantity it is necessary to include in our predictions the probability of emission of an arbitrary number of soft gauge bosons, as we have done in section 3.1 for QED. As already known, from the celebrated KNL theorem [20, 17], this procedure for QCD (as for QED) produces cross-sections free of infra-red divergences and so free of the dependences on μ . This result is more involved for massive gauge theories because the cross-section are not averaged over the color of the initial particles. Hence the KNL theorem cannot be applied and the large double log persist also in fully inclusive cross-section, as first found in Ref [8].

In the following, we are going to explain how to predict inclusive cross-section with two different methods: first summing together real and soft emissions, then via the formalism of the coherent states and of the overlapping matrix.

3.4.1 A diagrammatic approach

Let us consider the generic process, described in sect. 3.2, with Born amplitude $\mathcal{M}_B^\alpha(\mathbf{P})$ plus one real emission of a soft gauge boson with a color index a and momentum k . Thanks to eq. (3.30), we have

$$\mathcal{M}_B^\alpha(\mathbf{P}) \longrightarrow \mathcal{M}_{1R}^{\alpha;a}(\mathbf{P}, k) \sim \mathcal{M}_B^{\alpha'} \left(\sum_{l=1}^n g \frac{\epsilon^* \cdot p_l}{k \cdot p_l} T^a(l) \right)_{\alpha'}^\alpha. \quad (3.52)$$

In the previous equation, and in the rest of this section, we underline the indices we are not summing over to avoid confusion. In the case of real emission double logs corrections come from the integration over the phase space of the soft boson emitted. Let us consider, therefore, the amplitude modulo-squared

$$|\mathcal{M}_{1R}^{\alpha;a}|^2 = \mathcal{M}_B^{\alpha'} \left(\sum_{l=1}^N g \frac{\epsilon^* \cdot p_l}{k \cdot p_l} T^a(l) \right)_{\alpha'}^\alpha \mathcal{M}_B^{\alpha''*} \left(\sum_{k=1}^N g \frac{\epsilon^* \cdot p_k}{k \cdot p_k} T^a(k) \right)_{\alpha''}^{\alpha*}. \quad (3.53)$$

Next, we sum over the polarization of the soft bosons emitted, sum over their color a and integrate over the phase space, in the region of softness and collinearity, obtaining the following differential cross-section

$$\begin{aligned} \sigma_{1R}^\alpha &\equiv \sum_{a, pol} \int_{\mu^2 \leq \mathbf{k}_\perp^2} \frac{d^3 k}{(2\pi)^3 2\omega_k} |\mathcal{M}^{\alpha;a}|^2 = \\ &\int_{\mu^2 \leq \mathbf{k}_\perp^2} \frac{d^3 k}{(2\pi)^3 2\omega_k} \mathcal{M}^{\alpha'} \left(- \sum_{l,k=1}^n g^2 \frac{p_k \cdot p_l}{(k \cdot p_k)(k \cdot p_l)} \right) (T^a(l))_{\alpha'}^\alpha (T^a(k))_{\alpha''}^{\alpha*} \mathcal{M}^{\alpha''*}, \end{aligned}$$

where a cut-off μ on the the transverse momentum of the soft particle has been used.

We can focus only on the factors with $l \neq k$ because the ones in which $l = k$ do not give double logs contributions. Using that

$$\int_{\mu^2 \leq \mathbf{k}_\perp^2} \frac{d^3 k}{(2\pi)^3 2\omega_k} g^2 \frac{p_k \cdot p_l}{(k \cdot p_k)(k \cdot p_l)} = \left(\frac{W_l(E^2, \mu^2)}{C_l} + \frac{W_l(E^2, \mu^2)}{C_k} \right), \quad (3.54)$$

and the total charge conservation of the gauge group, it follows that

$$\sigma_{1R}^\alpha = \mathcal{M}_B^{\alpha'} \mathcal{M}_B^{\alpha''*} \left(\sum_{a,l} T_{\alpha_l}^{a\alpha_l} T_{\alpha''}^{a\alpha_l*} \frac{W_l(E^2, \mu^2)}{C_l} \right). \quad (3.55)$$

Figure 3.6: Primary radiation(left), secondary real radiation (center), secondary virtual radiation (right)

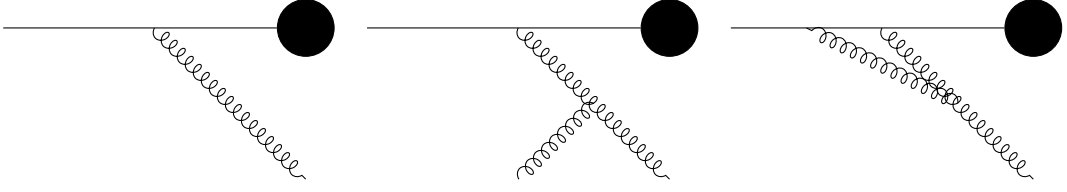
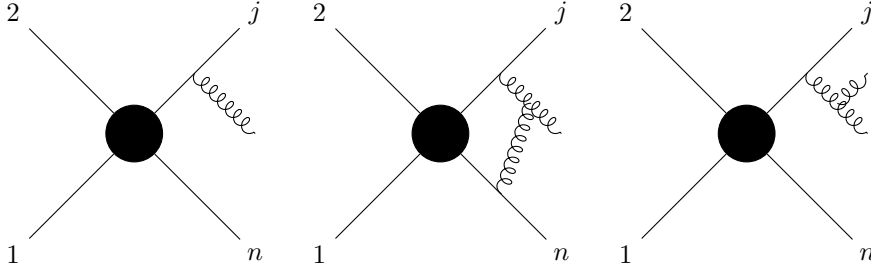


Figure 3.7: Secondary emissions in an hard process with primary soft emission



The group generators are chosen hermitian $T_{\alpha'_i}^{a\alpha_i} = T_{\alpha_i}^{a\alpha'_i}$, hence

$$\sigma_{1R}^{\alpha} = \mathcal{M}^{\alpha'} \mathcal{M}^{\alpha''*} \left(\sum_l T_{\alpha'_i}^{a\alpha_l} T_{\alpha_l}^{a\alpha''} \frac{W_l(E^2, \mu^2)}{C_l} \right) = \mathcal{A}_{\alpha'}^{\alpha}(E^2, \mu^2) d\sigma_B^{\alpha'} \quad (3.56)$$

Notice that in the previous we expected the fact that $T_{\alpha_l}^{a\alpha'_i} T_{\alpha'_i}^{a\alpha_l}$ is diagonal⁶ in α'_i and α_l , in order to define

$$\sum_l W_l(E^2, \mu^2) T_{\alpha'_i}^{a\alpha_l} T_{\alpha_l}^{a\alpha''} \equiv \mathcal{A}_{\alpha'}^{\alpha}(E^2, \mu^2) \delta_{\alpha''}^{\alpha'} . \quad (3.57)$$

Let us, now, sum together the first order in the fine structure α double logs corrections coming from one virtual emission (eq. (3.39)) and from one real emission (eq. (3.56)). The first order inclusive cross section σ_1^{α} reads:

$$\sigma_1^{\alpha} = (1 + A_{\alpha'}^{\alpha} + \mathcal{B}\delta_{\alpha'}^{\alpha}) \sigma_B^{\alpha'} . \quad (3.58)$$

We now guess how to extend the previous result to all orders in perturbation theory. The key statement we need to prove is the following: virtual and real double logs contributions due to secondary radiation sum up to zero. To be more specific, we call primary radiation the one emitted directly from an external leg of the hard process and secondary the radiation emitted from the primary one, as described in fig. 3.6. Without loss of generality, let us consider a hard process whose leg “ j ” has emitted a soft gauge boson with momentum “ k ”, and let us compute virtual and real IR corrections for such a process. Differently from the Abelian case, the presence of self-interactions obliges us to consider also secondary gauge bosons. Using the result of eq. (3.44) at first order, we find that adding one virtual correction to the single emission diagram lead to

$$\sigma_{1V}^{\alpha;a}(\mathbf{P}, k) = \sigma_B^{\alpha;a}(\mathbf{P}, k) \times \left(1 - \frac{1}{2} \sum_{l=1}^n W_l(E^2, \mu^2) - \frac{1}{2} W_A(\mathbf{k}_{\perp}^2, \mu^2) \right)^2 , \quad (3.59)$$

⁶It can be proved for the fundamental representation of $SU(N)$ and it is also true for all the case of interest in the following discussion.

where the second term in the bracket comes from the secondary virtual emission from the soft real boson, as in the central diagram of fig. 3.7. Analogously, we can generalize eq. (3.56) to include one external real emission, obtaining

$$\sigma_{1R}^{\alpha;a}(\mathbf{P}, k) = \left(\mathcal{A}_{\alpha}^{\alpha}(E^2, \mu^2) \delta_{a'}^{\bar{a}} + \delta_{\alpha'}^{\alpha} \mathcal{A}_{a'}^{\alpha}(\mathbf{k}_{\perp}^2, \mu^2) \right) \sigma_B^{\alpha';a'}(\mathbf{P}, k), \quad (3.60)$$

where $\mathcal{A}_{a'}^{\alpha}(\mathbf{k}_{\perp}^2, \mu^2) \equiv \frac{W(\mathbf{k}_{\perp}^2, \mu^2)}{C_A} \left(\sum_c T_{a'}^{(c)a} T_{a'}^{(c)a} \right)$. If now, we sum together virtual and real radiation color index \underline{a} and we sum together virtual and real radiation corrections of eq. (3.59) and eq. (3.60), we readily get

$$\sum_R \sigma_{1R}^{\alpha;a}(\mathbf{P}, k) + \sigma_{1V}^{\alpha;a}(\mathbf{P}, k) = \left(\mathcal{B} \delta_{\alpha'}^{\alpha} - \cancel{W_A(\mathbf{k}_{\perp}^2, \mu^2)} + \cancel{W_A(\mathbf{k}_{\perp}^2, \mu^2)} + \mathcal{A}_{\alpha'}^{\alpha} \right) \sum_a \sigma_B^{\alpha';a}. \quad (3.61)$$

This result shows that double logs contributions cancel by summing over the color index of the soft boson emitted. Since this scheme can be repeated for each uncolored bosons we can conclude that, we can take into account only primary radiation in computing double log corrections to inclusive cross-section.

Now we are ready to compute the inclusive cross-section for our process σ^{α} to all orders in perturbation theory. We work in analogy to the QED case and so we built an infrared evolution equation allowing to dress the exclusive cross section of eq. (3.39) of real emissions. We start from a cross-section $\bar{\sigma}(E'^2, \mu^2)$ with a threshold E' for the emitted real soft particle, supposing they are only primary radiation. Obviously $\bar{\sigma}(E'^2, \mu^2)$ has no physical meaning, since the presence of a threshold will make the cancellation of double logs coming from secondary radiation false. At the end of the computation, therefore, we will take $E'^2 = E^2$, obtaining a physical inclusive cross-section. The evolution equation is

$$\frac{\partial \bar{\sigma}^{\alpha}(E'^2, \mu^2)}{\partial E'^2} = K'_{\alpha'}(E'^2) \bar{\sigma}^{\alpha'}(E'^2, \mu^2), \quad (3.62)$$

where

$$K'_{\alpha'}(E'^2) = \frac{\partial \mathcal{A}_{\alpha'}^{\alpha}(E^2, E'^2)}{\partial \log E'^2} \quad (3.63)$$

By integrating the previous equation with the boundary that at $E' = \mu$ we obtain the exclusive of eq. (3.39), we get

$$\sigma^{\alpha} = [\exp(\mathcal{A} + \mathcal{B})]_{\alpha'}^{\alpha} \sigma_B^{\alpha'}. \quad (3.64)$$

In sect. 3.4.3, we will see how this formula works with an explicit example.

3.4.2 The Coherent States Formalism

The starting point of this method is that, given an hard process

$$\{\{p_I^1, \alpha_I^1\}, \dots\}_I \equiv \{\mathbf{P}_I, \boldsymbol{\alpha}_I\} \longrightarrow \{\{p_F^1, \alpha_F^1\}, \dots\} \equiv \{\mathbf{P}_F, \boldsymbol{\alpha}_F\}, \quad (3.65)$$

where with $\{\mathbf{P}_{I/F}, \boldsymbol{\alpha}_{I/F}\}$ we have denoted the set of momenta and color indexes of the initial/final particles, then the S matrix relative for such a process can be factorized as

$$\mathcal{S}_{\alpha,\beta}(\mathbf{P}_F, \mathbf{P}_I) = \mathcal{U}_{\beta,\beta'}^F(a_s, a_s^\dagger) \mathcal{S}_{\beta',\alpha'}^H(\mathbf{P}_F, \mathbf{P}_I) \mathcal{U}_{\alpha',\alpha}^I(a_s, a_s^\dagger). \quad (3.66)$$

The operators $\mathcal{U}^{I/F}(a_s, a_s^\dagger)$, called soft coherent state operators are functionals of the soft emission operators a_s and a_s^\dagger , involving gauge bosons with frequencies $\lambda \ll \omega \ll E$. Eq. (3.66) is considered to be universal (as explained in Ref. [27, 6]) and it is based on

the separation of the interaction hamiltonian of the theory H_I into an hard part, containing short time interactions, and a soft one, containing long time interactions

$$H_I(t) = H_H(t) + H_S(t). \quad (3.67)$$

As a consequences, also the Hilbert space of the theory can be factorized as $\mathcal{H} = \mathcal{H}_H \otimes \mathcal{H}_s$, where for each hard particle state of \mathcal{H}_H , \mathcal{H}_s contains an infinite set of “dangerous” states [27], of gauge bosons which are soft with respect to the hard state. The a_s and a_s^\dagger operator of eq. (3.66), therefore, act on this \mathcal{H}_s .

In the following, we will derive the form of the coherent states operators for the case of QED, starting from the method of the asymptotic dyammics. The discussion for non Abelian gauge theories is less transparent, there are a series of work [6, 5, 8, 7], providing eq. (3.66) and the form of $\mathcal{U}_{I/F}$ but we will only discuss qualitatively the general properties of them, in order to make a comparison with our approach of sect. 3.4.1.

Let us discuss the set up of the asymptotic dynamics, which leads to the separation of hard and soft interaction (3.66), following the original proposal of [19]. The canonical QED interaction is

$$H_I(t) = e \int d^3x \bar{\psi}(\mathbf{x}, t) \gamma^\mu \psi(\mathbf{x}, t) A_\mu(\mathbf{x}, t). \quad (3.68)$$

The fields can be further defined as functionals of creation and annihilation operators as

$$\psi(\mathbf{x}, t) = \sum_{\sigma=\pm} \int \frac{d^3k}{2\omega_k (2\pi)^3} [c_\sigma(k) u_\sigma(k) e^{-ik \cdot x} + d_\sigma^\dagger v_\sigma(k) e^{ik \cdot x}]_{k_0=\omega_k} \quad (3.69)$$

$$\bar{\psi}(\mathbf{x}, t) = \sum_{\sigma=\pm} \int \frac{d^3p}{2\omega_p (2\pi)^3} [c_\sigma(p) \bar{u}_\sigma(p) e^{ip \cdot x} + d_\sigma^\dagger \bar{v}_\sigma(p) e^{-ip \cdot x}]_{p_0=\omega_p} \quad (3.70)$$

$$A^\mu(\mathbf{x}, t) = \int \frac{d^3q}{2\omega_q (2\pi)^3} [A^\mu(q) e^{-iq \cdot x} + A^{\mu\dagger}(q) e^{iq \cdot x}]_{q_0=\omega_q}. \quad (3.71)$$

A more useful way to rewrite the Hamiltonian (3.68) is through

$$H_I(t) = \int_\lambda^\infty d\nu (h_+(t) e^{-i\nu t} + h_-(t) e^{i\nu t}). \quad (3.72)$$

This formula is simply obtained substituting the explicit expressions of the fields (3.69) and then performing the Fourier transform with the respect to the time conjugate variable ν (typically called transfer energy). The cut-off λ has been introduced, to account with IR divergences.

The main point in writing $H_I(t)$ as eq. (3.72) is that, in this way, one can easily separate short term interaction from the hard one just introducing a energy scale E

$$H_I(t) = \int_\lambda^E d\nu (h_+(t) e^{-i\nu t} + h_-(t) e^{i\nu t}) + \int_E^\infty d\nu (h_+(t) e^{-i\nu t} + h_-(t) e^{i\nu t}) \quad (3.73)$$

$$\equiv H_S^E(t) + H_H^E(t). \quad (3.74)$$

Then the analytic expression of $H_S^E(t)$ is determined by the leading behaviour of (3.72) in the limit $|t| \rightarrow \infty$. Following the discussion of [19], we can note that (3.72) is an integral over the momenta \mathbf{k} , \mathbf{p} , \mathbf{q} of the fermions and photon (respectively), which are related by the relation $\mathbf{p} = \mathbf{q} + \mathbf{k}$. It is simple to observe that the terms in (3.72) can be splitted in two cases. A first one containing two creation or annihilation operators of the charged particles, a second one containing a creation and a annihilation operators for the fermions. In both cases dependences on time is $\exp(\pm i\nu t)$. For the former $\nu = \omega_{\mathbf{k}} + \omega_{\mathbf{p}} \pm \omega_{\mathbf{q}}$ and it is simply to observe that $\forall q$ and $\forall k$ this is different from zero. The latter case, instead, has a dependences which is $\nu = \omega_{\mathbf{k}} - \omega_{\mathbf{p}} \pm \omega_{\mathbf{q}}$ that vanishes for all values of \mathbf{k} when \mathbf{q} is zero. Therefore, we can conclude that 3.68, in the limit $|t| \rightarrow \infty$, is dominated by

$$H_S(t) = \int d\nu (h_{s+}(t) e^{-i\nu t} + h_{s-}(t) e^{i\nu t}), \quad (3.75)$$

where

$$h_{s+}(t) = e \int \frac{d^3\mathbf{k}}{2\omega_{\mathbf{k}}(2\pi)^3} \frac{d^3\mathbf{p}}{2\omega_{\mathbf{p}}(2\pi)^3} \hat{p} \cdot A(\mathbf{k}) \rho(\mathbf{p}) \delta(\hat{p} \cdot k - \nu), \quad (3.76)$$

$$h_{s-}(t) = e \int \frac{d^3\mathbf{k}}{2\omega_{\mathbf{k}}(2\pi)^3} \frac{d^3\mathbf{p}}{2\omega_{\mathbf{p}}(2\pi)^3} \hat{p} \cdot A^{\mu\dagger}(\mathbf{k}) \rho(\mathbf{p}) \delta(\hat{p} \cdot k - \nu). \quad (3.77)$$

and

$$\hat{p}^\mu \equiv \frac{p^\mu}{E_{\mathbf{p}}} \quad \rho(\mathbf{p}) \equiv \sum_{\sigma} (c_{\sigma}^{\dagger}(\mathbf{p}) c_{\sigma}(\mathbf{p}) - d_{\sigma}^{\dagger}(\mathbf{p}) d_{\sigma}(\mathbf{p}))$$

As the Hamiltonian, also the Hilbert space of the states has to be splitted into an hard and soft part $\mathcal{H} \equiv \mathcal{H}_H \otimes \mathcal{H}_s$. The key feature of eq. (3.76) is that, since it makes photons coupling with hard charged particles only via their momentum, it is diagonal in \mathcal{H}_H states and it has a c-number commutators in \mathcal{H}_S .

Now, we have to solve the soft evolution equation for the soft Hamiltonian is

$$i \frac{\partial}{\partial t} \mathcal{U}_s(t, -\infty) = H_s^E(t) \mathcal{U}_s(t, -\infty). \quad (3.78)$$

In doing this, we use the method of [6], with can be easily generalized to non-Abelian gauge theories, as we will see later on. In particular the equation can be solved in perturbation theory as

$$\mathcal{U}_s^{(n)}(t, \pm\infty) = \sum_{\eta_i} d\nu_i \dots d\nu_n \frac{e^{-i(\sigma_n \nu_n + \dots + \sigma_1 \nu_1)t} h^{\sigma_n}(\nu_n) \dots h^{\sigma_1}(\nu_1)}{(\sigma_n \nu_n + \dots + \sigma_1 \nu_1 \pm \epsilon) \dots (\sigma_1 \nu_1 \pm i\epsilon)}, \quad (3.79)$$

this from in general does not show a factorization structure, however in QED the operators commute and so using the eikonal identity

$$\sum_{perm} \frac{1}{a_1 + \dots + a_n} \dots \frac{1}{a_1 + a_2} \frac{1}{a_1} = \prod_{i=1}^n \frac{1}{a_i}, \quad (3.80)$$

we get

$$\mathcal{U}_s(0, -\infty) = P_{\nu} \exp \left[\int_{\lambda}^E \frac{d\nu}{\nu} (h_{s+}(\nu) - h_{s-}(\nu)) \right]. \quad (3.81)$$

Or, using eq. (3.76)

$$\mathcal{U}_s(0, -\infty) = P_{\omega} \exp \left[ig \int_{\lambda}^E \frac{d^3k}{2\omega_{\mathbf{k}}(2\pi)^3} \frac{d^3p}{2\omega_{\mathbf{p}}(2\pi)^3} \rho(\mathbf{p}) \frac{p}{k \cdot p} \cdot \Pi(\mathbf{k}) \right], \quad (3.82)$$

where

$$\Pi_{\mu}(k) \equiv -i (A_{\mu}(k) - A_{\mu}^{\dagger}). \quad (3.83)$$

We are now ready to introduce the definition of choerent states of [6]. Ff the IN/OUT states are generic hard n/m -particle states:

$$|h_I\rangle \equiv |p_1, \dots, p_n\rangle \in \mathcal{H}_H, \quad |h_F\rangle \equiv |p_1, \dots, p_m\rangle \in \mathcal{H}_H, \quad (3.84)$$

then the IN/OUT coherent state operators is obtained evaluating eq. (3.82) on $|h\rangle$. With the result

$$\mathcal{U}_{I/F}^E(p_1, \dots, p_{n/m}) = e^{\pm i\phi_c} \prod_{i=1}^{n/m} \exp \left[\int_{\nu}^E d^3\mathbf{q} \frac{p_i \cdot (A(\mathbf{q}) - A^{\dagger}(\mathbf{q}))}{p_i \cdot q} \right], \quad (3.85)$$

where we have neglected an infinite unobservable phase and

$$\phi_c = \sum_{i < j} \frac{e_i e_j}{v_{ij}} \log \frac{E}{\lambda}, \quad (3.86)$$

with v_{ij} the relative velocity. The S_{FI} can be, therefore decomposed as

$$S_{FI} = (\mathcal{U}_F^E)^\dagger S_{FI}^H \mathcal{U}_I^E. \quad (3.87)$$

The case of non Abelian gauge theories is more involved. Restricting our analysis on the leading contributions, it is proved in Ref. [6] that, as we argued before, the S matrix element for a given hard process could be written in the form of eq. (3.66) as

$$S_{\alpha,\beta}(\mathbf{P}_F, \mathbf{P}_I) = \mathcal{U}_{\beta,\beta'}^{F,l}(a_s, a_s^\dagger) \mathcal{S}_{\beta',\alpha'}^H(\mathbf{P}_F, \mathbf{P}_I) \mathcal{U}_{\alpha',\alpha}^{I,l}(a_s, a_s^\dagger), \quad (3.88)$$

where $\mathcal{U}_{\alpha',\alpha}^{I,l}(a_s, a_s^\dagger)$ it is the leading coherent state operator. Now, this operator, even if it acts on \mathcal{H}_s , can change the hard state color set of indexes. Indeed, when an hard colored particle emits a soft boson, it could change its color. There are other two fundamental properties. First of all, the commutativity for any given color index

$$\left[\mathcal{U}_{\alpha',\alpha}^{I/F,l}, \mathcal{U}_{\beta',\beta}^{I/F,l} \right] = 0, \quad (3.89)$$

then the factorization with respect to hard particles, it holds

$$\mathcal{U}_{\alpha',\alpha}^{I/F,l}(1, \dots, n) = \mathcal{U}_{\alpha'_1, \alpha_1}(1) \dots \mathcal{U}_{\alpha'_n, \alpha_n}(n). \quad (3.90)$$

As we are going to see, these properties would be fundamental in the next section.

3.4.3 Comparison of the two formalisms

We now use the methods of sect. 3.4.2 and sect. 3.4.1 to predict inclusive cross-section in a special case, that will be useful later on in this thesis. In particular we consider a process between an hard initial state of two particles which transform under the fundamental representation and the anti-fundamental of $SU(2)$, and a final state which is singlet of the gauge group.

Let us start from the more clear diagrammatic approach of sec. 3.4.1. According to eq. (3.56) we know that, for our process

$$\mathcal{B}_{i'i'}^{ii} = (-W_1(E^2, \mu^2) - W_2(E^2, \mu^2)) \delta_{i'}^i \delta_{i'}^i, \quad (3.91)$$

where the indexes i and \dot{i} live, respectively, in the fundamental and anti-fundamental representation and are referred to our initial particle. In particular we refer to the two component of the double/anti-doublet as $i = \pm / \dot{i} = \pm$. For the matrix $\mathcal{A}_{i'_1 i'_2}^{i_1 i_2}$ we have, according to eq. (3.57),

$$\mathcal{A}_{i'_1 i'_2}^{i_1 i_2} = \mathcal{A}_{i'_1}^{i_1} \delta_{i'_2}^{i_2} + \delta_{i'_1}^{i_1} \mathcal{A}_{i'_2}^{i_2} \quad (3.92)$$

Let us compute explicitly the first factor of the right hand side of the previous equation. The generator of the fundamental representation are

$$T_{i'}^{1i} = \frac{1}{2} \begin{pmatrix} 0 & 1 \\ 1 & 0 \end{pmatrix}, \quad T_{i'}^{3i} = \frac{1}{2} \begin{pmatrix} 0 & -i \\ i & 0 \end{pmatrix}, \quad T_{i'}^{3\dot{i}} = \frac{1}{2} \begin{pmatrix} 1 & 0 \\ 0 & -1 \end{pmatrix}, \quad (3.93)$$

and so we have that from eq. (3.57) we get

$$\sum_a T_{i'_1}^{a1} T_1^{ai'_1} = -\frac{1}{4} \begin{pmatrix} 1 & 0 \\ 0 & 2 \end{pmatrix} \quad \sum_a T_{i'_1}^{a2} T_2^{ai'_1} = -\frac{1}{4} \begin{pmatrix} 2 & 0 \\ 0 & 1 \end{pmatrix}. \quad (3.94)$$

Finally $\mathcal{A}_{i_1'}^{i_1}$ results

$$\mathcal{A}_{i_1'}^{i_1} = \frac{W_1(E^2, \mu^2)}{C_1} \frac{1}{4} \begin{pmatrix} 1 & 2 \\ 2 & 1 \end{pmatrix}, \quad (3.95)$$

and the same result can be found for $\mathcal{A}_{i_1'}^{i_1}$. Now, it is straightforward to find $\mathcal{A}_{i_1' i_2'}^{i_1 i_2}$, we add it to \mathcal{B} and apply the result of eq. (3.64). We have

$$\begin{pmatrix} \sigma_I^{+\dot{+}} \\ \sigma_I^{+\dot{-}} \\ \sigma_I^{-\dot{+}} \\ \sigma_I^{-\dot{-}} \end{pmatrix} = \exp \left(\frac{\alpha}{16\pi} \log \left(\frac{E^2}{\mu^2} \right) \begin{pmatrix} -4 & 2 & 2 & 0 \\ 2 & -4 & 0 & 2 \\ 2 & 0 & -4 & 2 \\ 0 & 2 & 2 & -4 \end{pmatrix} \right) \begin{pmatrix} \sigma_B^{+\dot{+}} \\ \sigma_B^{+\dot{-}} \\ \sigma_B^{-\dot{+}} \\ \sigma_B^{-\dot{-}} \end{pmatrix}, \quad (3.96)$$

where the 4×4 matrix above is $\mathcal{A} + \mathcal{B}$. We can see, moreover, that since $\sigma^{+\dot{-}} \equiv \sigma^{-\dot{+}}$ and $\sigma^{+\dot{+}} \equiv \sigma^{-\dot{-}}$, then we can restrict our analysis on the two independent components

$$\begin{pmatrix} \sigma_I^{++} \\ \sigma_I^{+-} \end{pmatrix} = \exp \left(-\frac{\alpha}{4\pi} \log \left(\frac{E^2}{\mu^2} \right) \begin{pmatrix} 1 & -1 \\ -1 & 1 \end{pmatrix} \right) \begin{pmatrix} \sigma_B^{++} \\ \sigma_B^{+-} \end{pmatrix}. \quad (3.97)$$

The previous equation is clearly diagonalizable as follows

$$\begin{pmatrix} \sigma_I^{++} + \sigma_I^{+-} \\ \sigma_I^{++} - \sigma_I^{+-} \end{pmatrix} = \exp \left(-\frac{\alpha}{4\pi} \log \left(\frac{E^2}{\mu^2} \right) \begin{pmatrix} 0 & 0 \\ 0 & 2 \end{pmatrix} \right) \begin{pmatrix} \sigma_B^{++} + \sigma_B^{+-} \\ \sigma_B^{++} - \sigma_B^{+-} \end{pmatrix}. \quad (3.98)$$

This new set of cross-sections, in the color space, is diagonal in the soft evolution, we get

$$\sigma_I^{++} + \sigma_I^{+-} = \sigma_B^{++} + \sigma_B^{+-}, \quad \sigma_I^{++} - \sigma_I^{+-} = \exp \left(-\frac{\alpha}{2\pi} \log \left(\frac{E^2}{\mu^2} \right) \right) (\sigma_B^{++} - \sigma_B^{+-}). \quad (3.99)$$

Finally, from the above equation

$$\sigma_I^{++} = \frac{(\sigma^{++} + \sigma^{+-})_B}{2} + \frac{(\sigma^{++} - \sigma^{+-})_B}{2} \exp \left(-\frac{\alpha}{2\pi} \log^2(E^2/m_W^2) \right), \quad (3.100)$$

$$\sigma_I^{+-} = \frac{(\sigma^{++} + \sigma^{+-})_B}{2} - \frac{(\sigma^{++} - \sigma^{+-})_B}{2} \exp \left(-\frac{\alpha}{2\pi} \log^2(E^2/m_W^2) \right). \quad (3.101)$$

In the case we will consider in chapter 4 it will be $\sigma_B^{+-} = 0$

Let us prove eq. (3.99) with the formalism of Sec. 3.4.2. We have to introduce, the so-called overlapping matrix and hard overlapping matrix

$$\mathcal{O} \equiv S^\dagger S, \quad \mathcal{O}_H \equiv S_H^\dagger S_H, \quad (3.102)$$

where S is the Scattering matrix. Let us analyse the overlapping matrix as suggested in Ref. [7], for our given process. The key idea is that, in the high energy limit, where the gauge group is approximatively unbroken, the S-Matrix $S_{FI} \equiv \mathcal{M}^{i_1 i_2^*} \mathcal{M}^{i_1 i_2} \equiv S^I$ (where $I \equiv \{i_1 i_2\}$) has two color indexes, in the $SU(2)$ fundamental/anti-fundamental representations, and no one for the final state, since we assume it is a singlet of the gauge group. Therefore, the overlapping matrix has four color indexes

$$\mathcal{O}_H^{I'I} \equiv S_H^{\dagger I'} S_H^I \quad (3.103)$$

where we leave open the possibility that $I \neq I'$, while, obviously for physical differential cross section we have $I \equiv I'$. We can observe, now, that the overlap matrix of eq. (3.103) is a tensor in the indexes of the gauge group and so we can decompose it as

$$\mathcal{O}_H^{I'I} = C_0 \delta^{i_1 i_1'} \delta^{i_2 i_2'} + C_1 t^{a, i_1 i_1'} t^{a, i_2 i_2'}. \quad (3.104)$$

Now, we have to dress the Hard matrix with soft interaction, essentially we include the soft coherent state, according to eq. (3.66). We get

$$\mathcal{O}^{I'I} = {}_S\langle 0 | \mathcal{U}^{I'J\dagger} \mathcal{O}_H^{JK} \mathcal{U}^{KI} | 0 \rangle_S, \quad (3.105)$$

where $|0\rangle_S$ is soft vacuum relative to the initial state. In order to go on, we need the properties that, at leading order, the coherent state operators can be factorized in single particle operators and so we get

$$\mathcal{U}^{I'I} = U(i'_1 i_1) U(i'_2 i_2). \quad (3.106)$$

Therefore, without entering in detail, we find

$$\mathcal{O}_s^{I'I} = C_0 \delta^{i_1 i'_1} \delta^{i_2 i'_2} + C_1 {}_S\langle 0 | (U^\dagger(1) t^a U(1))_{i'_1 i_1} (U^\dagger(2) t^a U(2))_{i'_2 i_2} | 0 \rangle_S \quad (3.107)$$

$$= C_0 \delta^{i_1 i'_1} \delta^{i_2 i'_2} + C_1 F(s, m_W^2) t^{a, i_1 i'_1} t^{a, i_2 i'_2}. \quad (3.108)$$

where we have used that

$$(U^\dagger(1) t^a U(1))_{i'_1 i_1} = (U_A)_{ab} t_b, \quad (3.109)$$

with $(U_A)_{ab}^c$ the coherent state operator in the adjoint representation. The previous result can be proved to be (see Ref. [5])

$$\sigma_I^{++} = \frac{(\sigma^{++} + \sigma^{+-})_H}{2} + \frac{(\sigma^{++} - \sigma^{+-})_H}{2} \exp\left(-\frac{\alpha}{2\pi} \log^2(E^2/m_w^2)\right), \quad (3.110)$$

since $F_A(E^2, m_W^2) = \exp\left(-C_A \frac{\alpha}{4\pi} \log^2\left(\frac{E^2}{m_W^2}\right)\right)$ and $C_A \equiv 2$ is the Casimir representation.

Chapter 4

NLO heavy singlet VBF production

In this chapter we study the production of the singlet “S”, within the “singlet-extended” Higgs-Kibble model (SEHK model) defined in the chapter 2, through the process $W^+W^- \rightarrow SS$. This process, dubbed “Vector Boson Fusion”(VBF) production, might take place at a future high energy collider, where nearly on-shell initial state vector bosons are emitted from the colliding beams in the so-called “Effective W” configuration [4]. It is expected that this one would actually be the dominant production mode for S, given that all its couplings to quarks, gluons and leptons are absent at tree level¹. We consider the phenomenologically interesting configuration in which the singlet is heavy, i.e. $M_S > 1 \text{ TeV} \gg m_W$, and the initial WW c.o.m. energy, \sqrt{s} , is of the order of twice M_S . In this configuration it is possible to apply the Equivalence Theorem introduced in sect. 2.4, and immediately conclude that the dominant production is the one initiated by longitudinally polarized (i.e., helicity equal 0) vector bosons. Hence we will focus on the $W_0^+W_0^-$ in what follows.

The process will be computed at Next-to-Leading Order (NLO) accuracy, i.e. at one loop for the “exclusive” SS process and at tree-level for the extra emission processes $SS + X$. The interest of this calculation is twofold. First, it shows explicitly the quantitative importance of NLO contributions because of the double log enhancements discussed in the previous section. Actually we will see that those enhances are too large to be computed in perturbation theory above a certain threshold, and resummation is needed. This shows that all these effects will have to be taken into account in phenomenological analysis. Second, by the explicit NLO result we will be able to cross-check the high-energy theorems about massive gauge theories we illustrated in the previous chapters. Namely we will verify the exclusive and inclusive resummation results (though of course only at NLO), given in chapter 3. We will also verify the validity of the Equivalent Gauge approach discussed in section 2.4.

The calculations presented in this chapter, though verified manually whenever possible, have been performed by employing computer tools such as FEYNARTS, FORMCALC FEYNRULES and LOOPTOOLS. Let us briefly describe these tools and their application in the present context. First of all we have implemented the model into the MATHEMATICA package FEYNRULES [2] in order to generate Feynman rules for the vertexes and the propagators (the full list can be found in sect. A.1). Then, thanks to FEYNARTS [14], we have produced the expressions for the amplitude, without the algebra simplification and the loop integration. FORMCALC is used to perform the numerator algebra and the loop integration. In particular FORMCALC is optimized to perform the Passarino-Veltman reduction of tensor integrals into scalar ones, whose analytical values was obtained from PACKAGE X [22] and compared with the literature². Alternatively, when analytical expressions are too involved to be useful, we

¹We don’t investigate here the actual detectability of the process, which might be challenging if S is absolutely stable because of the \mathbb{Z}_2 symmetry, as in the SEHK model. One could either rely on same small amount of \mathbb{Z}_2 breaking or on the detection of particles (e.g. additional vector bosons as in sect. 4.3) produced in association with S.

²A brief review of the Passarino Veltman decomposition strategy, and the result concretely relevant for

make use of LOOPTOOLS [13] for numerical evaluation. In particular we will need it for the full one loop computation, in both the Equivalent Gauge and the standard formalism. Following the convention of Appendix A, we work in the t' Hooft Feynman gauge ($\xi = 1$ and $\tilde{m} = m_W$) and in the $\overline{\text{MS}}$ renormalization scheme.

The rest of the chapter is organized as follows. We first, in sect. 4.1, present the amputated 1 Particle Irreducible (1PI) two point functions for the bosonic sector of the theory. These are needed for the subsequent calculations and furthermore to verify the ST identity in eq. (2.59), which underlies the formulation of the Equivalent Gauge. Next, in sect. 4.2, we will consider exclusive production at one loop and compute all 1PI diagrams that appear in the amplitude. The full expression is too large to be displayed, hence for each class of diagrams we only report the divergent part and the leading terms in the m_W/\sqrt{s} expansion in Appendix C. The latter will allow us to verify the exclusive results of sect. 3.3. In this section we further investigate the validity of the general discussion of sect. 3.3 by showing that the double logs of each diagram actually match the general expectations. Tree level real emissions are included in sect. 4.3. This will allow us to compute the inclusive cross-section and verify eq. (3.56). Finally, the one loop computation is repeated by using the Equivalence Gauge showing perfect agreement.

4.1 Self-energies and Slavnov-Taylor identities

First of all, we compute all the form factors appearing in the propagators of the fields of the theory $\{W, \pi, S, h\}$ at one loop. The form factors will be useful for the computation of the next section. We moreover check at one loop the Slavnov-Taylor identities of eq. (2.59).

4.1.1 Transverse W , S and h

Let us start from the “physical” fields of the theory, namely the transverse W boson, the singlet S and the Higgs boson. From those correlators we will obtain the mass and the wave function renormalization factors, the physical mass and the residual (Z_W, Z_S, Z_h) at the propagator pole.

Transverse W

In order to find the one loop result of the $\Pi_{WW}(p^2)$ self energy, we have to compute all the diagrams of fig. C.1 and then to extract the transverse part i.e. Π_{WW}^T of eq. (2.56). In the following we report the full one-loop bare result, in terms of Passarino-Veltman scalar integral, along with their divergent part

$$\begin{aligned} \Pi_{WW}^T(p^2) = & \frac{g^2}{576\pi^2 m_h^2 p^2} \left\{ 3g^2 m_h^2 A_0(m_h^2) (m_h^2 - m_W^2 + 7p^2) + 36\lambda_S m_W^2 p^2 A_0(M_S^2) + \right. \\ & \left[p^2 (9m_h^2 (20m_W^2 + 13p^2) B_0(p^2, m_W^2, m_W^2) + 6m_h^4 + 2m_h^2 (57m_W^2 + 2p^2) - 108m_W^4) \right. \\ & \quad \left. - 3m_h^2 (m_h^4 - 2m_h^2 (m_W^2 + p^2) + m_W^4 + 10m_W^2 p^2 + p^4) B_0(p^2, m_h^2, m_W^2) \right. \\ & \quad \left. \left. - 3A_0(m_W^2) (m_h^4 - m_h^2 (m_W^2 - 29p^2) - 54m_W^2 p^2) \right] \right\}, \end{aligned} \quad (4.1)$$

$$\Pi_{WW,D}^T(p^2) \equiv p^2 \Pi_{WW,D1}^T + \Pi_{WW,D2}^T = p^2 \frac{19g^2}{n96\pi^2 \epsilon} + \frac{g^2 (3m_h^4 + 7m_h^2 m_W^2 + 18m_W^4) + 4\lambda_S M_S^2 m_W^2}{64\pi^2 m_h^2 \epsilon}. \quad (4.2)$$

our work, are reported in the Appendix B.

In order to end up with finite quantities, we have to pursue into the renormalization procedure, therefore, after the redefinition of eq. (A.9), we get

$$(A(p^2))_D = 0 \implies \delta Z_3(m_W^2 - p^2) + \delta m_W^2 + \Pi_{WW,D}^T(p^2) = 0, \quad (4.3)$$

$$(4.4)$$

The counterterms δm_W^2 and δZ_3 read

$$\delta Z_3 = \frac{1}{\epsilon} \Pi_{WW,D1}^T = \frac{19g^2}{96\pi^2}, \quad \delta m_W^2 = -(\delta Z_3 m_W^2 + \Pi_{WW,D2}^T). \quad (4.5)$$

For the pole mass, we have that

$$\begin{aligned} (m_W^{pole})^2 = & \bar{m}_W^2 + \frac{\bar{g}^2}{576\pi^2 \bar{m}_h^2 \bar{m}_W^2} \left\{ \left(3\bar{m}_h^2 \left(99\bar{m}_W^4 B_0(\bar{m}_W^2, \bar{m}_W^2, \bar{m}_W^2) - \right. \right. \right. \\ & \left. \left. \left(\bar{m}_h^4 - 4\bar{m}_h^2 \bar{m}_W^2 + 12\bar{m}_W^4 \right) B_0(\bar{m}_W^2, \bar{m}_h^2, \bar{m}_W^2) \right) - 3A_0(\bar{m}_W^2) \left(\bar{m}_h^4 + 28\bar{m}_h^2 \bar{m}_W^2 - 54\bar{m}_W^4 \right) \right. \\ & \left. \left. + 2\bar{m}_W^2 \left(3\bar{m}_h^4 + 59\bar{m}_h^2 \bar{m}_W^2 - 54\bar{m}_W^4 \right) \right) + 3\bar{g}^2 \bar{m}_h^2 A_0(\bar{m}_h^2) \left(\bar{m}_h^2 + 6\bar{m}_W^2 \right) + 36\bar{\lambda}_S \bar{m}_W^4 A_0(\bar{M}_S^2) \right\}, \end{aligned} \quad (4.6)$$

where all the scalar integrals, computed on the renormalized parameters, are understood free of the divergent part. For what concern the residual at the pole, $\sqrt{Z_W}$, we do not report the analytical expression, since we will make use of it only numerically

$$Z_W = \left. \frac{\partial \bar{\Pi}_{WW}(p^2)}{\partial p^2} \right|_{p^2=m_W^{pole}}, \quad (4.7)$$

where with $\bar{\Pi}_{WW}$ we denotes the finite part computed with the renormalized parameters.

Singlet S

The tree-level mass of the scalar S consist of two contributions, its own mass plus a factor coming from the spontaneous symmetry breakdown

$$M_S^2 = m_s^2 + \frac{1}{2} \lambda_S v^2.$$

At one loop, from the diagrams in fig. C.6 we get the two point function

$$\begin{aligned} \Pi_{SS}(p^2) = & \frac{\lambda_S}{16\pi^2 g^2 m_h^2} \left\{ m_W^2 \left(4\lambda_S m_h^2 B_0(p^2, m_h^2, M_S^2) - 9g^2 A_0(m_W^2) \right. \right. \\ & \left. \left. - 2\lambda_S A_0(M_S^2) + 6g^2 m_W^2 \right) - g^2 m_h^2 A_0(m_h^2) \right\}, \end{aligned} \quad (4.8)$$

where the divergent part is

$$\Pi_{SS}^D = -\frac{1}{\epsilon} \frac{\lambda_S (g^2 (m_h^4 + 9m_W^4) + 2\lambda_S m_W^2 (M_S^2 - 2m_h^2))}{16\pi^2 g^2 m_h^2}. \quad (4.9)$$

Therefore $\delta Z_S = 0$ and

$$\delta M_S^2 = \frac{1}{\epsilon} \frac{\lambda_S (g^2 (m_h^4 + 9m_W^4) + 2\lambda_S m_W^2 (M_S^2 - 2m_h^2))}{16\pi^2 g^2 m_h^2}. \quad (4.10)$$

For what concern the residual and the pole mass, we have

$$Z_S = \left. \frac{\partial \bar{\Pi}_{SS}(p^2)}{\partial p^2} \right|_{p^2=(M_S^{pole})^2}, \quad (4.11)$$

$$(M_S^{pole})^2 = -\frac{\bar{\lambda}_S (-4\bar{\lambda}_S \bar{m}_h^2 \bar{m}_W^2 B_0(\bar{M}_S^2, \bar{m}_h^2, \bar{M}_S^2) + \bar{g}^2 (\bar{m}_h^4 + 3\bar{m}_W^4) + 2\bar{\lambda}_S \bar{M}_S^2 \bar{m}_W^2)}{16\pi^2 \bar{g}^2 \bar{m}_h^2}. \quad (4.12)$$

Physical Higgs h

In order to perform the same analysis for the physical Higgs, we have to compute the diagrams in fig. C.2 with the result

$$\begin{aligned} \Pi_{hh}(p^2) = & \frac{1}{128\pi^2 g^2 m_W^2} \left\{ 3g^4 m_h^4 B_0(p^2, m_W^2, m_W^2) + 9g^4 m_h^4 B_0(p^2, m_h^2, m_h^2) \right. \\ & - 12g^4 m_W^2 p^2 B_0(p^2, m_W^2, m_W^2) + 36g^4 m_W^4 B_0(p^2, m_W^2, m_W^2) + 16\lambda_S^2 m_W^4 B_0(p^2, M_S^2, M_S^2) \\ & \left. + 3g^4 m_h^2 A_0(m_W^2) + 3g^4 m_h^2 A_0(m_h^2) + 18g^4 m_W^2 A_0(m_W^2) + 4g^2 \lambda_S m_W^2 A_0(M_S^2) - 36g^4 m_W^4 \right\}. \end{aligned} \quad (4.13)$$

The divergent part is

$$\Pi_{hh,D}(p^2) = \Pi_{hh,D1} p^2 + \Pi_{hh,D2} = -\frac{1}{\epsilon} \frac{3g^2 p^2}{32\pi^2} + \frac{1}{\epsilon} \frac{3g^4 m_h^4 - 3g^4 m_h^2 m_W^2 - 4g^2 \lambda_S M_S^2 m_W^2 + 8\lambda_S^2 m_W^4}{64\pi^2 g^2 m_W^2}, \quad (4.14)$$

and so the counterterms are

$$\delta Z_{2,\mathcal{H}} = \frac{1}{\epsilon} \frac{3g^2}{32\pi^2}, \quad \delta m_h^2 = \delta Z_{2,\mathcal{H}} m_h^2 - \Pi_{hh,D2} = \frac{1}{\epsilon} \frac{-3g^4 (m_h^4 - 3m_h^2 m_W^2) + 4g^2 \lambda_S M_S^2 m_W^2 - 8\lambda_S^2 m_W^4}{64\pi^2 g^2 m_W^2}. \quad (4.15)$$

Finally for the pole mass, we get

$$\begin{aligned} (m_h^{pole})^2 = & \frac{1}{128\pi^2 \bar{g}^2 \bar{m}_W^2} \left\{ 16\bar{\lambda}_S^2 \bar{m}_W^4 B_0(\bar{m}_h^2, \bar{M}_S^2, \bar{M}_S^2) + 3\bar{g}^4 (\bar{m}_h^4 + \bar{m}_h^2 \bar{m}_W^2 - 6\bar{m}_W^4) \right. \\ & \left. + 4\bar{g}^2 \bar{\lambda}_S \bar{M}_S^2 \bar{m}_W^2 + 3\bar{g}^4 ((\bar{m}_h^4 - 4\bar{m}_h^2 \bar{m}_W^2 + 12\bar{m}_W^4) B_0(\bar{m}_h^2, \bar{m}_W^2, \bar{m}_W^2) + 3\bar{m}_h^4 B_0(\bar{m}_h^2, \bar{m}_h^2, \bar{m}_h^2)) \right\} \end{aligned} \quad (4.16)$$

and

$$Z_h = \left. \frac{\partial \Pi_{hh}(p^2)}{\partial p^2} \right|_{p^2=(m_h^{pole})^2}. \quad (4.17)$$

4.1.2 “Unphysical fields” and Slavnov-Taylor

We now turn to the calculation of the two-point functions for the longitudinal W (W_0) and Goldstone system. The corresponding form factors Π_{WW}^L , $\Pi_{W\pi}$, $\Pi_{\pi\pi}$, as defined in eq. (2.53) will be needed in sect. 4.4, in order to perform the calculation in the Equivalent Gauge.

Longitudinal W

Computing the diagrams in fig. C.1, we get

$$\begin{aligned} \Pi_{WW}^L(p^2) = & \frac{g^2}{64\pi^2 m_h^2 p^2} \left\{ g^2 m_h^2 A_0(m_h^2) (-m_h^2 + m_W^2 + 3p^2) + 4\lambda_S m_W^2 p^2 A_0(M_S^2) + \right. \\ & \left[4m_W^2 p^2 (2m_h^2 B_0(p^2, m_W^2, m_W^2) - 3m_W^2) + A_0(m_W^2) (m_h^4 + 3p^2 (m_h^2 + 6m_W^2) - m_h^2 m_W^2) \right. \\ & \left. \left. + m_h^2 (m_h^4 - 2m_h^2 m_W^2 + m_W^4 - 4m_W^2 p^2) B_0(p^2, m_h^2, m_W^2) \right] \right\}, \end{aligned} \quad (4.18)$$

$$\Pi_{WW,D}^L(p^2) \equiv \Pi_{WW,D}^L = \frac{1}{\epsilon} \frac{19g^2}{96\pi^2} + \frac{1}{\epsilon} \frac{g^2 (3m_h^4 + 7m_h^2 m_W^2 + 18m_W^4) + 4\lambda_S M_S^2 m_W^2}{64\pi^2 m_h^2} = \Pi_{WW,D2}^T. \quad (4.19)$$

In order to fix the divergent part, we have to impose that the renormalized two-point function is finite, i.e.

$$\left(B(p^2) - \frac{p^2}{\xi} \right)_D = 0 \implies \delta Z_3(m_W^2 - p^2) + \delta m_W^2 + p^2 \delta \xi + \Pi_{WW,D}^L(p^2) = 0, \quad (4.20)$$

and then

$$\delta \xi = \delta Z_3 = \frac{1}{\epsilon} \frac{19}{96\pi^2} g^2. \quad (4.21)$$

Golstones system

For the $\Pi_{\pi\pi}$ form factor the diagrams to consider are in fig. C.4 and the results is

$$\begin{aligned} \Pi_{\pi\pi} = \frac{g^2}{64\pi^2 m_W^2} \left\{ -2m_h^2 m_W^2 B_0(p^2, m_h^2, m_W^2) - 2m_W^2 p^2 B_0(p^2, m_h^2, m_W^2) + \right. \\ \left. m_W^4 B_0(p^2, m_h^2, m_W^2) + m_h^4 B_0(p^2, m_h^2, m_W^2) - 4m_W^2 p^2 B_0(p^2, m_W^2, m_W^2) \right. \\ \left. + A_0(m_h^2)(m_W^2 - m_h^2) + A_0(m_W^2)(m_h^2 - m_W^2) \right\}, \end{aligned}$$

with the divergent part

$$\Pi_{\pi\pi,D}(p^2) \equiv p^2 \Pi_{\pi\pi,D} = -\frac{1}{\epsilon} \frac{3g^2}{32\pi^2} p^2.$$

For the counter terms, we have that

$$(p^2 F(p^2) - \xi \tilde{m}^2)_D \longrightarrow \delta Z_{2,\mathcal{H}}(p^2 - m_W^2) - m_W^2 \delta \xi - \delta \tilde{m}^2 + \Pi_{\pi\pi,D}(p^2) = 0,$$

and so

$$\delta \tilde{m}^2 = -m_W^2 (\delta Z_{2,\mathcal{H}} + \delta \xi) = -\frac{1}{\epsilon} \frac{7g^2 m_W^2}{24\pi^2}. \quad (4.22)$$

$W - \pi$ mixed propagator

Beyond the tree level, in our model, a non-vanishing mixed $W-\pi$ propagator appears. Computing the diagrams of fig. C.5 we get

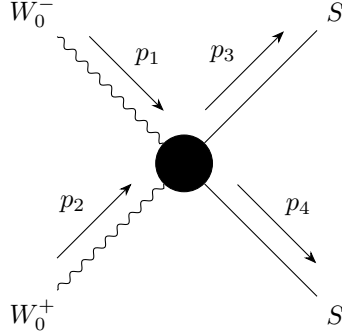
$$\begin{aligned} \Pi_{W\pi} = \frac{g}{128\pi^2} \left\{ \frac{g}{m_W p^2} \left[(2(m_h^4 - 2m_h^2 m_W^2 + m_W^4 - 3m_W^2 p^2) B_0(p^2, m_h^2, m_W^2) \right. \right. \\ \left. \left. + A_0(m_h^2)(-2m_h^2 + 2m_W^2 + 3p^2) + A_0(m_W^2)(2m_h^2 - 2m_W^2 + 3p^2) \right] \right. \\ \left. + 4gm_W B_0(p^2, m_W^2, m_W^2) + \frac{6g^2 m_W (3A_0(m_W^2) - 2m_W^2) + 4\lambda_S m_W A_0(M_S^2)}{gm_h^2} \right\}, \quad (4.23) \end{aligned}$$

with a divergence

$$\Pi_{W\pi,D} = \frac{1}{\epsilon} \frac{(g^2 (3m_h^4 + m_h^2 m_W^2 + 18m_W^4) + 4\lambda_S M_S^2 m_W^2)}{128\pi^2 m_h^2 m_W}.$$

We can check that the counter-terms computed before make the mixed two point function finite

$$(C(p^2) - \tilde{m})_D = 0 \longrightarrow \frac{\delta m_W^2}{2m_W} - \frac{\delta \tilde{m}^2}{2m_W} + \Pi_{W\pi,D}(p^2). \quad (4.24)$$

Figure 4.1: $W_0^-(p_1) W_0^+(p_2) \longrightarrow S(p_3) S(p_4)$ 

Slavnov Taylor

We are now able to check at one-loop level the result of eq. (2.59), namely

$$B(p^2)F(p^2) = C(p^2)^2.$$

At tree level it is trivially true and at one loop the relation we want explicitly to prove becomes

$$m_W^2 \Pi_{\pi\pi}(p^2) + p^2 \Pi_{WW}^L(p^2) = 2m_W \Pi_{W\pi}(p^2) p^2. \quad (4.25)$$

By an explicit computation it is straightforward to prove that, in the light of the result previously exposed, the RHS and the LHS of eq. (4.25) are the same.

4.2 $W_0 W_0 \rightarrow SS$ at one loop

Let us move now to the specific process of $W_0^-(p_1) W_0^+(p_2) \longrightarrow S(p_3) S(p_4)$, schematically depicted in fig. 4.1. According to the LSZ reduction formula, the matrix element of the process reads

$$\mathcal{M} = Z_W Z_S \mathcal{A}, \quad (4.26)$$

where Z_S and Z_W are the pole propagator residues for W and S , and \mathcal{A} denotes the Feynman amplitude.

At tree-level, $Z_W = Z_S = 1$ and the amplitude, corresponding to the diagram in fig. 4.2, is simply

$$\mathcal{M}^{tree} = \frac{g^2 v^2 \lambda_S \epsilon_1^L \cdot \epsilon_2^L}{2(s - m_h^2)} = \frac{g^2 v^2 \lambda_S}{2(s - m_h^2)} \left(\frac{s}{2m_W^2} - 1 \right). \quad (4.27)$$

We are particularly interested in the high-regime behaviour of the process, i.e.

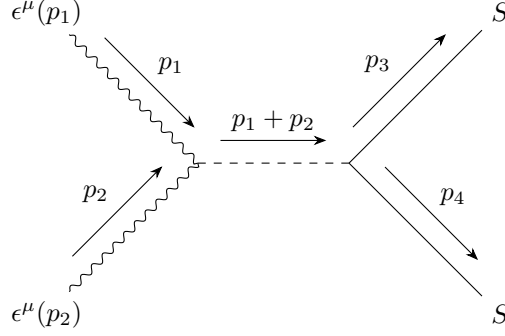
$$s \sim |t| \sim |u| \sim M_S \gg m_W \sim m_h, \quad (4.28)$$

where s, t, u are the standard Mandelstam invariants

$$t \equiv (p_1 - p_3)^2, \quad u \equiv (p_1 - p_4)^2, \quad s \equiv (p_1 + p_2)^2. \quad (4.29)$$

In this regime the tree level process is proportional to the coupling constant with no dependence on the energy, namely

$$\mathcal{M} = \lambda_S + \mathcal{O}\left(\frac{m_W}{\sqrt{s}}\right). \quad (4.30)$$

Figure 4.2: Tree-level diagram for the process $WW \rightarrow SS$ 

Let us switch to the one-loop calculation. At this order the amplitude in eq. (4.26) can be written as

$$\mathcal{M}^{1L} = (Z_W^{1L} + Z_S^{1L}) \mathcal{M}^{tree} + \mathcal{M}^{tree} \left(m_W^{pole}, M_S^{pole} \right) + \mathcal{A}^{1L}, \quad (4.31)$$

where, as indicated in the equations, the external particles masses are the poles ones. Wave functions and masses have been computed in the previous section. The one loop Feynman amplitude is conveniently expressed as

$$\begin{aligned} \mathcal{A}^{1L} = & \Gamma_{W_0W_0 \rightarrow SS}^{1L} + \Gamma_{W_0W_0 \rightarrow h}^{1L} G_{hh}^{tree}(s) \Gamma_{h \rightarrow SS}^{tree} \\ & + \Gamma_{W_0W_0 \rightarrow h}^{tree} G_{hh}^{tree}(s) \Gamma_{h \rightarrow SS}^{1L} + \Gamma_{W_0W_0 \rightarrow h}^{tree} G_{hh}^{1L}(s) \Gamma_{h \rightarrow SS}^{tree}, \end{aligned} \quad (4.32)$$

where we are using the following notation:

- $\Gamma_{W_0W_0 \rightarrow h}$ one-particle irreducible diagrams for the process $W_0(p_1)W_0(p_2) \rightarrow h(p_3)$ with $p_1^2 = p_2^2 = m_W^2$ and the Higgs off-shell $p_3^2 = (p_1 + p_2)^2 = s$;
- $\Gamma_{SS \rightarrow h}$ one-particle irreducible diagrams for the process $S(p_1)S(p_2) \rightarrow h(p_3)$ with $p_1^2 = p_2^2 = M_S^2$ and the Higgs off-shell $p_3^2 = (p_1 + p_2)^2 = s$;
- $\Gamma_{W_0W_0 \rightarrow SS}$ one-particle irreducible diagrams for the process $W_0(p_1)W_0(p_2) \rightarrow S(p_3)S(p_4)$ with $p_1^2 = p_2^2 = m_W^2$ and $p_3^2 = p_4^2 = M_S^2$.

Each of these diagrams has been computed analytically using the computer tools previously described. However the resulting expression are too involved to be useful. In what follows we will only report the divergent part of the result and the leading terms in the high energy expansion of eq. (4.28). The former will be needed for renormalization, the latter to verify that the result matches with the one expected at the leading double logs order.

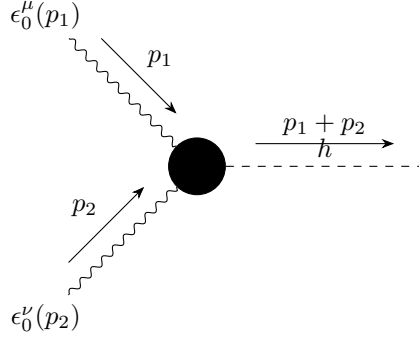
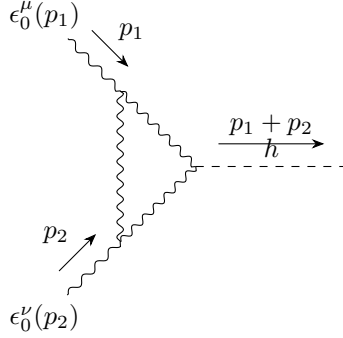
$\Gamma_{W_0W_0 \rightarrow h}$

At tree-level, the process $\Gamma_{W_0W_0 \rightarrow h}^{tree}$ (schematically represented in fig. 4.3), present the following amplitude

$$\Gamma_{WW \rightarrow h}^{tree} = g m_W \epsilon_L(p_1) \cdot \epsilon_L(p_2) = g \frac{s}{2m_W} + \mathcal{O}(s^0). \quad (4.33)$$

At one loop we have a divergent part

$$\left(\Gamma_{WW \rightarrow h}^{1L,D} \right)^{\mu\nu} = \frac{1}{\epsilon} \frac{\eta^{\mu\nu} \left(g^3 \left(3m_h^4 + 17m_h^2 m_W^2 + 18m_W^4 \right) + 4g\lambda_S M_S^2 m_W^2 \right)}{128\pi^2 m_h^2 m_W} \quad (4.34)$$

Figure 4.3: $W_0^-(p_1)W_0^+(p_2) \rightarrow h(p_1 + p_2)$ Figure 4.4: one-loop diagram giving the leading contribution to the process $W_0^-(p_1)W_0^+(p_2) \rightarrow h(p_1 + p_2)$ 

To obtain a finite result, then, we perform the rescaling of eq. (A.9) and so we get

$$Z_3\sqrt{Z_{2,\mathcal{H}}}\Gamma_{WW\rightarrow h}^D = 0 \rightarrow \bar{g} \left(\delta g \bar{M}_W + \frac{\delta m_W^2}{2\bar{M}_W} \right) + \bar{\Gamma}_{WW\rightarrow h}^D = 0,$$

where $\bar{\Gamma}$ is the vertex operator Γ computed with the renormalized parameters. We obtain

$$\delta g = \frac{1}{\epsilon} \frac{g^2}{48\pi^2}. \quad (4.35)$$

For the present discussion we need the leading terms of the one loop amplitude at high energy. The computation is presented in Appendix C and the result is the one of eq. (C.2) which reads

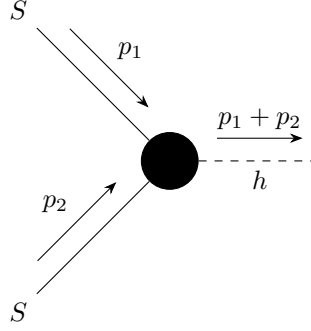
$$\Gamma_{W_0W_0\rightarrow h}^{1L} = \Gamma_{W_0W_0\rightarrow SS}^{tree} \left(-\frac{\alpha}{8\pi} \log^2 \left(\frac{s}{m_W^2} \right) + \mathcal{O} \left(\log \left(\frac{s}{m_W^2} \right) \right) \right). \quad (4.36)$$

Notice that the double logs terms of eq. (4.36) come only from the kind of diagrams reported in fig. 4.4.

$\Gamma_{SS\rightarrow h}$

At tree level amplitude (depicted in fig. 4.5) is the following

$$\Gamma_{SS\rightarrow h}^{tree} = -2\lambda_S \frac{m_W}{g}. \quad (4.37)$$

Figure 4.5: $S(p_1)S(p_2) \rightarrow h(p_1 + p_2)$ 

At one loop the diagrams to consider are the ones reported in appendix C, and the result reported in eq. (C.3), is found to be free of double logs. Here we report only the divergent part, in order to find $\delta\lambda_S$ counterterm

$$\Gamma_{SS \rightarrow h}^D = \frac{1}{\epsilon} \frac{\lambda_S (3g^2 (m_h^4 - m_h^2 m_W^2 - 6m_W^4) + 4\lambda_S m_W^2 (4m_h^2 - M_S^2))}{64\pi^2 g m_h^2 m_W}.$$

We impose $\sqrt{Z_{\mathcal{H}}} Z_2 \Gamma_{SS \rightarrow h}$ to be finite

$$\bar{\Gamma}_{SS \rightarrow h}^D + \frac{2\lambda_S m_W}{g} \delta\lambda_S - \frac{2\lambda_S m_W}{g} \delta g + \frac{\lambda_S \delta m_W^2}{m_W g} = 0,$$

and then

$$\delta\lambda_S = -\frac{1}{\epsilon} \frac{3g^2 (m_h^2 - m_W^2) + 8\lambda_S m_W^2}{64\pi^2 m_W^2}.$$

$\Gamma_{W_0W_0 \rightarrow SS}$

Now, we are going to compute the one loop one particle irreducible correction to the Feynman amplitude of the process. The list of all the diagrams, with the relative values, can be found in Appendix C. The result is eq. (C.4) with no divergent part. This was expected in the light of the fact that we have not such a vertex operator in our tree level Lagrangian in eq. (2.52). Taking the high-energy limit $s \gg m_W^2$ we can find that

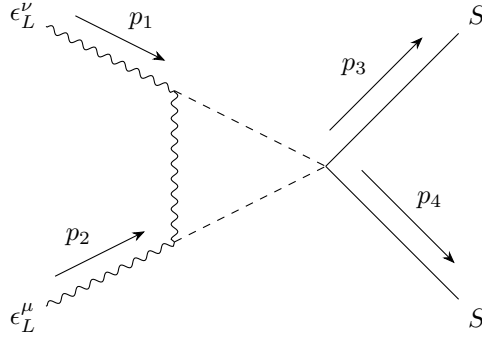
$$\Gamma_{W_0W_0 \rightarrow SS}^{1L} = \Gamma_{W_0W_0 \rightarrow SS}^{tree} \left(-\frac{\alpha}{16\pi} \log^2 \left(\frac{s}{m_W^2} \right) + \mathcal{O} \left(\log \left(\frac{s}{m_W^2} \right) \right) \right), \quad (4.38)$$

and this contribution can be identified coming from the diagram in fig. 4.6.

To summarize, in this section until now, we have computed the S-matrix element for the process $W_0^- W_0^+ \rightarrow SS$ at one-loop. The total result, according to the decomposition of eq. (4.26), for the Feynman amplitude \mathcal{A}^{1L} at one loop, is in eq. (C.5). The complete result will be used for the numerical calculation. Let us now concentrate on the leading double log corrections, in order to compare the result with the theoretical predictions. From eq. (4.38) and eq. (4.36) we can easily find

$$\mathcal{A}^{1L} =_{DL} \mathcal{A}^{tree} \left(-\frac{3\alpha}{16\pi} \log^2 \left(\frac{s}{m_W^2} \right) \right), \quad (4.39)$$

which shows that the double log terms, in each of the sets of diagrams contributing to eq. (3.50), match the general result for the leading virtual correction derived in eq. 3.39.

Figure 4.6: One loop diagram giving the leading contribution to $\Gamma_{W_0 W_0 \rightarrow SS}$ 

Cross-section

In order to verify the agreement between the expected theoretical result and the one loop one, we are going to compute the cross-section for the given process. We work in the center of mass, where the momenta of the ingoing/outgoing particles are defined as follows

$$\begin{aligned} p_1^\mu &= (E_{\mathbf{p}}, 0, 0, p), & p_2^\mu &= (E_{\mathbf{p}}, 0, 0, -p), & E_{\mathbf{p}}^2 &= m_W^2 + p^2, \\ p_3^\mu &= (E_{\mathbf{p}'}, 0, p' \sin \theta, p' \cos \theta), & p_4^\mu &= (E_{\mathbf{p}'}, 0, -p' \sin \theta, -p' \cos \theta), & E_{\mathbf{p}'}^2 &= M_S^2 + p'^2. \end{aligned}$$

The tree level cross-section is very trivial to compute and the result is the following.

$$\sigma^{tree} = \frac{1}{16\pi s} \frac{p'}{p} |\mathcal{M}^{tree}|^2, \quad (4.40)$$

The one loop result is

$$\sigma^{1L} \equiv \frac{1}{32\pi s} \frac{\sqrt{\frac{s}{4} - M_S^2}}{\sqrt{\frac{s}{4} - m_W^2}} \int_0^\pi \sin \theta d\theta |\mathcal{M}^{tree} + \mathcal{M}^{1L}|^2. \quad (4.41)$$

In order to compute it we employ the software LOOPTOOLS to get the numerical values of the Feynman-Integral and then we perform the numerical computation of the cross-section above. The results is reported in chapter 5 (fig. 5.1 (a)) and discussed there in some details. In the figure 5.1 (b) it is compared with the resummed expression which, according to eq. 3.39, is

$$\sigma^{excl} = \sigma^{tree} \exp\left(-\frac{3\alpha}{8\pi} \log^2\left(\frac{s}{m_W^2}\right)\right). \quad (4.42)$$

Let us discuss briefly the results. In both the figures of fig. 5.1, we report the chosen cross-sections normalized with the tree level one. It can be noticed that, both the cross-sections are remarkable different from the tree-level, and the gap increases with the energy. This shows, as anticipated, a breakdown of the perturbation theory: a fixed order perturbative expansion is not sufficient to obtain a useful result. We can notice, moreover, that both the curves go down rapidly and, therefore, we can identify the exclusive cross-section as a not good candidate for a physical observable.

4.3 $W_0 W_0 \rightarrow SS + X$

In order to end up with a cross-section with phenomenological relevance, we need to consider the possible emission of additional particles. As the matter of fact, since the possibility of non additional emissions becomes more and more improbable with the increasing of

energy, as we stressed before, the exclusive cross section is high energy suppressed. We limit our analysis, here, to the leading contribution to the Born cross section of our VBF process plus the emission of an additional particle. Resummed formulas, allowing for an arbitrary number of emission, were found in eq. (3.100). Notice that, because of symmetries, the only additional particle to the process $W_0W_0 \rightarrow SS$ could be only an Higgs h or a W^3 boson. Then, according to the discussion of chapter 3, we know that the cross-section with the emission of a soft and collinear higgs is subleading with respect to the ones with an additional W^3 and so the latter is the only case we are going to study explicitly.

We report in table 4.1 the three tree-level diagrams for the process and the respective full amplitude and the amplitude in the limit of soft and collinear W^3 emitted.

In order to check the validity of eq. (3.64) at leading log, we need to compute the cross section for the process. For simplicity, we are going to integrate only over the phase space configurations, in which q is collinear and soft with respect to p_1 and p_2 . It is immediate to see that ${}^1\mathcal{M}_{W_0W_0 \rightarrow SSW^3}$ is high energy suppressed and after a straightforward computation we find

$$d\sigma^{(1)} =_{DL} \int \frac{d^3q}{(2\pi)^3 2\omega_q} ({}^3\mathcal{M}_{W_0W_0 \rightarrow SSW^3}^* {}^2\mathcal{M}_{W_0W_0 \rightarrow SSW^3} + {}^2\mathcal{M}_{W_0W_0 \rightarrow SSW^3}^* {}^3\mathcal{M}_{W_0W_0 \rightarrow SSW^3}) \quad (4.49)$$

$$=_{DL} \lambda_S^2 \frac{\alpha}{8\pi} \log\left(\frac{s}{m_W^2}\right) \quad (4.50)$$

times the 2-body phase-space factor (for the SS system), which we omitted from the previous expression. By a simple integration we get

$$\sigma^1 = \sigma_B \times \left(\frac{\alpha}{8\pi}\right) \log\left(\frac{s}{m_W^2}\right). \quad (4.51)$$

Now, remembering that

$$\sigma^{inc,1L} = \sigma^{exc,1L} + \sigma^1 \quad (4.52)$$

we find an evident matching with eq. (3.100) at one loop.

The result of eq. (4.52) is reported in fig. 5.1, for both the first order inclusive cross-section (a) and the resummed one (b). Notice that, both the cross-section are very different from the tree level amplitude, showing the necessity of a resummation. We can also note that the resummed inclusive cross-section, with the increasing of the energy, level up to a half of the Born one and do not go to zero (relative to the tree-level result) as the exclusive one. The inclusive cross-section is, for sure, the most probable configuration that can be observed in an experiment.

4.4 $W_0W_0 \rightarrow SS$ in the Equivalent Gauge

In this section we repeat the computation of the one loop exclusive amplitude within the formalism of the Equivalent Gauge, introduced in sect. 2.4. The advantage of the Equivalent Gauge is that the high energy power counting is manifest. The disadvantage is that the number of diagrams to compute increase. Those relevant for our process are depicted in fig. 4.7, leading to a scattering amplitude

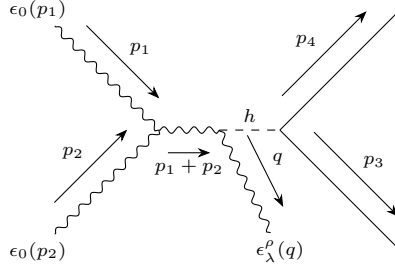
$$\mathcal{M} = Z_W Z_S \mathcal{A}, \quad (4.53)$$

with

$$\mathcal{A} \equiv \mathcal{A}_{W_L W_L \rightarrow SS}^L + m_W \mathcal{A}_{\pi W_L \rightarrow SS} + m_W \mathcal{A}_{W_L \pi \rightarrow SS} + m_W^2 \mathcal{A}_{\pi\pi \rightarrow SS}, \quad (4.54)$$

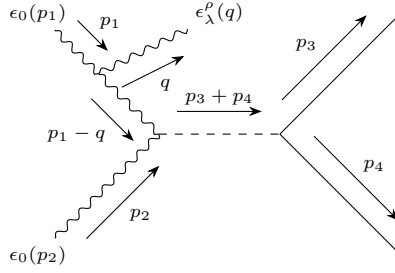
where, as in sect. 4.2, we have defined

$$\begin{aligned} \mathcal{A}_{W_L W_L \rightarrow SS}^L &\equiv \epsilon_L^\mu(p_1) \epsilon_L^\mu(p_2) \mathcal{A}[W_\mu(p_1), W_\nu(p_2), S(p_3), S(p_4)], \\ \mathcal{A}_{W_L \pi \rightarrow SS} &\equiv \epsilon_\pi \epsilon_L^\mu(p_2) \mathcal{A}[\Pi(p_1), W_\mu(p_2), S(p_3), S(p_4)], \\ \mathcal{A}_{W_L \pi \rightarrow SS} &\equiv \epsilon_\pi \epsilon_L^\mu(p_1) \mathcal{A}[W_\mu(p_1), \Pi(p_2), S(p_3), S(p_4)]. \end{aligned} \quad (4.55)$$

Table 4.1: Tree-level diagrams for the process $W_0^+ W_0^- \rightarrow S S W^3$ 

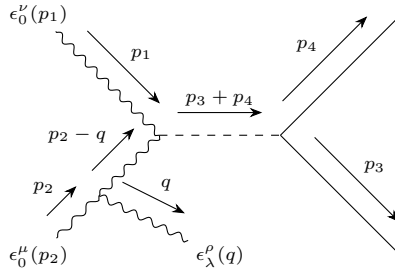
$${}^1 \mathcal{M}_{W_0 W_0 \rightarrow S S W^3} = -\frac{g^3 \lambda_S v^2}{2} \left\{ \frac{2(\epsilon_0(p_1) \cdot p_2)(\epsilon_0(p_2) \cdot \epsilon_\lambda(q))}{(s - m_W^2)((p_3 + p_4)^2 - m_W^2)} - \frac{2(\epsilon_0(p_2) \cdot p_1)(\epsilon_0(p_1) \cdot \epsilon_\lambda(q)) + \epsilon_0(p_1) \cdot \epsilon_0(p_2)(\epsilon_\lambda(q) \cdot p_1 - \epsilon_\lambda(q) \cdot p_2)}{(s - m_W^2)((p_3 + p_4)^2 - m_W^2)} \right\} \quad (4.43)$$

$$\simeq_{q \rightarrow 0} -\frac{g^3 \lambda_S v^2}{2} \left\{ \frac{2(\epsilon_0(p_1) \cdot p_2)(\epsilon_0(p_2) \cdot \epsilon_\lambda(q))}{(s - m_W^2)(s - m_W^2)} - \frac{2(\epsilon_0(p_2) \cdot p_1)(\epsilon_0(p_1) \cdot \epsilon_\lambda(q)) + \epsilon_0(p_1) \cdot \epsilon_0(p_2)(\epsilon_\lambda(q) \cdot p_1 - \epsilon_\lambda(q) \cdot p_2)}{(s - m_W^2)(s - m_W^2)} \right\} \quad (4.44)$$



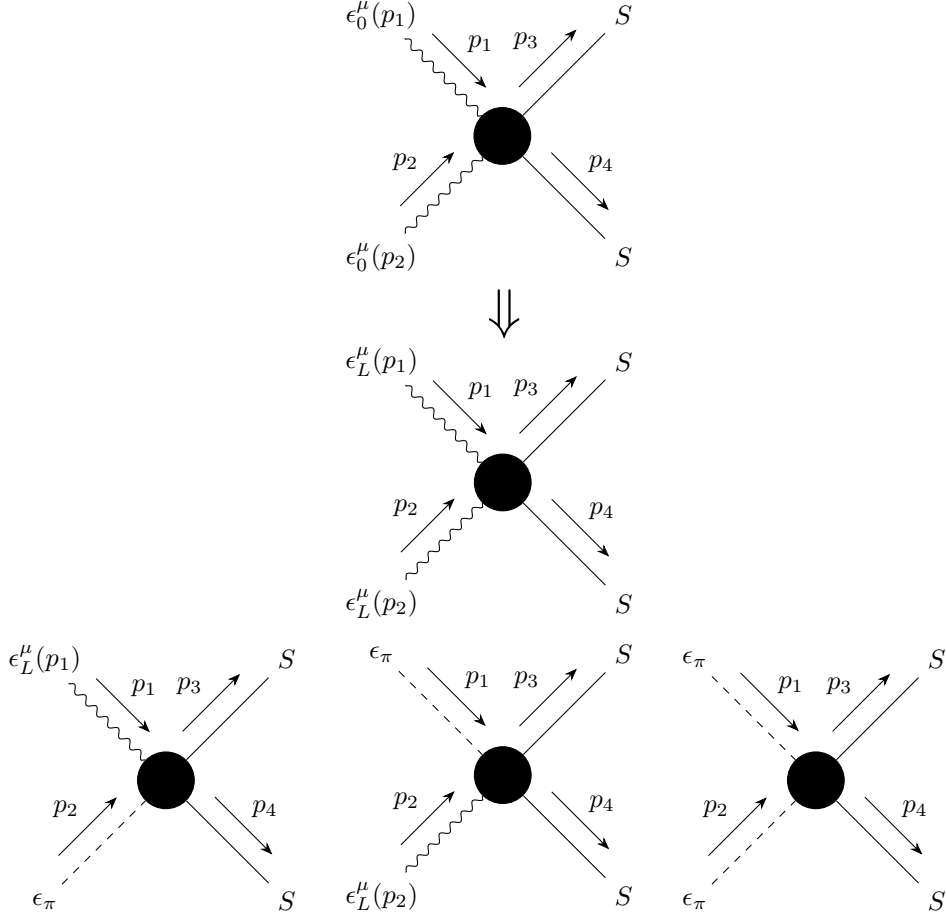
$${}^2 \mathcal{M}_{W_0 W_0 \rightarrow S S W^3} = -\frac{g^3 \lambda_S v^2}{2} \left\{ \frac{2\epsilon_0(p_1) \cdot q \epsilon_0(p_2) \cdot \epsilon_\lambda(q) - \epsilon_0(p_1) \epsilon_\lambda(q) (\epsilon_0(p_2) \cdot p_1 + \epsilon_0(p_1) \cdot p_2)}{((p_1 + p_2 - q)^2 - m_W^2)((p_1 - q)^2 - m_W^2)} + \frac{2\epsilon_0(p_1) \cdot \epsilon_0(p_2) \epsilon_\lambda(q) \cdot p_1}{((p_1 + p_2 - q)^2 - m_W^2)((p_1 - q)^2 - m_W^2)} \right\} \quad (4.45)$$

$$\simeq_{q \rightarrow 0} -\frac{g^3 \lambda_S v^2}{2} \frac{-2\epsilon_0(p_1) \cdot \epsilon_0(p_2) \epsilon_\lambda(q) \cdot p_1 + \epsilon_0(p_1) \cdot \epsilon_\lambda(q) \epsilon_0(p_2) \cdot p_1}{(2p_1 \cdot q)(s - m_W^2)} \quad (4.46)$$



$${}^3 \mathcal{M}_{W_0 W_0 \rightarrow S S W^3} = -\frac{g^3 \lambda_S v^2}{2} \left\{ \frac{2\epsilon_0(p_2) \cdot q \epsilon_0(p_1) \cdot \epsilon_\lambda(q) - \epsilon_0(p_2) \epsilon_\lambda(q) (\epsilon_0(p_1) \cdot p_2 + \epsilon_0(p_2) \cdot p_1)}{((p_2 + p_1 - q)^2 - m_W^2)((p_2 - q)^2 - m_W^2)} + \frac{2\epsilon_0(p_2) \cdot \epsilon_0(p_1) \epsilon_\lambda(q) \cdot p_2}{((p_2 + p_1 - q)^2 - m_W^2)((p_2 - q)^2 - m_W^2)} \right\} \quad (4.47)$$

$$\simeq_{q \rightarrow 0} -\frac{g^3 \lambda_S v^2}{2} \frac{-2\epsilon_0(p_2) \cdot \epsilon_0(p_1) \epsilon_\lambda(q) \cdot p_2 + \epsilon_0(p_2) \cdot \epsilon_\lambda(q) \epsilon_0(p_1) \cdot p_2}{(2p_2 \cdot q)(s - m_W^2)} \quad (4.48)$$

Figure 4.7: $W_0W_0 \rightarrow SS$ in the Equivalent Gauge

The (modified) polarization vector ϵ_L^μ and the “Goldstone wave function” ϵ_π are defined in sect. 2.4.

The tree-level process, in the Equivalent Gauge, is described by the diagrams of Fig 4.8. whose values are

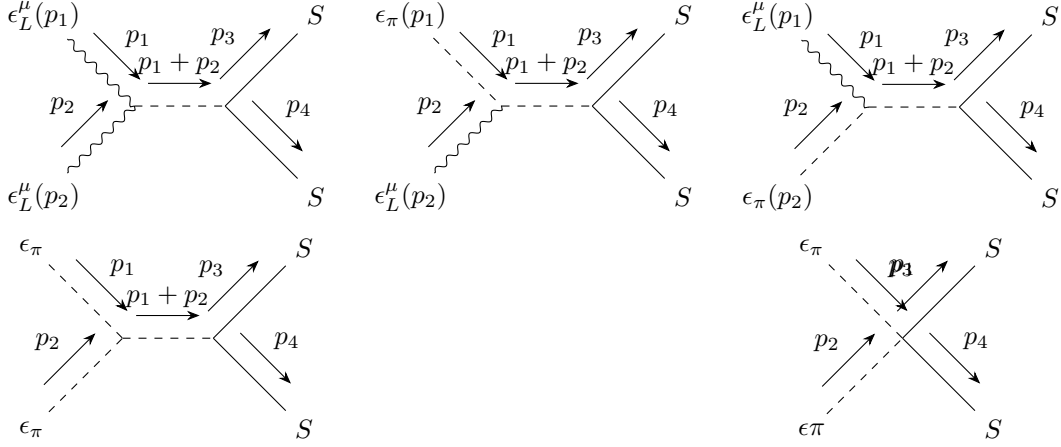
$$\begin{aligned}
 \mathcal{M}_{W_0W_0 \rightarrow SS} &= \overbrace{\left(\lambda_S \frac{2m_W^2}{s - m_h^2} \epsilon_L(p_1) \cdot \epsilon_L(p_2) \right)}^{\mathcal{A}_{W_LW_L \rightarrow SS}} - im_W \overbrace{\left(-\lambda_S \frac{1}{s - m_h^2} \epsilon(p_1) \cdot (p_1 + p_2) \epsilon_\pi \right)}^{\mathcal{A}_{W_L\pi \rightarrow SS}} \\
 &- im_W \overbrace{\left(-\lambda_S \frac{1}{s - m_h^2} \epsilon(p_2) \cdot (p_1 + p_2) \epsilon_\pi \right)}^{\mathcal{A}_{\pi W_L \rightarrow SS}} + \overbrace{\left(-\lambda_S \frac{s}{s - m_h^2} \right)}^{\mathcal{A}_{\pi\pi \rightarrow SS}} \epsilon_\pi^2 = \lambda_S \frac{2M_W^2}{s - m_h^2} \left(\frac{s}{2m_W^2} - 1 \right),
 \end{aligned} \tag{4.56}$$

where we have used that

$$\epsilon_L(p_1) \cdot \epsilon_L(p_2) = 2 \frac{(p - E_p)^2}{m_W^2}, \quad \epsilon_L(p_{1/2}) \cdot p_{1/2} = -m_W, \quad \epsilon_L(p_1) \cdot p_2 = -\frac{(p - E_p)^2}{m_W} = \epsilon_L(p_2) \cdot p_1,$$

and that, obviously, at tree level $\epsilon_\pi = -i$.

The result of eq. (4.8) concedes with the one we have obtained in eq. (4.27) with the standard formalism. The full one loop result, as we have seen, is too much involved. Therefore, we limit our analytical computation to the leading terms in the high energy expansion. We have, also, verified that the full Equivalent Gauge result is numerically identical to the one derived in the previous section. At high energy, thanks to the properties of the polarization

Figure 4.8: Tree-level diagrams for the process $W_0W_0 \rightarrow SS$ in the Equivalent Gauge

vectors we employ in the Equivalent Gauge, the only non mass suppressed terms is the one with the Goldstones, i.e. the amplitude $A_{\pi\pi \rightarrow SS}$. At one loop this can be written as

$$\mathcal{A}_{\pi\pi \rightarrow SS}^{1L} = \Gamma_{\pi\pi \rightarrow h}^{1L} G_{hh}^{tree} \Gamma_{h \rightarrow SS}^{tree} + \Gamma_{\pi\pi \rightarrow h}^{tree} G_{hh}^{1L} \Gamma_{h \rightarrow SS}^{tree} + \Gamma_{\pi\pi \rightarrow h}^{tree} G_{hh}^{tree} \Gamma_{h \rightarrow SS}^{1L} + \Gamma_{\pi\pi \rightarrow SS}^{1L}, \quad (4.57)$$

where a notation analogue to eq. (4.32) has been employed.

It is easy to see that

$$\mathcal{A}_{\pi\pi \rightarrow SS}^{1L} = \Gamma_{\pi\pi \rightarrow SS}^{1L} + \mathcal{O}\left(\frac{m_W}{\sqrt{s}}\right) \quad (4.58)$$

by, simply, power-counting analysis. In fact, we know that both $\Gamma_{\pi\pi \rightarrow h}$ and $\Gamma_{h \rightarrow SS}$ are mass suppressed at tree level and that the propagators also vanish at high energy.

The diagrams to consider are, thus, only the ones of Fig. C.4 and, as eq. (4.2), we report, along with the approximate result, the divergent part and the leading behaviour

$$\Gamma_{\pi\pi \rightarrow SS} = {}_{DL} - \lambda_S \frac{3\alpha}{8\pi} \log^2\left(\frac{s}{m_W^2}\right) \quad (4.59)$$

$$\Gamma_{\pi\pi \rightarrow SS}^D = \frac{\lambda_S (3g^2 m_h^2 - m_W^2) + 8\lambda_S m_W^2}{64\pi^2 m_W^2}. \quad (4.60)$$

A more detailed result, can be found in eq. (C.1). In order to complete the calculation we need to compute the scalar wave function ϵ_π , defined in eq. (2.66). At one loop, this is given by

$$\epsilon_\pi = -i \left(1 + \frac{\Pi_{WW}^L(m_W^2)}{m_W^2} + \frac{\Pi_{W\pi}(m_W)}{m_W} \right), \quad (4.61)$$

for bare quantities³ or explicitly

$$\begin{aligned} \epsilon_\pi = 1 + \frac{1}{128\pi^2 m_h^2 m_W^2} g^2 \left\{ \right. & \left[3A_0(m_W^2)(m_h^2 + 6m_W^2) \right. \\ & \left. - 2m_W^2(m_h^2 B_0(m_W^2, m_h^2, m_W^2) - 6m_h^2 B_0(m_W^2, m_W^2, m_W^2) + 6m_W^2) \right] \\ & \left. + 3g^2 m_h^2 A_0(m_h^2) + 4\lambda_S m_W^2 A_0(M_S^2) \right\}. \end{aligned}$$

³For renormalized ones, instead, we have to consider $\frac{\sqrt{Z_2}}{\sqrt{Z_{3,\mathcal{H}}}} \bar{\epsilon}_\pi$

Therefore, at one loop we, finally, have

$$\mathcal{A}_{W_0W_0 \rightarrow SS}^{1L} = \epsilon_\pi^2 \mathcal{A}_{\pi\pi \rightarrow SS}^{tree} + \mathcal{A}_{\pi\pi}^{1L} + \mathcal{O}\left(\frac{m_W}{\sqrt{s}}\right), \quad (4.62)$$

and substituting all the factors we have back the result of eq. (C.5). The full computation of eq. (4.54) also brings to the same result of eq. (4.26).

Chapter 5

Conclusions

In this thesis we discussed the high energy properties of massive gauge theories, far above their characteristic mass scale. After a general introduction, we focused on two main specific topics: the Equivalence Theorem and the resummation of double logs of Sudakov type. We discussed and examined these topics in two ways. First of all we reviewed the existing literature on the subject trying to clarify the derivation of existing result. In particular this led us, in sect. 3.4.1 to an alternative derivation of double logs resummation formulas for inclusive cross-section. Second, we performed a concrete NLO calculation for a specific process, in order to verify the validity of the general results.

The well-known Equivalence Theorem is discussed in its general formulation, presenting it via the so-called “Equivalent Gauge”, a less-known reformulation of the standard computation strategy for massive gauge theories. Verifying the validity of this approach at one loop level and at all order energy expansion, is one of the main original results of the present work. For what concerns the other main topic, i.e. Sudakov double logs, we review in details the existing literature and we give a generalization of the method of the infrared evolution equation of Ref. [12], for double logs coming from virtual emission, to the case of real emission. In particular, for inclusive cross-section, we get the same result of Ref. [6] with a more transparent and effective approach.

Concerning the explicit calculation, let us briefly summarize what we have found. We started with the computation of the S-matrix element for the process $W_0W_0 \rightarrow SS$ at NLO, within the singlet-extended Higgs-Kibble model (introduced in the thesis). By taking the high energy limit of the result we have found that the leading one loop contributions to the tree level, are the double logs of infrared nature we predicted on the basis of the general formulas in the previous chapters. Furthermore, we computed the leading contribution to $W_0W_0 \rightarrow SS + X$ production, due by the emission of a soft and collinear gauge bosons. These corrections are significant as well as the ones due to virtual emissions and need to be taken into account, at energies above order 10 TeV in order to obtain accurate predictions. Resummation further changes the result and need to be taken into account.

As a final summary for our work, we display in Fig. 5.1 all the predictions we have obtained for the $W_0W_0 \rightarrow SS$ production cross-sections, normalized to the tree level one. Namely, we report on the left panel the one loop exclusive cross-section, together with the NLO inclusive one. The resummed expressions, exclusive and inclusive, are reported in the right panel. The figure displays a number of interesting features. We see a large and growing-with-energy negative one-loop contribution to the exclusive cross-section, which reduces it relative to the tree-level. These are the famous “negative Sudakov logs”. Second we notice that the one loop result is rather close to the resummed exclusive expansion, even if the two cross sections eventually depart at a very high energy because of the double log exponentiation in the resummed formula. The behaviour of the inclusive cross-section is also very interesting. Unlike the exclusive one, which goes to zero as

$$\frac{\sigma^{excl}}{\sigma_B} = \exp\left(-\frac{3\alpha}{8\pi} \log^2\left(\frac{s}{m_W^2}\right)\right), \quad (5.1)$$

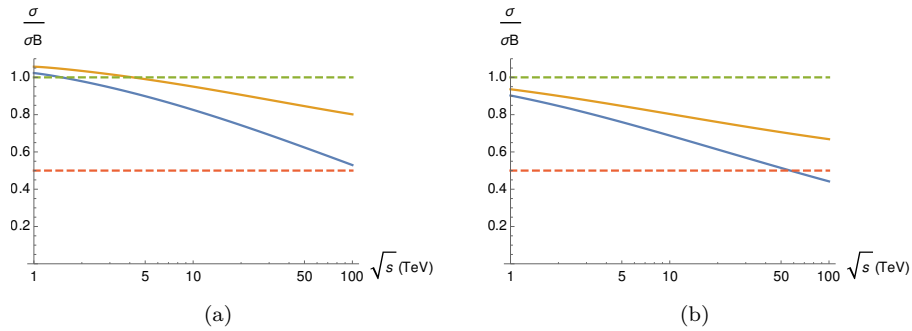


Figure 5.1: (a) Comparison between one loop exclusive (blue line), inclusive (orange line) cross sections (b). Comparison between resummed exclusive (blue line), inclusive (orange line) cross sections. The parameters chosen for both the plots are $g = 0.65$, $m_W = 0.08 \text{ TeV}$, $m_h = 0.125 \text{ TeV}$, $\lambda_S = 0.1$, $M_S = \sqrt{s}/3$, $\mu = \sqrt{s}$.

relative to the three level, the inclusive one goes to a constant (as we saw in sect. 3.4.1)

$$\frac{\sigma^{inc}}{\sigma_B} = \frac{1 + \exp\left(-\frac{\alpha}{2\pi} \log^2\left(\frac{s}{m_W^2}\right)\right)}{2}. \quad (5.2)$$

This means that at asymptotically high energy the exclusive process becomes rare, and the vast majority of the SS production events come accompanied by the emission of soft gauge bosons which are nearly collinear to the beam axis. On top of computing accurately the inclusive cross-section as we did in this thesis, an accurate modelling of the soft vector boson radiation will be needed for a concrete experimental analysis of the process. So-called ‘‘Electroweak showering’’ techniques to QCD parton showering will have to be further developed. This shows once again that Electroweak high energy physics is an intricate and stimulating theoretical subject on which a lot of work will be needed in the forthcoming years.

Appendix A

Feynman rules and renormalization scheme

In all the computations performed in the thesis we adopted the t'Hooft Feynman gauge (i.e. $\xi = 1$ and $\tilde{m} = m_W$). Differently from eq. (2.48) we have worked in the following basis for the gauge fields

$$W_\mu \equiv \frac{1}{2} W_\mu^a \sigma_a = \frac{1}{2} \begin{pmatrix} W_\mu^3 & W_\mu^2 - iW_\mu^1 \\ W_\mu^2 + iW_\mu^1 & -W_\mu^3 \end{pmatrix} \equiv \frac{1}{2} \begin{pmatrix} W_\mu^3 & \sqrt{2}W_\mu^+ \\ \sqrt{2}W_\mu^- & -W_\mu^3 \end{pmatrix}, \quad (\text{A.1})$$

and for the \mathcal{H} field

$$\omega^+ = \frac{\omega^1 - i\omega^2}{\sqrt{2}}, \quad \omega^- = \frac{\omega^1 + i\omega^2}{\sqrt{2}}, \quad \pi^+ = \frac{\pi^1 - i\pi^2}{\sqrt{2}}, \quad \pi^- = \frac{\pi^1 + i\pi^2}{\sqrt{2}}. \quad (\text{A.2})$$

For what concern the fields ω^3 and π^3 , otherwise, we have used the same definition of eq. (2.48).

A.1 Feynman Rules

Here, we list the full set of Feynman rules of the theory

Propagators

$$\begin{aligned} \begin{array}{c} \xrightarrow{p} \\ \text{wavy line} \\ W^{\pm/3} \end{array} &= \frac{-i\eta^{\mu\nu}}{p^2 - m_W^2 + i\epsilon}, & \begin{array}{c} \xrightarrow{p} \\ \text{dashed line} \\ h \end{array} &= \frac{i}{p^2 - m_h^2 + i\epsilon}, \\ \begin{array}{c} \xrightarrow{p} \\ \text{dotted line} \\ \omega^{\pm/3} \end{array} &= \frac{i}{p^2 - m_W^2 + i\epsilon}, & \begin{array}{c} \xrightarrow{p} \\ \text{dashed line} \\ \pi^{\pm/3} \end{array} &= \frac{i}{p^2 - m_W^2 + i\epsilon}, \\ \begin{array}{c} \xrightarrow{p} \\ \text{solid line} \\ S \end{array} &= \frac{i}{p^2 - M_S^2 + i\epsilon}. \end{aligned} \quad (\text{A.3})$$

Ghost interactions

$\omega^{\pm/3}$ $\omega^{\pm/3}$ $h = -\frac{i}{2}gm_W$ ω^{\pm} ω^{\pm} $\phi^3 = \pm\frac{1}{2}gm_W$

ω^{\pm} ω^z $\phi^{\pm} = \pm\frac{1}{2}gm_W$ ω^z ω^{\pm} $\phi^{\mp} = \pm\frac{1}{2}gm_W$

ω^{\pm} p $W_{\mu}^3 = \pm igp_{\mu}$ ω^{\pm} p $W_{\mu}^{\pm} = \mp igp_{\mu}$

ω^3 p $W_{\mu}^{\mp} = \mp igp_{\mu}$

(A.4)

Scalar "S" interactions

h S S h S S $= -i\lambda_S$ π^{\pm} S S π^{\mp} S S $= -i\nu\lambda_S$

h S S h S S $= -i\lambda_S$ π^3 S S π^3 S S $= -i\lambda_S$

(A.5)

Gauge self-interactions

$$\begin{aligned}
 & \text{Diagram 1: } W_\mu^+ \text{ and } W_\mu^- \text{ meet at a vertex, } W_\nu^+ \text{ and } W_\nu^- \text{ meet at another vertex.} \\
 & \qquad = ig^2 \left(2\eta_{\mu\nu}\eta_{\rho\sigma} - \eta_{\mu\rho}\eta_{\nu\sigma} - \eta_{\mu\sigma}\eta_{\nu\rho} \right) \\
 & \text{Diagram 2: } W_\mu^+ \text{ and } W_\mu^3 \text{ meet at a vertex, } W_\nu^- \text{ and } W_\rho^3 \text{ meet at another vertex.} \\
 & \qquad = ig^2 \left(\eta_{\mu\rho}\eta_{\nu\sigma} + \eta_{\mu\sigma}\eta_{\nu\rho} - 2\eta_{\mu\nu}\eta_{\rho\sigma} \right)
 \end{aligned} \tag{A.6}$$

$$\text{Diagram: } W_\mu^+ \text{ (momentum } p \text{), } W_\nu^- \text{ (momentum } q \text{), } W_\sigma^3 \text{ (momentum } r \text{).} \\
 = -ig \left[\eta_{\mu\nu}(p-q)_\rho + \eta_{\nu\rho}(q-r)_\mu + \eta_{\rho\mu}(r-p)_\nu \right]$$

Gauge interactions

$$\begin{aligned}
 & \text{Diagram 1: } h \text{ and } \phi^{\pm/3} \text{ meet at a vertex, } W_\mu^{\mp/3} \text{ is the outgoing line.} \\
 & \qquad = \frac{1}{2}g(p_\mu - q_\mu) \\
 & \text{Diagram 2: } \phi^3 \text{ and } \phi^\pm \text{ meet at a vertex, } W_\mu^\mp \text{ is the outgoing line.} \\
 & \qquad = \frac{1}{2}g(p_\mu - q_\mu) \\
 & \text{Diagram 3: } \phi^+ \text{ and } \phi^- \text{ meet at a vertex, } W_\mu^3 \text{ is the outgoing line.} \\
 & \qquad = \frac{i}{2}g(p_\mu - q_\mu) \\
 & \text{Diagram 4: } W_\mu^{\pm/3} \text{ and } W_\nu^{\mp/3} \text{ meet at a vertex, } h \text{ is the outgoing line.} \\
 & \qquad = \frac{i}{2}g^2 v \eta_{\mu\nu} \\
 & \text{Diagram 5: } \phi^{\pm/3} \text{ and } \phi^{\mp/3} \text{ meet at a vertex, } W_\nu^- \text{ and } W_\mu^+ \text{ are outgoing lines.} \\
 & \qquad = \frac{i}{2}g^2 \eta_{\mu\nu} \\
 & \text{Diagram 6: } \phi^{\pm/3} \text{ and } \phi^{\mp/3} \text{ meet at a vertex, } W_\nu^3 \text{ and } W_\mu^3 \text{ are outgoing lines.} \\
 & \qquad = \frac{i}{2}g^2 \eta_{\mu\nu} \\
 & \text{Diagram 7: } h \text{ and } h \text{ meet at a vertex, } W_\nu^{\mp/3} \text{ and } W_\mu^{\pm/3} \text{ are outgoing lines.} \\
 & \qquad = \frac{i}{2}g^2 \eta_{\mu\nu}
 \end{aligned} \tag{A.7}$$

Higgs and Goldstone interactions

$$\begin{aligned}
& \begin{array}{ccc}
\begin{array}{c} h \\ \diagdown \\ \diagup \\ h \end{array} & \begin{array}{c} h \\ \diagup \\ \diagdown \\ h \end{array} & = -i \frac{3}{4} \frac{m_h^2}{m_W^2} g^2 \\
\begin{array}{c} \phi^\pm \\ \diagdown \\ \diagup \\ \phi^\mp \end{array} & \begin{array}{c} \phi^\mp \\ \diagup \\ \diagdown \\ \phi^\pm \end{array} & = -i \frac{1}{2} \frac{m_h^2}{m_W^2} g^2 \\
\begin{array}{c} \phi^\pm \\ \diagdown \\ \diagup \\ \phi^\mp \end{array} & \begin{array}{c} h \\ \diagup \\ \diagdown \\ h \end{array} & = -i \frac{1}{4} \frac{m_h^2}{m_W^2} g^2 \\
\begin{array}{c} h \\ \diagdown \\ \diagup \\ h \end{array} & \begin{array}{c} h \\ \diagup \\ \diagdown \\ h \end{array} & = -i \frac{3m_h^2}{v}
\end{array}
\end{aligned}
\tag{A.8}$$

A.2 Renormalization scheme

We adopt the $\overline{\text{MS}}$ renormalization scheme¹ and we choose to redefine the fields and independent parameters $\{W_\mu, \mathcal{H}, S, m_W, M_S, m_h, g, \lambda_s, \xi, m\}$ as

$$\begin{aligned}
W_\mu &\equiv \sqrt{Z_3} \bar{W}_\mu & \mathcal{H} &\equiv \sqrt{Z_{2,\mathcal{H}}} \bar{\mathcal{H}} & S &\equiv \sqrt{Z_{2,S}} \bar{S} \\
m_W^2 &\equiv \bar{M}_W^2 + \delta m_W^2 & M_S^2 &\equiv \bar{M}_S^2 + \delta M_S^2 & m_h^2 &\equiv \bar{M}_h^2 + \delta m_h^2 \\
g &\equiv Z_3^{-1} Z_{\epsilon,\mathcal{H}}^{-\frac{1}{2}} \bar{g} (1 + \delta g) & \lambda_s &\equiv \bar{\lambda}_s Z_s^{-1} Z_{2,\mathcal{H}}^{-1} (1 + \delta \lambda_s) & \xi &\equiv 1 + \delta \xi & \tilde{m}^2 &\equiv \bar{M}_W^2 + \delta \tilde{m}^2,
\end{aligned}
\tag{A.9}$$

where we denoted with a bar the renormalized quantities. We underline that we have redefined the whole bare scalar “ S ” mass ($M_S^2 = m_s^2 + \frac{2\lambda_s}{g} m_W^2$).

¹We have omitted the universal constant, which comes out from divergent integral in dimensional regularization, already in the definition of the scalar integrals in Appendix B and so, in order to adopt the $\overline{\text{MS}}$ scheme, we have to take care only of the divergent part

Appendix B

One-loop integrals

The explicit computations of chapter 4 lead us to deal with a quite heavy set of Feynman integrals. Since all of the particles of our model are massive we don't have to deal with true infrared divergences. Some of the integrals we encountered, otherwise, present an ultraviolet divergences. In order to handle with this we employ dimensional regularization [25], where the dimensionality of space time becomes $D = 4 - 2\epsilon$ and we will take $\epsilon \rightarrow 0$ at the end of the computation. The generic integral we need to compute, therefore, generally takes the form

$$I_N^{\mu_1 \dots \mu_\rho} = \frac{(2\pi\mu)^{4-D}}{i\pi^2} \int d^4l \frac{l^\mu \dots l^{\mu_\rho}}{D_1 \dots D_N}, \quad (\text{B.1})$$

where

$$D_j = (l + q_j)^2 - m_j^2, \quad q_j = \sum_{i=1}^j p_i, \quad (\text{B.2})$$

and in our cases, N has a maximum value of 4 and we adopt the conventions of Ref. [11]. In particular we forget about the usual multiplicative factor, coming from dimensional regularization, in eq. (B.1). With this conventions we can forget to deal with finite terms in the renormalization procedure in the $\overline{\text{MS}}$ scheme.

B.1 Passarino-Veltman tensor integral decomposition

The Passarino-Veltman [21] reduction is an efficient way allowing to express the generic Feynman tensor integrals of eq. (B.1) as a sum of basic scalar integrals times some coefficients which depends only on external kinematical quantities. We adopt now a convention similar to the one of Passarino Veltman and we call the one, two, three and four point integrals A , B , C and D as

$$A_0(m^2) = \frac{(2\pi\mu)^{4-D}}{i\pi^2} \int d^4l \frac{1}{D} \quad (\text{B.3})$$

$$B_0, B^\mu, B^{\mu\nu}(p^2, m_1^2, m_2^2) = \frac{(2\pi\mu)^{4-D}}{i\pi^2} \int d^4l \frac{1, l^\mu, l^\mu l^\nu}{D_1 D_2} \quad (\text{B.4})$$

$$C_0, C^\mu, C^{\mu\nu}, C^{\mu\nu}(p_1^2, p_2^2, (p_1 + p_2)^2, m_1^2, m_2^2, m_3^2) = \frac{(2\pi\mu)^{4-D}}{i\pi^2} \int d^4l \frac{1, l^\mu, l^\mu l^\nu}{D_1 D_2 D_3} \quad (\text{B.5})$$

$$\begin{aligned} D_0, \dots (p_1^2, p_2^2, p_3^2, (p_1 + p_2 + p_3)^2, (p_1 - p_3)^2, (p_2 - p_3)^2, m_1^2, m_2^2, m_3^2, m_4^2) \\ = \frac{(2\pi\mu)^{4-D}}{i\pi^2} \int d^4l \frac{1, \dots}{D_1 D_2 D_3 D_4} \end{aligned} \quad (\text{B.6})$$

In the next section we will give the values we need for such integrals in our model. We now discuss the general decomposition.

The idea of this decomposition is to write the tensor integrals as

$$\begin{aligned}
B_\mu(p^2, m_1^2, m_2^2) &= p_\mu B_1(p^2, m_1^2, m_2^2), \\
B_{\mu\nu}(p^2, m_1^2, m_2^2) &= \eta_{\mu\nu} B_{00}(p^2, m_1^2, m_2^2) + p_\mu p_\nu B_{11}(p, m_1, m_2) \\
C_\mu(p_1^2, p_2^2, p_3^2, m_1^2, m_2^2, m_3^2) &= p_{1\mu} C_1(p_1^2, p_2^2, p_3^2, m_1^2, m_2^2, m_3^2) + p_{2\mu} C_2(p_1^2, p_2^2, p_3^2, m_1^2, m_2^2, m_3^2) \\
C_{\mu\nu}(p_1^2, p_2^2, p_3^2, m_1^2, m_2^2, m_3^2) &= \eta_{\mu\nu} C_{00}(p_1^2, p_2^2, p_3^2, j_1^2, m_2^2, m_3^2) + \sum_{i,j=1}^2 C_{ij} p_{i,\mu} p_{j,\nu}, \text{ where } C_{21} = C_{12}.
\end{aligned} \tag{B.7}$$

The relation between tensor integrals and scalar integrals can be obtained by saturating both side of eq. (B.7) with $\eta^{\mu\nu}$ or the external momenta p_i^μ . This procedure is implemented in the computer tools FORMCALC we adopted for the computation. Therefore, here, we discuss in details only the case of the rank-one tensor triangle integral. For simplicity we set the internal masses at zero (i.e. $m_1 = m_2 = m_3 = 0$) and we drop the dependencies on the Lorentz invariants of the case ($p_1^2, p_2^2, p - 3^2 = (p - 1 + p_2)^2, m_1^2, m_2^2, m_3^2$). Multiplying both side of

$$\frac{(2\pi\mu)^{4-D}}{i\pi^2} \int d^D l \frac{l \cdot p_1}{l^2(l+q_1^2)(l+q_2)^2} = C_1 p_1^\mu + C_2 p_2^\mu \tag{B.8}$$

with p_1^μ , we get

$$\frac{(2\pi\mu)^{4-D}}{i\pi^2} \int d^D l \frac{l \cdot p_1}{l^2(l+q_1)^2(l+q_2)^2} = C_1 p_1^2 + C_2 p_1 \cdot p_2. \tag{B.9}$$

Now, we note that

$$l \cdot p_1 = \frac{1}{2} ((l+q_1)^2 - l^2 - p_1^2) \tag{B.10}$$

and so

$$p_1^2 C_1 + p_1 \cdot p_2 C_2 = \frac{1}{2} (B_0((p_2 + p_1)^2, 0, 0) - B_0(p_2^2, 0, 0) - p_1^2 C_0). \tag{B.11}$$

Analogously, multiplying for p_2^μ , we get

$$p_1 \cdot p_2 C_1 + p_2^2 C_2 = \frac{1}{2} (B_0(p_1^2, 0, 0) - B_0(p_2^2, 0, 0) - (2p_1 \cdot p_2 + p_2^2) C_0). \tag{B.12}$$

Therefore the Passarino-Veltman coefficients can be written as

$$\begin{aligned}
C_1 &= \frac{1}{(p_1^2 p_2^2 - (p_1 \cdot p_2)^2)} ((p_2^2 + p_1 \cdot p_2) B_0((p_1 + p_2)^2, 0, 0) - p_2^2 B_0(p_2^2, 0, 0) - p_1 \cdot p_2 B_0(p_1^2, 0, 0) \\
&\quad - (p_1^2 p_2^2 - 2(p_1 \cdot p_2)^2 - p_2^2 (p_1 \cdot p_2)) C_0),
\end{aligned} \tag{B.13}$$

$$\begin{aligned}
C_2 &= \frac{1}{(p_1^2 p_2^2 - (p_1 \cdot p_2)^2)} ((p_1^2 + p_1 \cdot p_2) B_0((p_1 + p_2)^2, 0, 0) + p_1^2 B_0(p_1^2, 0, 0) - p_1 \cdot p_2 B_0(p_2^2, 0, 0) \\
&\quad - (p_1^2 p_2^2 + p_1^2 (p_1 \cdot p_2)) C_0).
\end{aligned} \tag{B.14}$$

B.2 One-loop scalar integrals

Here, we list all the one-loop scalar integral we need in the analytic computations of ch. 4. We report the full result of Refs. [11, 26] for bubbles and tadpoles. Instead for triangles and boxes we give only an approximation in our kinematical region of interest.

Tadpole

The full result for the tadpole integral is [11]

$$A_0(m^2) = m^2 \left(\frac{\mu^2}{m^2 - i\epsilon} \right)^\epsilon \left\{ 1 + \frac{1}{\epsilon} \right\} + \mathcal{O}(\epsilon). \quad (\text{B.15})$$

In the limit $\mu^2 \sim s \gg m^2$ it becomes

$$A_0^2(m^2) \simeq m^2 \log \left(\frac{s}{m^2} \right). \quad (\text{B.16})$$

Bubble

The full result for the bubble integral is [11]

$$B_0(p^2, m_1^2, m_2^2) = \mu^{2\epsilon} \left\{ \frac{1}{\epsilon} + 2 - \log(p^2 - i\epsilon) + \sum_{i=1}^2 \left[\gamma_i \log \left(\frac{\gamma_i - 1}{\gamma_i} \right) - \log(\gamma_i - 1) \right] \right\} + \mathcal{O}(\epsilon), \quad (\text{B.17})$$

where

$$\gamma_{1,2} = \frac{s - m_2^2 + m_1^2 \pm \sqrt{(p^2 - m_2^2 + m_1^2)^2 - 4s(m_1^2 - i\epsilon)}}{2p^2}. \quad (\text{B.18})$$

In the limit $\mu^2 \sim s \gg p^2 \sim m^2 \sim m_2^2$ it becomes [23]

$$B_0(p^2, m_1^2, m_2^2) \simeq \log \left(\frac{s}{m^2} \right). \quad (\text{B.19})$$

Triangle

In our computation, it comes out that the only triangle integrals which survive, in the high energy limit $s \sim M_S^2 \gg m_h^2, m_W^2$, are the ones of the form $C_0(p_1^2, p_2^2, p_3^2 = (p_1 + p_2)^2, m_0^2, m_1^2, m_2^2)$, where $p_3^2 \gg m_0^2, m_1^2, m_2^2$.¹ [9]

$$C_0(p_1^2, p_2^2, p_3^2, m_0^2, m_1^2, m_2^2) = \frac{1}{p_3^2} \left(\frac{1}{2} \log^2 \left(\frac{-p_3^2}{m_0^2} \right) + \sum_{l=1,2} I_C(p_l^2, m_0^2, m_l^2) \right), \quad (\text{B.20})$$

where

$$I_C(p^2, m_0^2, m^2) \equiv - \int_0^1 \frac{dx}{x} \left(1 + \frac{m^2 - m_0^2 - p^2}{m_0^2 - i\epsilon} x + \frac{p^2}{m_0^2 - i\epsilon} x^2 \right). \quad (\text{B.21})$$

The integral I_C leads to large logarithms when the mass m_0^2 is small compared to p^2 and/or $p^2 - m^2$.

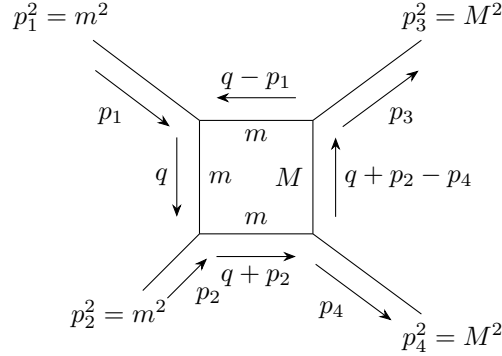
Box

In the explicit computation, we have to match with the box scalar integrals, with the configuration of masses (as depicted in fig. B.1)

$$D_0 = \int \frac{d^4q}{(2\pi)^4} \frac{1}{D_1 D_2 D_3 D_4}, \quad (\text{B.22})$$

¹In fact, even if we encounter integrals that depend on the M_S^2 mass, they turn out to be polynomially suppressed in our diagrams (i.e. of the form C_0/s).

Figure B.1: Box integral relative to eq. (B.22)



where

$$\begin{aligned} D_1 &= q^2 - m^2, & D_2 &= (q + p_2)^2 - m^2, \\ D_3 &= (q + p_2 - p_4)^2 - M^2, & D_4 &= (q - p_2)^2 - m^2. \end{aligned}$$

For analytical purposes we just need the leading behaviour in the asymptotic regime ($s \sim -t \sim -u \sim M^2 \gg m^2$), where in our process M and m play the role of, respectively, M_S and m_W .

This integral is clearly UV convergent, since it had a $D = -4$ grade of superficial divergence and it is, also, free from IR divergences, since it has no massless propagators. In order to find the behaviour of this D_0 with the kinematical invariants in our regime of interest, without performing the full integration, we can identify the three region giving the biggest contribution as

- A) q soft and almost collinear with respect to p_1 and p_2 ,
- B) q soft and almost collinear with respect to p_2 and p_4 ,
- C) q soft and almost collinear with respect to p_1 and p_3 .

Let us start with the region (A), we switch to the Sudakov parametrization as in eq. (3.4)

$$q = up_1 + vp_2 + p_\perp \quad (\text{B.23})$$

where p_\perp is ortogonal to the plane defined by p_1 and p_2 . In this coordinate we have that region (A) corresponds to

$$q_0 \ll \min|su|, |sv|, \quad |su|, |sv| \ll 1. \quad (\text{B.24})$$

After a straightforward computation it follows that

$$I_4 =_A \left(\frac{1}{M_S^2 - t} \right) \times I_3 = \frac{1}{2s(M_S^2 - t)} \log^2 \left(\frac{s}{m_W^2} \right) + \mathcal{O} \left(\frac{1}{s(M_S^2 - t)} \log^2 \left(\frac{s^2}{m_W^2} \right) \right) \quad (\text{B.25})$$

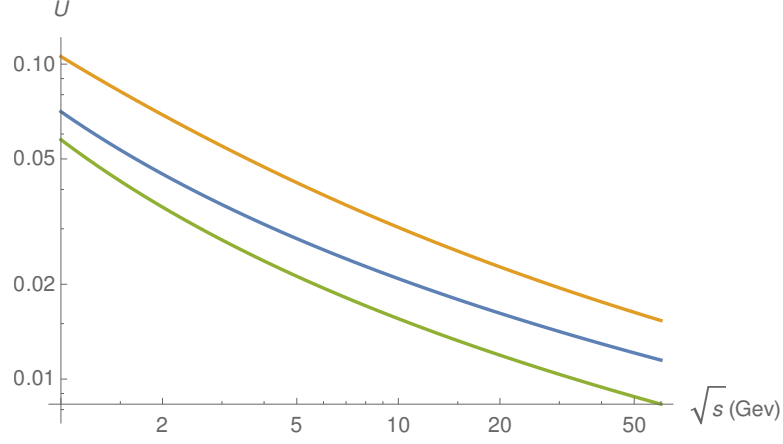
We can follow a similar scheme for the region (B), we switch to coordinates

$$q = up_2 + vp_4 + p_\perp, \quad (\text{B.26})$$

and we integrate in

$$q_0 \ll \min|tu|, |tv|, \quad |tu|, |tv| \ll 1. \quad (\text{B.27})$$

Figure B.2: Uncertainty between the exact value of the D_0 and the predicted one of eq. (B.29) with $t = t_{min}$ (green line), $t = t_{max}$ (orange line) and $t = \bar{t}$ (blue line). The other parameters of the plot are $m = 0.08$ and $M = \sqrt{s}/3$.



The result is

$$I_4 =_B \frac{1}{s(M_S^2 - t)s} \log^2 \left(\frac{M_S^2 - t}{m_W M_S} \right) \quad (\text{B.28})$$

Summing all the contributions² we have

$$I_4 \simeq I^A + I^B + I^C = \frac{1}{2s(M_S^2 - t)} \left(\log^2 \left(\frac{s}{m_W^2} \right) + 4 \log^2 \left(\frac{M_S^2 - t}{m_W M_S} \right) \right). \quad (\text{B.29})$$

In order to verify the validity of the previous result, we present a comparison between eq. (B.29) and the numerical value for the D_0 . In the plot of fig. B.31, therefore, is reported the value of the uncertainty between them

$$U = \frac{|I_4 - D_0|}{|I_4 + D_0|}, \quad (\text{B.30})$$

with three different values of the Mandelstam invariant $\{t_{min}, \bar{t}, t_{max}\}$, where

$$t_{min/max} = m^2 + M^2 - \frac{s}{2} \pm 2\sqrt{\left(\frac{s}{4} - m^2\right)\left(\frac{s}{4} - M^2\right)}, \quad \bar{t} = \frac{t_{max} + t_{min}}{2}. \quad (\text{B.31})$$

As we can see, there is good agreement between the exact and the leading result, and this agreement, obviously, increase with the energy.

²For instance, it comes out that the full result of eq. (B.29) is equal to the divergent part of D_0 , computed via the method of Ref. [10], with a IR cut-off m .

Appendix C

Feynman diagrams and analytical results

In this section we report the analytical result and the Feynman diagrams concerning the explicit computation of chapter 3.

C.1 High energy expansion

In order to find the leading double logs and to verify the Equivalence theorem of sect. 2.4 up to $\mathcal{O}(s^0)$, analytically, we have proceeded as following. Using the tools described in ch. 4, we generate the Feynman diagrams we are looking for and then we compute the relative amplitudes in terms of Passarino-Veltman scalar function. Then, using the asymptotic values of ch. B for the Scalar integral, we drop out all the terms which are polynomial sub-leading in our expansion (i.e. in our case as $1/s^n$, with $n > 0$). In order to find double logs, in particular, we know that, in our fauna of scalar integral only the Scalar C_0 could give us such contribution (the double logs coming from the Box integral are too much high-energy suppressed to be leading).

In the following, therefore, we report the list of the amplitudes computed in ch 4.

$$\begin{aligned} \Gamma_{\pi\pi\rightarrow SS} = & \frac{1}{256\pi^2} \left\{ \frac{2\lambda_S}{m_W^2} \left[4m_W^2 \left(2\lambda_S B_0(t, M_S^2, m_W^2) + 2\lambda_S B_0(u, M_S^2, m_W^2) \right) \right. \right. \\ & + g^2 s \left(C_0(m_W^2, S, m_W^2, m_W^2, m_h^2, m_h^2) + 2C_0(m_W^2, S, m_W^2, m_W^2, m_W^2, m_W^2) \right) \\ & + g^2 (m_h^2 + 2m_W^2) B_0(S, m_h^2, m_h^2) + g^2 (5m_h^2 + 4m_W^2) B_0(S, m_W^2, m_W^2) \left. \right] \\ & \left. - 8g^2 \lambda_S \left(B_0(m_W^2, m_h^2, m_W^2) + 2B_0(m_W^2, m_W^2, m_W^2) \right) \right\} + \mathcal{O}\left(\frac{m_W}{\sqrt{s}}\right) \quad (\text{C.1}) \end{aligned}$$

$$\begin{aligned} \Gamma_{WW\rightarrow h}^{1L} = & s \frac{g \left(g^2 (3A_0(m_W^2) (m_h^2 + 6m_W^2) - 2m_W^2 (9m_h^2 B_0(s, m_W^2, m_W^2))) \right)}{256\pi^2 m_h^2 m_W^3} \\ & s \left\{ \frac{g \left(g^2 (-2m_W^2 (-16m_h^2 B_0(m_W^2, m_W^2, m_W^2) + 4m_h^2 s C_0(m_W^2, s, m_W^2, m_W^2, m_W^2, m_W^2) + 6m_W^2)) \right)}{256\pi^2 m_h^2 m_W^3} \right. \\ & \left. + \frac{3g^2 m_h^2 A_0(m_h^2) + 4\lambda_S m_W^2 A_0(M_S^2)}{256\pi^2 m_h^2 m_W^3} \right\} + \mathcal{O}(s^0) \quad (\text{C.2}) \end{aligned}$$

$$\begin{aligned} \Gamma_{SS \rightarrow h}^{1L} = & \frac{\lambda_S}{64\pi^2 g m_h^2 m_W} \left(3g^2 m_h^4 B_0(S, m_W^2, m_W^2) + 3g^2 m_h^4 B_0(S, m_h^2, m_h^2) \right. \\ & + 16\lambda_S m_h^2 m_W^2 B_0(M_S^2, m_h^2, M_S^2) - 3g^2 m_h^2 A_0(m_W^2) - 3g^2 m_h^2 A_0(m_h^2) \\ & \left. - 18g^2 m_W^2 A_0(m_W^2) - 4\lambda_S m_W^2 A_0(M_S^2) + 12g^2 m_W^4 \right) \end{aligned} \quad (C.3)$$

$$\begin{aligned} \Gamma_{W_0 W_0 \rightarrow SS} = & \frac{\lambda_S}{64\pi^2 m_W^2} \left\{ g^2 (m_h^2 - m_W^2) B_0(s, m_h^2, m_h^2) - g^2 m_h^2 B_0(s, m_W^2, m_W^2) \right. \\ & + g^2 m_W^2 B_0(s, m_W^2, m_W^2) + 8\lambda_S m_W^2 B_0(M_S^2, m_h^2, M_S^2) - 4\lambda_S m_W^2 B_0(t, M_S^2, m_W^2) \\ & \left. - 4\lambda_S m_W^2 B_0(u, M_S^2, m_W^2) - 2g^2 m_W^2 s C_0(s, m_W^2, m_W^2, m_h^2, m_h^2, m_W^2) \right\} + \mathcal{O}\left(\frac{m_W}{\sqrt{s}}\right), \end{aligned} \quad (C.4)$$

$$\begin{aligned} \mathcal{A}_{W_0 W_0 \rightarrow SS}^{1L} = & -\frac{\lambda_S}{128\pi^2 m_h^2 m_W^2} \left\{ 5g^2 m_h^4 B_0(s, m_W^2, m_W^2) + 2g^2 m_h^2 m_W^2 B_0(s, m_h^2, m_h^2) \right. \\ & + 4g^2 m_h^2 m_W^2 B_0(s, m_W^2, m_W^2) - 32g^2 m_h^2 m_W^2 B_0(m_W^2, m_W^2, m_W^2) \\ & + g^2 m_h^4 B_0(s, m_h^2, m_h^2) + 8\lambda_S m_h^2 m_W^2 B_0(T, M_S^2, m_W^2) \\ & + 8\lambda_S m_h^2 m_W^2 B_0(U, M_S^2, m_W^2) + 8g^2 m_h^2 m_W^2 s C_0(m_W^2, s, m_W^2, m_W^2, m_W^2, m_W^2) \\ & + 4g^2 m_h^2 m_W^2 s C_0(s, m_W^2, m_W^2, m_h^2, m_h^2, m_W^2) - 6g^2 m_h^2 A_0(m_W^2) - 6g^2 m_h^2 A_0(m_h^2) \\ & \left. - 36g^2 m_W^2 A_0(m_W^2) - 8\lambda_S m_W^2 A_0(M_S^2) + 24g^2 m_W^4 \right\} + \mathcal{O}(s^0). \end{aligned} \quad (C.5)$$

C.2 Feynman diagrams

In the following, we report the list of all the Feynman diagrams computed and analysed in the thesis.

Figure C.1: The 1-loop diagrams which contributes the Π_{WW} form-factor

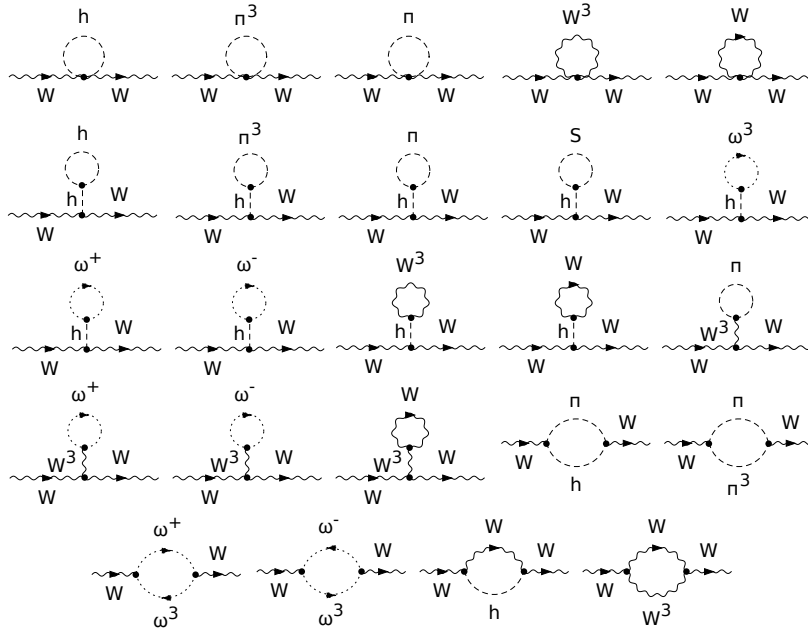


Figure C.2: The 1-loop diagrams which contributes the Π_{hh} form-factor

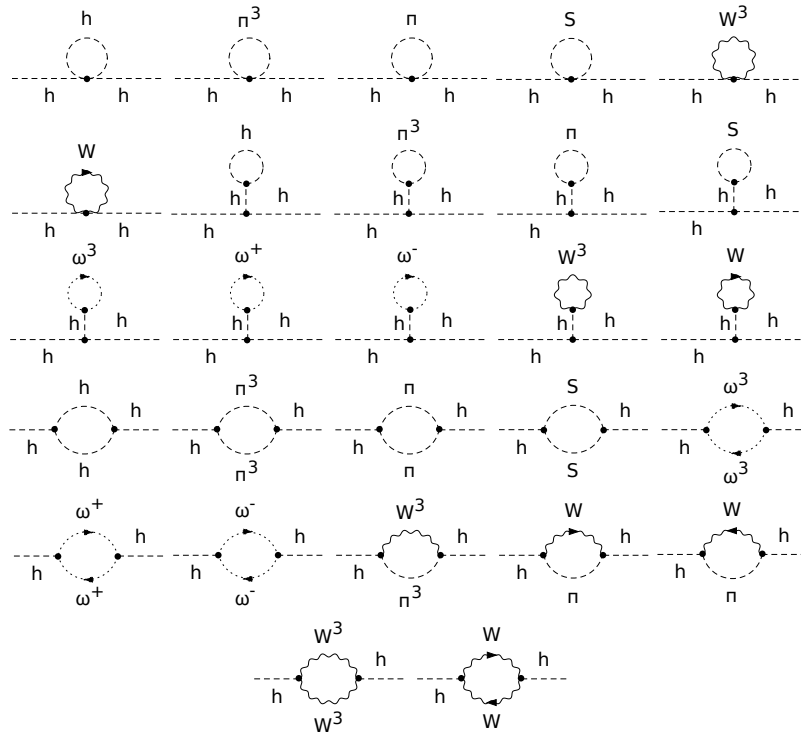


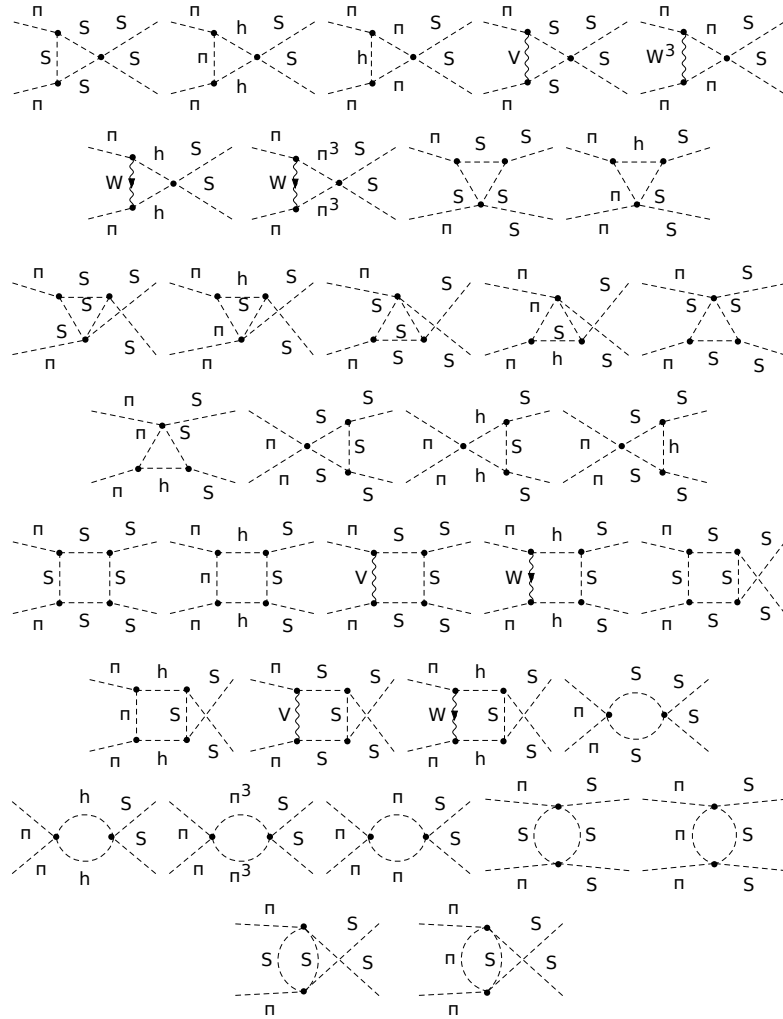
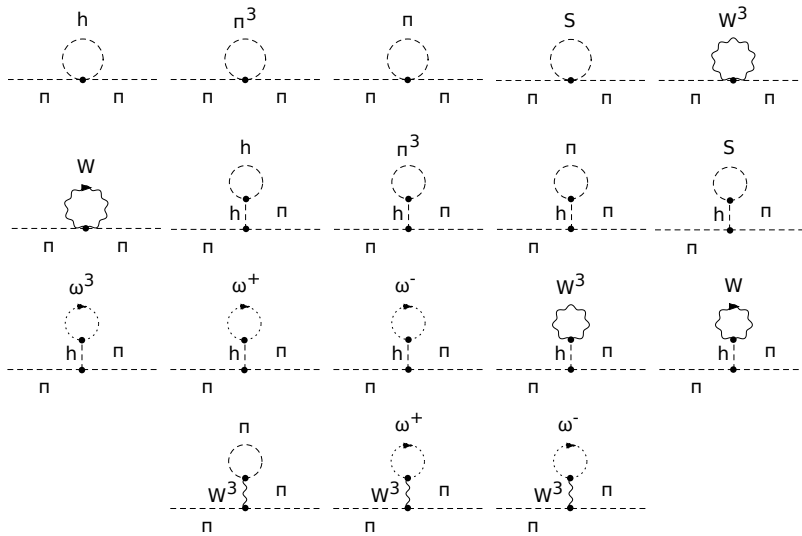
Figure C.3: 1-loop diagrams for $\Gamma_{\pi^+\pi^-\rightarrow SS}$ Figure C.4: The 1-loop diagrams which contribute to the $\Pi_{\pi\pi}$ form-factor

Figure C.5: The 1-loop diagrams which contributes the $\Pi_{W\pi}$ form-factor

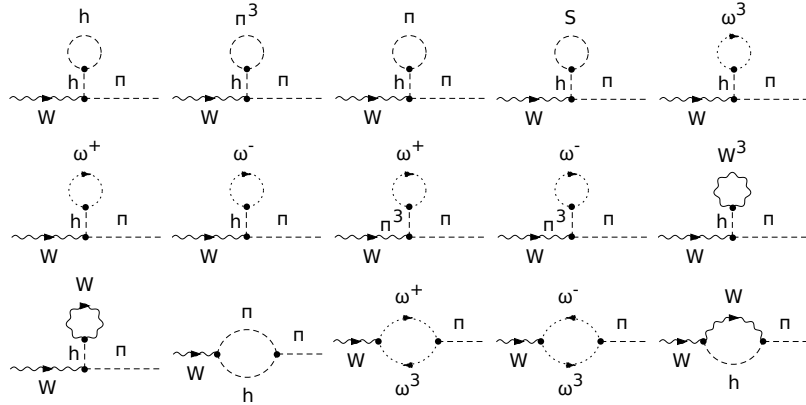


Figure C.6: The 1-loop diagrams which contributes the Π_{SS} form-factor

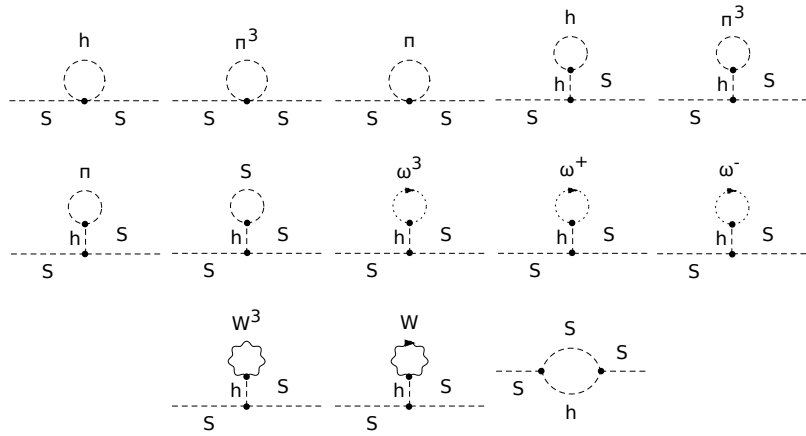


Figure C.7: 1-loop diagrams for $\Gamma_{SS \rightarrow h}$

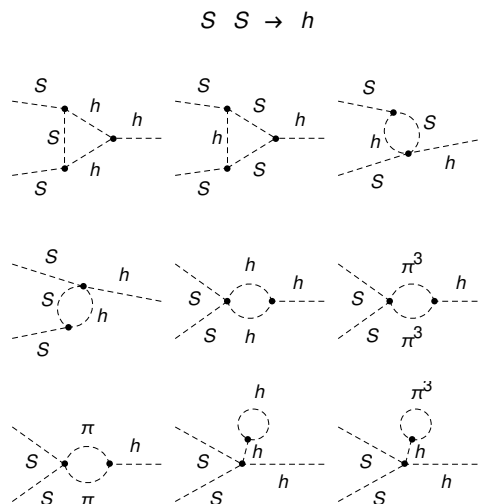
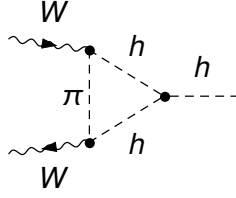
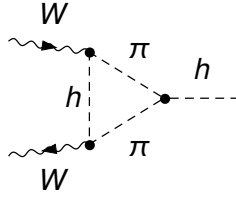
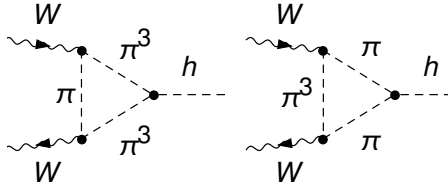


Table C.1: 1-loop diagrams for $\gamma_{W_0 W_0 \rightarrow h}^{1L}$ 

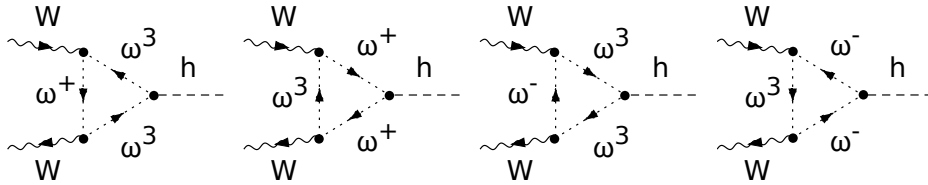
$${}^1D\Gamma_{WW \rightarrow h}^{1L} = \frac{3g^3 m_h^2 \epsilon_1 \cdot \epsilon_2}{128\pi^2 m_W} \quad {}^1\Gamma_{W_0 W_0 \rightarrow h}^{1L} = \frac{3g^3 m_h^2 B_0(s, m_h^2, m_h^2)}{256\pi^2 m_W^3} s + \mathcal{O}(s^0)$$



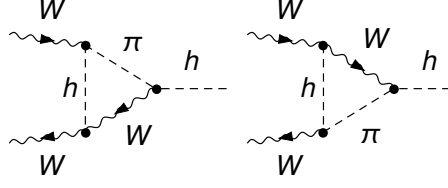
$${}^2D\Gamma_{WW \rightarrow h}^{1L} = \frac{g^3 m_h^2 \epsilon_1 \cdot \epsilon_2}{128\pi^2 m_W} \quad {}^2\Gamma_{W_0 W_0 \rightarrow h}^{1L} = \frac{g^3 m_h^2 B_0(s, m_W^2, m_W^2)}{256\pi^2 m_W^3} s + \mathcal{O}(s^0)$$



$${}^3D\Gamma_{WW \rightarrow h}^{1L} = \frac{g^3 m_h^2 \epsilon_1 \cdot \epsilon_2}{64\pi^2 m_W} \quad {}^3\Gamma_{W_0 W_0 \rightarrow h}^{1L} = \frac{g^3 m_h^2 B_0(s, m_W^2, m_W^2)}{128\pi^2 m_W^3} s + \mathcal{O}(s^0)$$

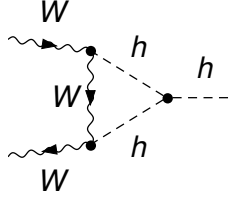


$${}^4D\Gamma_{WW \rightarrow h}^{1L} = -\frac{g^3 m_W \epsilon_1 \cdot \epsilon_2}{32\pi^2} \quad {}^4\Gamma_{W_0 W_0 \rightarrow h}^{1L} = -\frac{g^3 B_0(s, m_W^2, m_W^2)}{64\pi^2 m_W} s + \mathcal{O}(s^0)$$



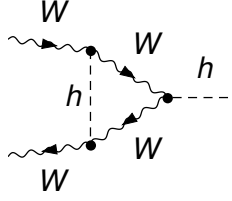
$${}^5D\Gamma_{WW\rightarrow h}^{1L} = \frac{g^3 m_W \epsilon_1 \cdot \epsilon_2}{64\pi^2}$$

$${}^5\Gamma_{W_0W_0\rightarrow h}^{1L} = \frac{g^3 (4B_0(m_W^2, m_h^2, m_W^2) - 3B_0(s, m_W^2, m_W^2))}{128\pi^2 m_W} s + \mathcal{O}(s^0)$$



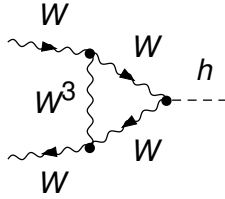
$${}^6D\Gamma_{WW\rightarrow h}^{1L} = 0$$

$${}^6\Gamma_{W_0W_0\rightarrow h}^{1L} = \mathcal{O}(s^0)$$



$${}^7D\Gamma_{WW\rightarrow h}^{1L} = 0$$

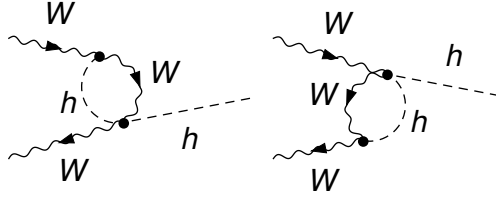
$${}^7\Gamma_{W_0W_0\rightarrow h}^{1L} = \mathcal{O}(s^0)$$



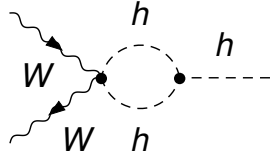
$${}^8D\Gamma_{WW\rightarrow h}^{1L} = \frac{9g^3 m_W \epsilon_1 \cdot \epsilon_2}{16\pi^2}$$

$${}^8\Gamma_{W_0W_0\rightarrow h}^{1L} = -s \frac{g^3 (-5B_0(s, m_W^2, m_W^2) - 4B_0(m_W^2, m_W^2, m_W^2))}{32\pi^2 m_W}$$

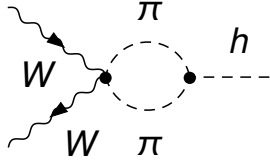
$$- \frac{(sC_0(m_W^2, S, m_W^2, m_W^2, m_W^2) + 4)}{32\pi^2 m_W} + \mathcal{O}(s^0)$$



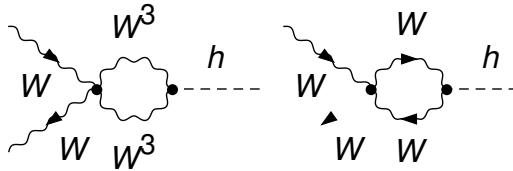
$${}^9D\Gamma_{WW\rightarrow h}^{1L} = -\frac{g^3 m_W \epsilon_1 \cdot \epsilon_2}{16\pi^2} \quad {}^9\Gamma_{W_0 W_0 \rightarrow h}^{1L} = -\frac{g^3 B_0(m_W^2, m_h^2, m_W^2)}{32\pi^2 m_W} s + \mathcal{O}(s^0)$$



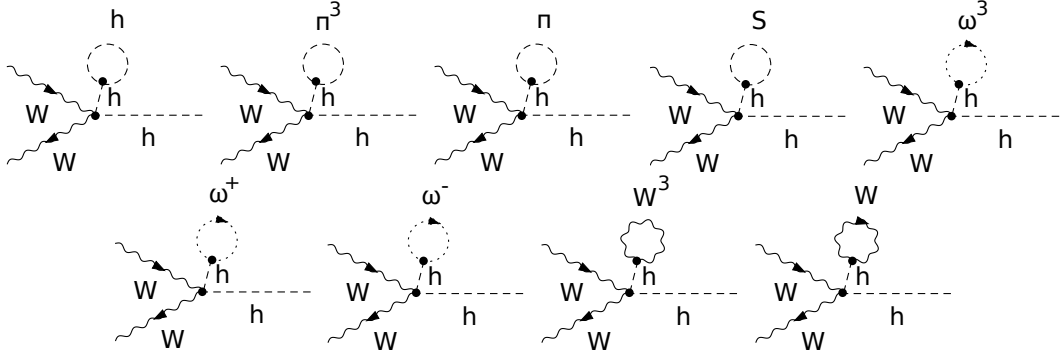
$${}^{10D}\Gamma_{WW\rightarrow h}^{1L} = -\frac{3g^3 m_h^2 \epsilon_1 \cdot \epsilon_2}{128\pi^2 m_W} \quad {}^{10}\Gamma_{W_0 W_0 \rightarrow h}^{1L} = -\frac{3g^3 m_h^2 B_0(s, m_h^2, m_h^2)}{256\pi^2 m_W^3} s + \mathcal{O}(s^0)$$



$${}^{11D}\Gamma_{WW\rightarrow h}^{1L} = -\frac{3g^3 m_h^2 \epsilon_1 \cdot \epsilon_2}{128\pi^2 m_W} \quad {}^{11}\Gamma_{W_0 W_0 \rightarrow h}^{1L} = -\frac{3g^3 m_h^2 B_0(S, m_W^2, m_W^2)}{256\pi^2 m_W^3} s + \mathcal{O}(s^0)$$

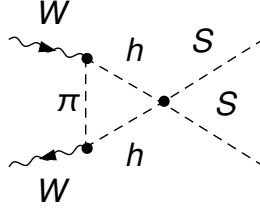


$${}^{12D}\Gamma_{WW\rightarrow h}^{1L} = -\frac{3g^3 m_W \epsilon_1 \cdot \epsilon_2}{8\pi^2} \quad {}^{12}\Gamma_{W_0 W_0 \rightarrow h}^{1L} = -\frac{g^3 (3B_0(s, m_W^2, m_W^2) - 2)}{16\pi^2 m_W} s + \mathcal{O}(s^0)$$



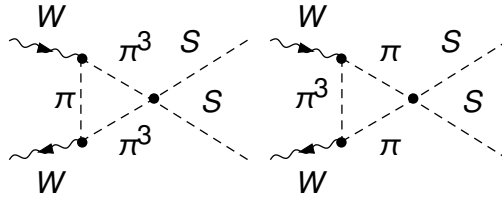
$${}^{13D}\Gamma_{WW \to h}^{1L} = -\frac{g^3 m_W \epsilon_1 \cdot \epsilon_2}{32\pi^2}$$

$${}^{13}\Gamma_{W_0 W_0 \to h}^{1L} = \frac{g}{256\pi^2 m_h^2 m_W^3} \left\{ 3g^2 (A_0(m_W^2)(m_h^2 + 6m_W^2) - 4m_W^4) + 3g^2 m_h^2 A_0(m_h^2) + 4\lambda_s m_W^2 A_0(M_S^2) \right\} s + \mathcal{O}(s^0)$$

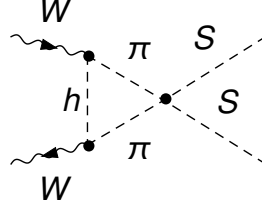
Table C.3: 1-loop diagrams for $\Gamma_{W_0 W_0 \to SS}^{1L}$ 

$${}^{1D}\Gamma_{WW \to SS}^{1L} = \frac{g^2 \lambda_S \epsilon_1 \cdot \epsilon_2}{64\pi^2}$$

$${}^1\Gamma_{W_0 W_0 \to SS}^{1L} = \frac{g^2 \lambda_S}{128\pi^2 m_W^2} \left\{ -4m_W^2 B_0(s, m_h^2, m_h^2) + 2m_h^2 B_0(s, m_h^2, m_h^2) + s B_0(s, m_h^2, m_h^2) - 2A_0(m_h^2) + 2A_0(m_W^2) \right\} + \mathcal{O}\left(\frac{m_W}{\sqrt{s}}\right)$$

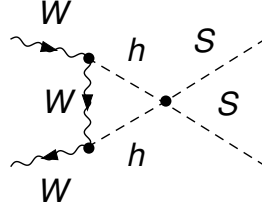


$${}^{2D}\Gamma_{WW \to SS}^{1L} = \frac{g^2 \lambda_S \epsilon_1 \cdot \epsilon_2}{32\pi^2} \quad {}^2\Gamma_{W_0 W_0 \to SS}^{1L} = \frac{g^2 \lambda_S (s - 2m_W^2) B_0(s, m_W^2, m_W^2)}{64\pi^2 m_W^2} + \mathcal{O}\left(\frac{m_W}{\sqrt{s}}\right)$$

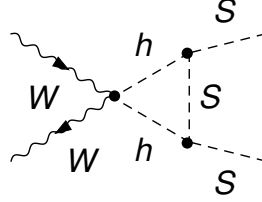


$${}^3D\Gamma_{WW \rightarrow SS}^{1L} = \frac{g^2 \lambda_S \epsilon_1 \cdot \epsilon_2}{64\pi^2}$$

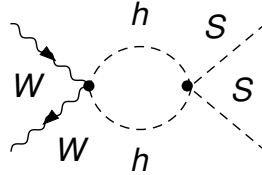
$${}^3\Gamma_{W_0 W_0 \rightarrow SS}^{1L} = \frac{g^2 \lambda_S ((s - 2m_h^2) B_0(s, m_W^2, m_W^2) + 2A_0(m_h^2) - 2A_0(m_W^2))}{128\pi^2 m_W^2} + \mathcal{O}\left(\frac{m_W}{\sqrt{s}}\right)$$



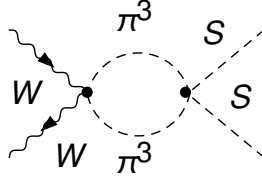
$${}^4D\Gamma_{WW \rightarrow SS}^{1L} = 0 \quad {}^4\Gamma_{W_0 W_0 \rightarrow SS}^{1L} = -\frac{g^2 \lambda_S s C_0(s, m_W^2, m_W^2, m_h^2, m_h^2, m_W^2)}{32\pi^2} + \mathcal{O}\left(\frac{m_W}{\sqrt{s}}\right)$$



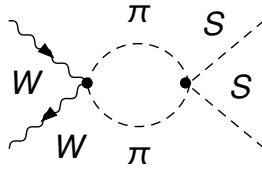
$${}^5D\Gamma_{WW \rightarrow SS}^{1L} = 0 \quad {}^5\Gamma_{W_0 W_0 \rightarrow SS}^{1L} = -\frac{\lambda_S^2 s C_0(s, M_S^2, M_S^2, m_h^2, m_h^2, M_S^2)}{16\pi^2} + \mathcal{O}\left(\frac{m_W}{\sqrt{s}}\right)$$



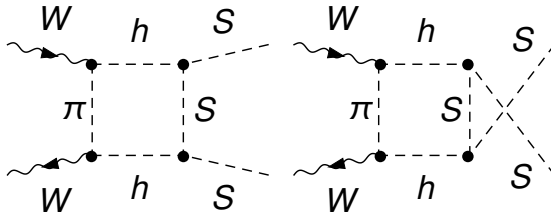
$${}^6D\Gamma_{WW \rightarrow SS}^{1L} = -\frac{g^2 \lambda_S \epsilon_1 \cdot \epsilon_2}{64\pi^2} \quad {}^6\Gamma_{W_0 W_0 \rightarrow SS}^{1L} = -\frac{g^2 \lambda_S (s - 2m_W^2) B_0(s, m_h^2, m_h^2)}{128\pi^2 m_W^2} + \mathcal{O}\left(\frac{m_W}{\sqrt{s}}\right)$$



$${}^7D\Gamma_{WW\rightarrow SS}^{1L} = -\frac{g^2\lambda_S\epsilon_1\cdot\epsilon_2}{64\pi^2} \quad {}^7\Gamma_{W_0W_0\rightarrow SS}^{1L} = -\frac{g^2\lambda_S(s-2m_W^2)B_0(s, m_W^2, m_W^2)}{128\pi^2 m_W^2} + \mathcal{O}\left(\frac{m_W}{\sqrt{s}}\right)$$

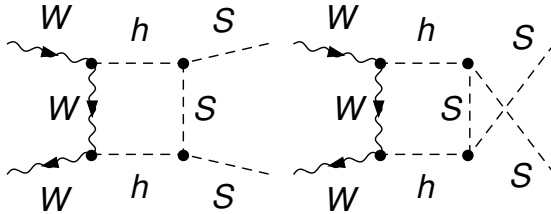


$${}^8D\Gamma_{WW\rightarrow SS}^{1L} = -\frac{g^2\lambda_S\epsilon_1\cdot\epsilon_2}{32\pi^2} \quad {}^8\Gamma_{W_0W_0\rightarrow SS}^{1L} = -\frac{g^2\lambda_S(s-2m_W^2)B_0(s, m_W^2, m_W^2)}{64\pi^2 m_W^2} + \mathcal{O}\left(\frac{m_W}{\sqrt{s}}\right)$$



$${}^9D\Gamma_{WW\rightarrow SS}^{1L} = 0$$

$${}^9\Gamma_{W_0W_0\rightarrow SS}^{1L} = \frac{\lambda_S^2}{16\pi^2} \left\{ 2B_0(M_S^2, m_h^2, M_S^2) - B_0(y, M_S^2, m_W^2) - B_0(u, M_S^2, m_W^2) + S + sC_0(s, M_S^2, M_S^2, m_h^2, m_h^2, M_S^2) \right\} + \mathcal{O}\left(\frac{m_W}{\sqrt{s}}\right)$$



$${}^{10D}\Gamma_{WW\rightarrow SS}^{1L} = 0$$

$${}^{10}\Gamma_{W_0W_0\rightarrow SS}^{1L} = \mathcal{O}\left(\frac{m_W}{\sqrt{s}}\right)$$

Bibliography

- [1] A.A. Abrikosov. Scattering of high-energy electrons and positrons by electrons. *Soviet Phys. JETP*, Vol: 3, 10 1956.
- [2] Adam Alloul, Neil D. Christensen, Céline Degrande, Claude Duhr, and Benjamin Fuks. FeynRules 2.0 - A complete toolbox for tree-level phenomenology. *Comput. Phys. Commun.*, 185:2250–2300, 2014.
- [3] F. Bloch and A. Nordsieck. Note on the radiation field of the electron. *Phys. Rev.*, 52:54–59, Jul 1937.
- [4] Pascal Borel, Roberto Franceschini, Riccardo Rattazzi, and Andrea Wulzer. Probing the Scattering of Equivalent Electroweak Bosons. *JHEP*, 06:122, 2012.
- [5] Marcello Ciafaloni. The QCD Coherent State From Asymptotic Dynamics. *Phys. Lett.*, 150B:379–382, 1985.
- [6] Marcello Ciafaloni. INFRARED SINGULARITIES AND COHERENT STATES IN GAUGE THEORIES. *Adv. Ser. Direct. High Energy Phys.*, 5:491–572, 1989.
- [7] Marcello Ciafaloni, Paolo Ciafaloni, and Denis Comelli. Bloch-Nordsieck violating electroweak corrections to inclusive TeV scale hard processes. *Phys. Rev. Lett.*, 84:4810–4813, 2000.
- [8] P. Ciafaloni and D. Comelli. Sudakov enhancement of electroweak corrections. *Phys. Lett.*, B446:278–284, 1999.
- [9] Ansgar Denner. Techniques for calculation of electroweak radiative corrections at the one loop level and results for W physics at LEP-200. *Fortsch. Phys.*, 41:307–420, 1993.
- [10] Stefan Dittmaier. Separation of soft and collinear singularities from one-loop n-point integrals. *Nuclear Physics B*, 675(1):447 – 466, 2003.
- [11] R. Keith Ellis and Giulia Zanderighi. Scalar one-loop integrals for QCD. *JHEP*, 02:002, 2008.
- [12] Victor S. Fadin, L. N. Lipatov, Alan D. Martin, and M. Melles. Resummation of double logarithms in electroweak high-energy processes. *Phys. Rev.*, D61:094002, 2000.
- [13] Thomas Hahn. Automatic loop calculations with FeynArts, FormCalc, and LoopTools. *Nucl. Phys. Proc. Suppl.*, 89:231–236, 2000.
- [14] Thomas Hahn. Generating Feynman diagrams and amplitudes with FeynArts 3. *Comput. Phys. Commun.*, 140:418–431, 2001.
- [15] Hong-Jian He, Yu-Ping Kuang, and Xiao-yuan Li. Further investigation on the precise formulation of the equivalence theorem. *Phys. Rev.*, D49:4842–4872, 1994.
- [16] Hong-Jian He, Yu-Ping Kuang, and Xiaoyuan Li. On the precise formulation of the equivalence theorem. *Phys. Rev. Lett.*, 69:2619–2622, Nov 1992.

-
- [17] T. Kinoshita. Mass singularities of Feynman amplitudes. *J. Math. Phys.*, 3:650–677, 1962.
- [18] Taichiro Kugo and Izumi Ojima. Local covariant operator formalism of non-abelian gauge theories and quark confinement problem. *Progress of Theoretical Physics Supplement*, 66:1–130, 1979.
- [19] P. P. Kulish and L. D. Faddeev. Asymptotic conditions and infrared divergences in quantum electrodynamics. *Theor. Math. Phys.*, 4:745, 1970. [Teor. Mat. Fiz.4,153(1970)].
- [20] T. D. Lee and M. Nauenberg. Degenerate systems and mass singularities. *Phys. Rev.*, 133:B1549–B1562, Mar 1964.
- [21] G. Passarino and M. J. G. Veltman. One Loop Corrections for $e^+ e^-$ Annihilation Into $\mu^+ \mu^-$ in the Weinberg Model. *Nucl. Phys.*, B160:151–207, 1979.
- [22] Hiren H. Patel. Package-X: A Mathematica package for the analytic calculation of one-loop integrals. *Comput. Phys. Commun.*, 197:276–290, 2015.
- [23] Stefano Pozzorini. *Electroweak radiative corrections at high-energies*. PhD thesis, Zurich U., Inst. Math., 2001.
- [24] V. V. Sudakov. Vertex parts at very high-energies in quantum electrodynamics. *Sov. Phys. JETP*, 3:65–71, 1956. [Zh. Eksp. Teor. Fiz.30,87(1956)].
- [25] Gerard 't Hooft and M. J. G. Veltman. Regularization and Renormalization of Gauge Fields. *Nucl. Phys.*, B44:189–213, 1972.
- [26] Gerard 't Hooft and M. J. G. Veltman. Scalar One Loop Integrals. *Nucl. Phys.*, B153:365–401, 1979.
- [27] Steven Weinberg. Infrared photons and gravitons. *Phys. Rev.*, 140:B516–B524, 1965.
- [28] Andrea Wulzer. An Equivalent Gauge and the Equivalence Theorem. *Nucl. Phys.*, B885:97–126, 2014.
- [29] Andrea Wulzer, Cuomo Gabriel, and Luca Vecchi. [In preparation].